ANTIBACTERIAL EFFECTS OF BIOGENIC SILVER NANOPARTICLES SYNTHESIZED USING *MANIHOT ESCULENTA* (CASSAVA) LEAF AQUEOUS EXTRACT

TONI CHARLIZE ALEXIA OLIVER

UNIVERSITY *of the*
WESTERN CAPE

A thesis submitted in fulfilment of the requirements for the degree of Magister Scientiae in the Department of Biotechnology, University of the Western Cape.

Supervisor: Prof. Abram Madiehe

Co-supervisor: Dr. Nicole Sibuyi

30 January 2023

KEYWORDS

Bacterial infections
Antimicrobial resistance
Antibiotic-resistant
Antibacterial activity
ESKAPE
Nanotechnology
Silver nanoparticles (AgNPs)
Green synthesis
Manihot esculenta
Cassava biowaste

ABSTRACT

Antibacterial effects of biogenic silver nanoparticles synthesized using *Manihot esculenta* (cassava) leaf aqueous extract

T.C.A. Oliver

MSc Thesis, Department of Biotechnology, University of the Western Cape

Antimicrobial resistance (AMR) is a growing global health concern that poses a serious threat to the health of humans, animals, and plants. The major public health problem of AMR is primarily caused by the incorrect use of antibiotics, which is further compounded by the reduced novel antibiotics discovery rate. AMR bacteria cause infections that are difficult to treat, resulting in prolonged hospital stays and increased healthcare costs. Moreover, AMR is associated with a high risk of morbidity and mortality. Current therapeutic strategies for AMR infections are often inefficacious, associated with side effects, and may further exacerbate AMR. Therefore, there is an urgent need to develop alternative strategies to treat AMR bacterial infections.

Nanotechnology has the potential to eradicate the burden of AMR by providing alternative novel or improved therapeutic strategies for AMR infections. Silver nanoparticles (AgNPs) have been shown to exhibit antimicrobial properties which aid in the prevention and treatment of infections. The green synthesis of AgNPs is beneficial and preferred over physical and chemical synthesis methods as it employs sustainable green chemistry principles, makes use of bioactive molecules with medicinal properties, is cost-effective, energy-efficient, and environmentally friendly. Previous literature has shown that *Manihot esculenta* (cassava) leaf extracts possess antimicrobial properties and can be used for AgNPs synthesis. In South Africa (SA), cassava leaves are an agricultural waste by-product of industrial starch production, which enables the utilization of cassava leaves in waste upcycling. This study reports on the green synthesis and characterization of AgNPs synthesized using an aqueous cassava leaf extract (CLE) and the antibacterial effects of the CLE-AgNPs against AMR pathogens, such as *Staphylococcus aureus,* Methicillin-resistant *Staphylococcus aureus, Escherichia coli, Klebsiella pneumoniae, Acinetobacter baumannii,* and *Pseudomonas aeruginosa*.

AgNPs synthesis conditions (i.e., pH, temperature, CLE concentration, and silver nitrate ($AgNO_3$) concentration) were optimized to obtain AgNPs with desirable physicochemical properties. CLE-AgNPs were successfully synthesized and characterized using Ultraviolet-visible (UV-vis) Spectroscopy, Dynamic Light Scattering (DLS), High-Resolution Transmission Electron Microscopy (HR-TEM), and Fourier-Transform Infrared (FTIR) Spectroscopy. The *in vitro* antibacterial effect of CLE-AgNPs was assessed by agar well diffusion, microdilution assay to obtain the minimum inhibitory concentration (MIC), and minimum bactericidal concentration (MBC).

The CLE-AgNPs had a surface plasmon resonance at 432 nm, a hydrodynamic diameter of 91.5 ± 50.82 nm, and an average core size of 16.11 ± 10.6 nm. The CLE-AgNPs had a PDI of 0.52 ± 0.014 and a ζ-potential of – 21.7 ± 11.3 mV. The CLE-AgNPs were anisotropic and relatively polydispersed, with most CLE-AgNPs being spherical. The functional groups of the phytochemicals present in the CLE were identified and confirmed to be involved in the reduction and capping of the CLE-AgNPs. The CLE-AgNPs displayed significant dose-dependent inhibitory activity against all the bacterial strains tested. The CLE-AgNPs also displayed bactericidal activity against all the bacterial strains tested. Moreover, the ability of CLE to synthesize biogenic AgNPs with exceptional antibacterial activity is exhibited. Therefore, CLE-AgNPs may serve as a novel antibacterial agent to aid in the prevention and treatment of AMR infections, and ultimately, in the eradication of AMR pathogens globally. In conclusion, the results presented in this study demonstrated that the upcycling of cassava biowaste through valorisation and use in the manufacturing of new high-value products is achievable.

30 January 2023

DECLARATION

I declare that "**Antibacterial effects of biogenic silver nanoparticles synthesized using *Manihot esculenta* (cassava) leaf aqueous extract "** is my own work, that it has not been submitted for any degree or examination in any other university, and that all the sources I have used or quoted have been indicated and acknowledged by complete references.

Full name: Toni Charlize Alexia Oliver **Date:** 30 January 2023

Signed: 

ACKNOWLEDGMENTS

Firstly, I would like to acknowledge and thank the Almighty Father for granting me the strength to get through this chapter. It has not been easy, but I am more than a conqueror. I give Him all the glory, honour, and praise. Proverbs 3:5-6 "***Trust in the Lord with all your heart and lean not on your own understanding; in all your ways acknowledge Him and He shall direct your paths***."

With a heart filled with immense gratitude and appreciation, I would like to thank my supervisor, Prof. Abram Madiehe, a man who has worn many hats and has gone over and beyond to be there for me the past few years that I have been under his supervision. His guidance, support, and tough love have been invaluable for my growth, not only as a student but as a human being too. Prof, I will never forget the space you held for me and how the numerous conversations in your office have carried me more than you will ever know. You have been more like a father to me, and I will always feel honoured to have been led and taught by you. *Ke a leboha haholo. Love, Charlize.*

My sincere gratitude to Prof. Mervin Meyer and Dr. Nicole Sibuyi who have both played important roles in my postgraduate journey. I am grateful for the assistance and support that you have provided me with. It has been an honour to have been a student under your leadership.

To all my colleagues in the Nanobiotechnology Research Group, Department of Science and Innovation-Mintek Nanotechnology Innovation Centre, and Department of Biotechnology, thank you for being there for me whenever I needed a helping hand, a listening ear, or a strong shoulder to lean on. I will cherish the memories we have made in and outside of the lab. I will never forget the laughs we shared and our spontaneous adventures. It has been fun! *Let's play 30 Seconds?!*

To my mother, Hazel Oliver, thank you for all the sacrifices you have made as a single mother to make sure that I had/have the best of what this life has to offer. I am because you are, and my achievements are yours too. To Ashwin, Nicole, Carlyle, and Athena – thank you for your love, care, and support. You bring joy into my life and give me the strength to carry on. To my family and closest friends (you know who you are), a heartfelt thank you for helping me achieve this goal.

Finally, I would like to extend a thank you to the National Research Foundation for providing me with the financial support to further my postgraduate studies, and the NBRG lab, DSI-Mintek NIC, and the University of the Western Cape for affording me the opportunity to pursue a Master of Science degree and providing me with the support and resources needed to complete my studies.

DEDICATION

To my mother, Hazel Oliver, I hope to continue making you proud and I pray that God gives me the chance to be able to give you the best of what this life has to offer one day.
Thank you for always reminding me to never allow anyone to make me feel inferior without my consent and that despite the adversities we have faced in life, nothing is impossible.
Love, Alexia.

To my nephew, Carlyle, and niece, Athena, I hope that Aunty always remains an inspiration to both of you. Never give up on your dreams and, most importantly, never give up on yourself.
May the choices you make reflect your hopes and not your fears.
"I love you too days!"

"It always seems impossible until it's done."

- Nelson Rolihlahla Mandela -

CONFERENCE CONTRIBUTION

Oliver, T.C.A., Sibuyi, N.R.S., Meyer, M., and Madiehe, A.M. "Antibacterial effects of biogenic silver nanoparticles synthesized using *Manihot esculenta* (cassava) leaf aqueous extract" at the Department of Science and Innovation-Mintek Nanotechnology Innovation Centre (DSI-Mintek NIC) Annual Workshop at Rhodes University, Makhanda, Eastern Cape, 23-24 November 2022. **Oral presentation (Second prize).**

TABLE OF CONTENTS

LIST OF ABBREVIATIONS

°C	Degrees Celsius or degree centigrade
%	Percentage
β	Beta
λmax	maximum absorbance/ absorption maximum
µl	Microliter
ζ-potential	Zeta potential
Abs.	Absorbance
Ag	Silver
Ag^+	Silver ion
Ag^0	Silver atom
AgNP(s)	Silver nanoparticle(s)
$AgNO_3$	Silver nitrate
Al	Aluminium
AMR	Antimicrobial resistance
AMU	Antimicrobial use
ATCC	American Type Culture Collection
Au	Gold
AuNP(s)	Gold nanoparticle(s)
BRICS	Brazil, Russia, India, China, and South Africa
BSA	Bovine serum albumin
BSIs	Bloodstream infections

CAM	Complementary and alternative medicine
CDC	Centers for Disease Control and Prevention
CDI	*Clostridium difficile* infection
CFU	Colony forming units
CLE	Cassava leaf extract
CLE-AgNPs	Cassava leaf extract-silver nanoparticles
Co	Cobalt
COVID-19	Coronavirus disease 2019
Cu	Copper
DDD	Defined Daily Dose
ddH_2O	Deionized distilled water
dH_2O	Distilled water
DLS	Dynamic Light Scattering
DFUs	Diabetic foot ulcers
DM	Diabetes mellitus
DNA	Deoxyribonucleic acid
EPS	Extracellular polymeric substances
ESBL	Extended spectrum b-lactamases
ESKAPE	*Enterococcus faecium, Staphylococcus aureus, Klebsiella pneumoniae, Acinetobacter baumannii, Pseudomonas aeruginosa*, and *Enterobacter*
FC	Folin-Ciocalteu
FDA	Food and Drug Administration
Fe	Iron

FEG	Field emission gun
FQAD	Fluoroquinolone-associated disability
FTIR	Fourier-transform Infrared spectroscopy
g	Gram(s)
GAE	Gallic Acid Equivalents
GRAS	Generally recognized as safe
HCl	Hydrochloric acid
HICs	Higher-income countries
HNO_3	Nitric acid
hr(s)	Hour(s)
HR-TEM	High Resolution-Transmission Electron Microscopy
IBM	International Business Machines
ICP-OES	Inductively Coupled Plasma Optical Emission Spectrometry
IDs	Infectious diseases
IONPs	Iron oxide nanoparticles
KBr	Potassium bromide
L	Liter
LMICs	Low- and middle-income countries
LSPR	Localized surface plasma resonance
M	Molar
MBC	Minimum bactericidal concentration
MDR	Multi-drug resistant
mg	Milligram(s)

mg/ml	milligram(s) per millilitre
MHA	Mueller Hinton agar
MHB	Mueller Hinton broth
MIC	Minimum inhibitory concentration
min(s)	Minute(s)
ml	Millilitre(s)
mm	Millimetre(s)
mM	Millimolar
MNPs	Metal nanoparticles
NaOH	Sodium hydroxide
Na_2CO_3	Sodium carbonate
NDoH-RSA	National Department of Health Republic of South Africa
NHLS	National Health Laboratory Service
Ni	Nickel
NiNPs	Nickel nanoparticles
nm	Nanometre
NP(s)	Nanoparticle(s)
OD	Optical density
PBS	Phosphate buffered saline
PDI	Polydispersity index
Pt	Platinum
PtNPs	Platinum nanoparticles
QS	Quorum sensing

RFU	Relative Fluorescence Units
ROS	Reactive oxygen species
RSA/ SA	Republic of South Africa/ South Africa
RT	Room temperature
rpm	Revolutions per minute
SADC	Southern African Development Community
SD	Standard deviation
Se	Selenium
SeNPs	Selenium nanoparticles
SEC	Size exclusion chromatography
SPR	Surface Plasmon Resonance
Ti	Titanium
TiO_2NPs	Titanium dioxide nanoparticles
TPC	Total Phenolic Content
UK	United Kingdom
U.S./ USA	United States/ United States of America
UTIs	Urinary tract infections
UV-vis	Ultraviolet-visible spectroscopy
v/v	Volume per volume
w/v	Weight per volume
WHO	World Health Organization
XDR	Extensively drug-resistant
ZnONPs	Zinc oxide nanoparticles

LIST OF FIGURES

LIST OF TABLES

CHAPTER 1: LITERATURE REVIEW

1.1. Introduction

Recently, several infections that were under control are now reappearing and new infectious diseases (IDs) are emerging (Khémiri *et al.,* 2019). The rapid emergence of IDs poses a serious threat to global public health. Approximately 17 million people have been killed by IDs worldwide with bacterial infections being the leading cause of mortalities (Cano *et al.*, 2020; Patil and Chandrasekaran, 2020; Yeh *et al.*, 2020; Zhang *et al.*, 2020b). It is imperative to prevent infection or decrease the duration of already existing bacterial infections as it may result in life-threatening consequences such as sepsis. The prevention of the development of sepsis is important as it may lead to death (Azeltine *et al.*, 2020). Approximately, 5-15% of patients admitted to the hospital are impacted by one or more bacterial infections (Urzedo *et al.*, 2020). Bacterial infections lead to increased healthcare costs and place immense pressure on healthcare systems due to prolonged hospital stays, treatment failures, the persistence of infections, and delayed healing of wounds which often lead to amputation and increased levels of morbidity and mortality (Chinnasamy *et al.*, 2021; Kalantari *et al.*, 2020). The threat of bacterial infections to global health is exacerbated by the emergence and spread of multi-drug resistant (MDR) bacteria due to antimicrobial resistance (AMR) (World Health Organization, 2021).

According to the U.S. Centers for Disease Control and Prevention (CDC), AMR is a naturally occurring process that occurs when microorganisms "develop the ability to defeat the drugs that are designed to kill them" (Centers for Disease Control and Prevention, 2022a). AMR has been declared by the World Health Organization (WHO) as "one of the top 10 global public threats facing humanity" and is generally regarded by all stakeholders as a 'One Health' issue because humans, animals, plants, and the environment are all impacted by it (Velazquez-Meza *et al.*, 2022; Krishna *et al.*, 2021). In 2019, 4.95 million deaths were linked to bacterial AMR with Sub-Saharan Africa having the highest death rate globally (Murray *et al.*, 2022). Projections by the CDC indicate that more deaths will be attributed to AMR (10 million/year) than all types of cancers (8.2 million/year) by 2050 which will cost the global economy an estimated US$100 trillion (Cano *et al.*, 2020; Hu *et al.*, 2020; Kalantari *et al.*, 2020). Although AMR occurs naturally, the main reason for the rise in AMR to drugs and the failure of available antimicrobial agents to treat infections is the overprescribing and/ or misuse of antibiotics resulting in recalcitrant infections (Khémiri *et al.*,

2019). Several reports have stated that the global coronavirus disease 2019 (COVID-19) pandemic aggravated the spread of AMR as there was an escalation in the misuse of antibiotics (Moolla *et al.*, 2021).

AMR has primarily been found in multi-drug resistant (MDR) bacterial strains such as the ESKAPE pathogens. The ESKAPE pathogens also known as "superbugs" have growing multidrug resistance and virulence, are responsible for most nosocomial infections, and can "escape" the killing action of antibacterial agents. ESKAPE stands for *Enterococcus faecium, Staphylococcus aureus, Klebsiella pneumoniae, Acinetobacter baumannii, Pseudomonas aeruginosa*, and *Enterobacter* species (Bhatia *et al.*, 2021; De Oliveira *et al.*, 2020; Mulani *et al.*, 2019). ESKAPE pathogens are associated with the highest risk of morbidity and mortality (Founou *et al.*, 2017).

Current therapeutic strategies available to treat AMR infections are often inefficacious, associated with side effects, and may further exacerbate AMR. Therefore, there is an urgent need to develop alternative strategies to battle rapidly evolving pathogens and existing bacterial infections associated with AMR. ESKAPE pathogens are on the WHO list of MDR bacteria that require the urgent development of new antibiotics (Bhatia *et al.*, 2021). The WHO advocates the use of complementary and alternative medicine (CAM) which deals with the use of natural products and/or their derivatives to treat various illnesses (WHO, 2019). Approximately 80% of the global population relies on CAM for the treatment of several diseases (Bhatia *et al.*, 2021). The use of CAM has also been found to be effective in the treatment of IDs (Nilashi *et al.*, 2020). Although CAM may be beneficial for the treatment of AMR infections, there are limitations associated with the use of medicinal plant extracts and other naturally derived products such as poor oral bioavailability due to inadequate solubility and limited permeability as a result of degradation in the gastrointestinal tract. In addition, natural compounds may exhibit serious side effects such as high fever, hypotension, chills, cardiac arrhythmias, and damage to major organs (Saka and Chella, 2021; Teoh and Das, 2018).

Nanotechnology can eradicate the burden of AMR by providing alternative novel or improved therapeutic strategies for AMR infections. Nanotechnology refers to the manipulation of particles on an atomic and molecular level for the design, manufacture, and application of new (nano)materials (Lozano, 2022; Agarwal *et al.*, 2021; Gour and Jain, 2019; Rafique *et al.*, 2017). Nanomaterials are tiny particles with a range of diameter between 1 and 100 nanometres (nm).

The physicochemical and structural properties of nanomaterials differ from those of atoms, molecules, and bulk counterparts making them ideal candidates for biomedical applications (Joudeh and Linke, 2022; Okkeh *et al.*, 2021; Srikar *et al.*, 2016; Guisbiers *et al.*, 2012). Noble metals have received great attention as they can provide NPs with appealing characteristics (Rafique *et al.*, 2017). Silver nanoparticles (AgNPs) possess excellent chemical stability, high electrical and thermal conductivity, catalytic activity, non-linear optical behaviour, and biological properties that make them attractive for applications within the nanobiotechnology field (Skóra *et al.*, 2021; Parveen *et al.*, 2016).

AgNPs have been shown to exhibit antimicrobial properties which aid in the prevention and treatment of AMR infections. The green synthesis of AgNPs is beneficial and preferred over physical and chemical methods as it employs sustainable green chemistry principles, makes use of biologically active compounds with medicinal properties, is cost-effective, energy-efficient, and environmentally friendly. Biologically active compounds found in plant extracts also referred to as phytochemicals act as reducing and stabilizing agents in the formation of NPs (Soltys *et al.*, 2021; Bhardwaj *et al.*, 2020; Rigo *et al.*, 2013). The medicinal properties of the biologically active compounds can also be introduced to the NPs resulting in enhanced biological activities (Gnanajobitha *et al.*, 2013). Previous literature has shown that the leaf extracts of *Manihot esculenta* (cassava) possess antimicrobial properties and can facilitate AgNPs synthesis. In South Africa (SA), cassava leaves are an agricultural waste by-product of industrial starch production which enables the utilization of cassava leaves in waste upcycling. The proper management of cassava biowaste can alleviate the burden of environmental pollution and lead to environmental, human health, and socio-economic benefits (Hadzi-Nikolova *et al.*, 2021; Oghenejoboh *et al.*, 2021; Ghimire *et al.*, 2015). Furthermore, the management of biowaste plays a key role in ensuring the sustainability of the bioeconomy (Ortega *et al.*, 2022).

Green silver nanotechnology can revolutionize the field of AMR by providing alternative novel or improved therapeutic strategies that are promising, cost-effective, and environmentally safe. Biogenic AgNPs with antibacterial efficacy may be employed as a promising alternative strategy to currently available treatments for antibiotic-resistant infections associated with AMR. Therefore, this study will focus on the green synthesis and characterization of AgNPs synthesized using an aqueous cassava leaf extract (CLE) and the antibacterial effects of the CLE-AgNPs

against six human pathogenic bacteria associated with AMR such as *S. aureus*, MRSA, *E. coli*, *P. aeruginosa*, *K. pneumoniae*, and *A. baumannii.*

1.2. Human bacterial infections

The rapid emergence of infectious diseases is a global health crisis that continues to negatively affect millions of humans, animals, plants, and the environment. Infectious diseases (IDs) are caused by bacteria, viruses, fungi, and parasites. Approximately 17 million people have been killed by IDs worldwide with bacterial infections being the leading cause of mortalities in children, the elderly and, immunocompromised individuals (Cano *et al.*, 2020; Patil and Chandrasekaran, 2020; Yeh *et al.*, 2020; Zhang *et al.*, 2020b). Pathogenic bacteria on the surface of the organism or inside the organism is the causative agent of bacterial infections, which leads to the dysfunction or death of cells, tissues, and organs by the production of toxins or other metabolic substances (Hu *et al.*, 2020). Bacteria are the oldest forms of life tracing back to over 3.5 billion years ago (Mubeen *et al.*, 2021). Bacteria were also the first living organisms found on Earth and have adapted over time (Sánchez-López *et al.*, 2020).

Human bacterial infections represent a serious public health risk. The most severe bacterial infections are tuberculosis, diarrhoea, meningitis, pneumonia, sexually transmitted diseases, and nosocomial infections (Cano *et al.*, 2020). Bacterial infections are of great concern as 5-15% of admitted hospital patients will be affected one or more infections (Urzedo *et al.*, 2020). Even though the human body lives with its own microbiota in an advantageous symbiosis, several pathogenic bacterial strains can infect and colonize the human body resulting in serious diseases (Cano *et al.*, 2020). Transmission of bacteria to humans can occur through food, water, air, or living vectors. Bacteria may infect any organ in the human body; however, each bacterial species has a predilection for a particular organ. Moreover, certain organs are generally more susceptible to being infected by bacteria (**Figure 1.1**) (Cano *et al.*, 2020).

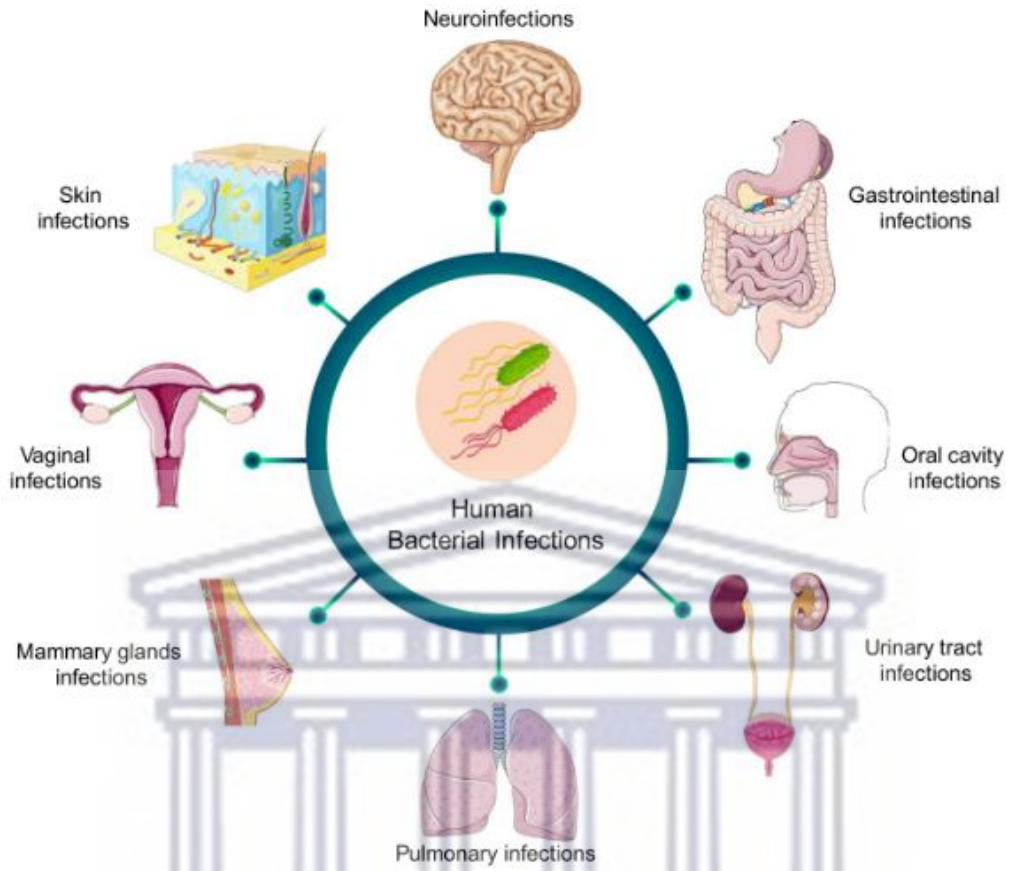

Figure 1.1: A schematic diagram displaying the organs which are more susceptible to being infected by bacteria (Adapted from Cano *et al.*, 2020).

The WHO report also highlighted that sepsis is commonly caused by nosocomial infections. Approximately 49% of intensive care unit patients with sepsis acquired the infection during their hospitalization. It was estimated that roughly 27% of sepsis patients hospitalized and 42% of people in intensive care units will die due to the complications associated with the illness (World Health Organization, 2020). However, survivors of sepsis are not out of danger as half of them will either die within one year or be left with the burden of long-term disabilities (World Health Organization, 2020).

Bacterial infections increase medical costs and place immense pressure on healthcare systems due to long stays in hospitals, treatment failures, the persistence of infections, and delayed healing of wounds often leading to amputation and increased mortality (Kalantari *et al.*, 2020). The high susceptibility of wounds to microbial infection exacerbates the public health concern of antibiotic-resistant infections and is the main reason for death relating to burns and diabetic wounds

(Kalantari *et al.*, 2020). Burns are most susceptible to infections, severe sepsis, and multiple organ failure due to the loss of the innate barrier constituted by the skin layer and a weakened immune system caused by a systemic inflammatory response triggered by the damaged skin tissue. Increases in the length of hospitalization and invasive medical procedures used in the treatment of wounds and diagnosis of bacterial infections put wound patients at high risk of developing nosocomial infections (Mulder *et al.*, 2022; Moins-Teisserenc *et al.*, 2021; Azimi *et al.*, 2011). Moreover, diabetic wounds usually do not heal quickly due to hyperglycaemia (i.e., high glucose levels in the blood) which causes dysfunction of the immune system resulting in the body's inability to repair itself (Rodríguez-Rodríguez *et al.*, 2022; Spampinato *et al.*, 2020). Both the innate and adaptive immune systems are disrupted by hyperglycaemia making diabetic patients more prone to developing infections (Rodríguez-Rodríguez *et al.*, 2022). Other complications associated with diabetes mellitus (DM), such as peripheral nerve damage and poor blood circulation, also play a role in the delayed healing of wounds and increase their susceptibility to infection (Spampinato *et al.*, 2020). Due to the complications associated with DM, diabetics have a 15-25% risk of developing diabetic foot ulcers (DFUs) in their lifetime. Severe DFUs can lead to osteomyelitis which may develop in 20% of diabetic foot infections. Patients with DFUs often require hospitalization, long-term antibiotic therapy, and surgical intervention with amputation of the body part where the infection is localized (Spampinato *et al.*, 2020; Geraghty and Laporta, 2019).

1.2.1 Antimicrobial resistance (AMR)

Another increasing threat to global health is the emergence of antimicrobial resistance (AMR) along with a reduced drug discovery rate of novel antibiotics (Azeltine *et al.*, 2020; Boateng and Catanzano, 2020). The discovery of antibiotics to treat infectious diseases had a remarkable impact on human and animal health (Kumar *et al.*, 2021a). The first treatment for an ID was Salvarsan which was capable of curing syphilis without any toxicity to humans. However, it was the accidental discovery of penicillin in 1928 by Alexander Fleming that truly sparked the dawn of the antibiotics research era (Sánchez-López *et al.*, 2020). Penicillin has been coined as the wonder drug as it has played a key role in the tremendous development of modern medicine (Mulani *et al.*, 2019). Research of antibiotics reached its peak between the 1950s and 1960s, a period commonly referred to as the "golden age" (Sánchez-López *et al.*, 2020). Since the beginning of the 1990s, the rate of discovery, development, and commercialization of novel antibiotics has been reduced. Only

11 new antibacterial agents were approved by the U.S. Food and Drug Administration (FDA) between 2017 and 2019 (De Oliveira *et al.*, 2020).

In 2013, the WHO declared that a tipping point has been reached for the global community, where we find ourselves entering a "post-antibiotic era" (Hu *et al.*, 2020). According to the U.S. CDC, AMR is a naturally occurring process that occurs when microorganisms "develop the ability to defeat the drugs that are designed to kill them" (Centers for Disease Control and Prevention, 2022a). AMR is caused by evolutionary processes happening during antibiotic treatment such as spontaneous modifications in the genetic material of bacteria (e.g., genetic mutation and horizontal gene transfer through chromosomes, plasmids, transposons, and other mobile genetic elements) and the development of molecular mechanisms that prevent the action of the antimicrobial agents. Resistant bacteria survive and pass this trait to future generations. AMR is found in both gram-positive and gram-negative bacteria (Bhatia *et al.*, 2021; Urzedo *et al.*, 2020; Konop *et al.*, 2016).

The CDC and WHO have classified pathogens that have developed AMR as an imminent threat to human health (De Oliveira *et al.*, 2020). AMR has been declared by the WHO as "one of the top 10 global public threats facing humanity" and is generally regarded by all stakeholders as a 'One Health' issue because humans, animals, plants, and the environment are all impacted by it (Velazquez-Meza *et al.*, 2022; Krishna *et al.*, 2021). The findings of a comprehensive study undertaken to investigate the global burden of AMR in 2019 were recently published in The Lancet and revealed that 4.95 million deaths were linked to bacterial AMR with more than a quarter of the total deaths (1.27 million) being directly caused by AMR. It was also reported that Sub-Saharan Africa had the highest death rate caused by antibiotic-resistant infections globally (27.3 deaths per 100 000) with Australasia having the lowest death rate (6.5 deaths per 100 000). An estimated 1.5 million deaths were attributable to lower respiratory infections associated with AMR making it the most burdensome infection (Murray *et al.*, 2022). Projections by the CDC indicate that more deaths will be attributed to AMR (10 million/year) than all types of cancers (8.2 million/year) by 2050 (Hu *et al.*, 2020; Kalantari *et al.*, 2020).

According to the WHO, the number of mortalities caused by AMR worldwide rose from 50 000 in 2010 to 700 000 in 2019 (Hu *et al.*, 2020). It has also been projected that death as a direct result of antibiotic-resistant infections will cost the global economy an estimated US$100 trillion by 2050 (Cano *et al.*, 2020). In the USA, more than 2 million infections are linked to AMR with a

death toll of 29 000 occurring each year, associated with a healthcare cost of approximately US$4.7 billion (De Oliveira *et al.*, 2020; Centers for Disease Control and Prevention, 2019). In Europe, over 33 000 deaths are linked to AMR infections accounting for US$1.5 billion in direct and indirect costs (De Oliveira *et al.*, 2020). It is evident that the cost of AMR to the economy is substantial. There are many financial challenges faced by patients as their productivity or their caretaker's productivity is affected by the persistent illness as it often results in prolonged hospitalization and requirements for more expensive medication and intensive care (World Health Organization, 2021).

AMR organisms are microscopic creatures that can be found almost everywhere around the environment, for example, in people, animals, plants, food, water, soil, and air. The transmission of AMR organisms can occur between two people or between people and animals (Mubeen *et al.*, 2021; World Health Organization, 2021). The main reason for the rise in AMR to drugs and the failure of available antimicrobial agents to treat infections is the overprescribing and/ or indiscriminate use of antibiotics (Khémiri *et al.*, 2019). Even though AMR occurs naturally in the environment over time, usually through genetic changes, the misuse of antibiotics has resulted in the selection for the presence of AMR genes which boosts the prevalence of AMR (World Health Organization, 2021; De Oliveira *et al.*, 2020). In the USA, over 47 million antibiotic courses are prescribed annually for infections that do not require antibiotic treatment (Centers for Disease Control and Prevention, 2022b). According to the CDC, the global COVID-19 pandemic aggravated the spread of AMR. During the first year of the pandemic, nosocomial infections and deaths linked to AMR both increased by approximately 15%. Moreover, there was an escalation in the abuse and misuse of antibiotics as an increase in patients being hospitalized led to an increase in antibiotics usage. Upon admission, antibiotics were administered to patients to treat any secondary infections of bacterial origin even though there was no clear diagnosis of coinfections. Recent studies have shown that many COVID-19 patients did not need antibiotics because coinfections were uncommon in patients at the time of admission with only 3-14% of patients having an early bacterial coinfection or superinfection (Moolla *et al.*, 2021). Late nosocomial infections (roughly two days after admission) were more prevalent than early community-acquired infections and were linked to intubation, length of hospitalization, and mortality (Kumar *et al.*, 2021a). There was no benefit to the early administration of antibiotics strategy, however, the risks associated with the incorrect use of antibiotics are well documented. The early administration of

antibiotic therapy should be avoided while strategies to prevent coinfections and outbreaks in hospitals should be adhered to (Moolla *et al.*, 2021).

Along with the persistent misuse of antibiotics, self-medication, and exposure to infections in hospital settings has exacerbated the emergence of MDR bacteria which is responsible for 15.5% of hospital-acquired infections globally (Kumar *et al.*, 2021a; Mulani *et al.*, 2019). Moreover, it has also been reported that the increasing prevalence of infectious diseases; poor public health conditions, lack of access to clean water, sanitation, and hygiene for humans and animals; poor access to quality, affordable medication, vaccines, and diagnostics; inadequate prevention and control of infection and disease in the healthcare and agricultural sectors; lack of awareness and knowledge about MDR bacteria and the consequences of overuse of antibiotics: and lack of enforcement of legislation helps towards the spread of AMR (Kumar *et al.*, 2021a; World Health Organization, 2021).

1.2.1.1 ESKAPE pathogens

For a long period of time, antibiotic resistance was overlooked, and it was the detection of bacteria carrying extended spectrum b-lactamases (ESBL) imparting resistance to penicillins and cephalosporins, extensively drug-resistant (XDR) *Mycobacterium tuberculosis*, and MDR *Acinetobacter baumannii*, Enterobacteriaceae, *Neisseria gonorrhoeae*, and *Pseudomonas aeruginosa* that caught the attention of the global scientific community (Kumar *et al.*, 2021a). In 2017, the WHO made it a precedence to focus on the research, discovery, and development of new and effective antibiotics and published a global priority list of pathogens for which new antibacterial development is required with urgency (Pinto *et al.*, 2020; Tacconelli, 2017). The list consists of 12 different bacterial species which have been categorized into three groups according to their level of resistance, namely critical, high, and medium. The critical species are *A. baumannii* and *P. aeruginosa*, which are both carbapenem-resistant, and Enterobacteriaceae (including *K. pneumoniae, E. coli, Enterobacter spp., Serratia spp., Proteus spp.*, and *Providencia spp., Morganella spp.*) which are resistant to carbapenem and third generation cephalosporin (Pinto *et al.*, 2020). In the broad list of pathogens, ESKAPE pathogens also known as "superbugs" were designated "priority status." ESKAPE is an acronym representing the following microorganisms: *Enterococcus faecium, Staphylococcus aureus, Klebsiella pneumoniae, Acinetobacter baumannii, Pseudomonas aeruginosa*, and *Enterobacter* species (Bhatia *et al.*, 2021; De Oliveira *et al.*, 2020;

Pinto *et al.*, 2020; Tacconelli, 2017). A schematic diagram of the ESKAPE pathogens and their morphological characteristics is displayed in **Figure 1.2** (Sinclair, 2016). These six pathogens have growing MDR and virulence, are responsible for most nosocomial infections, and can "escape" the killing action of antibacterial agents. Curiously, this acronym also references the ability of these microorganisms to escape the effects of commonly used antibiotics through evolutionarily developed mechanisms (Mulani *et al.*, 2019). ESKAPE pathogens are associated with the highest risk of mortality and morbidity leading to greater economic costs across the world, particularly in low- and middle-income countries (LMICs) (Kumar *et al.*, 2021a; Mulani *et al.*, 2019; Founou *et al.*, 2017).

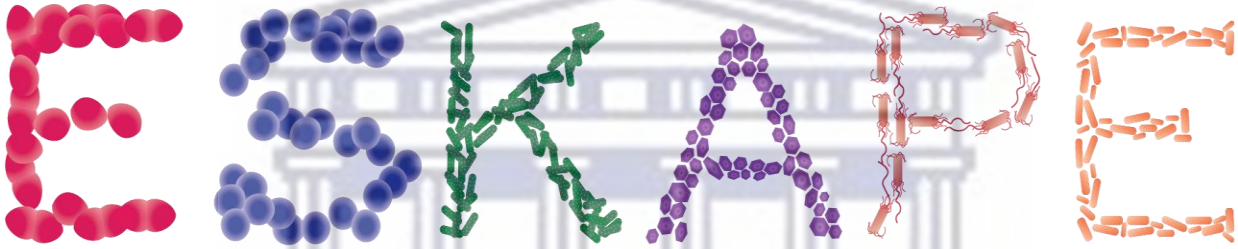

Figure 1.2: Schematic diagram depicting the ESKAPE pathogens and their morphological characteristics (Adapted from Sinclair, 2016).

ESKAPE pathogens have been able to develop resistance mechanisms due to genetic mutations and the acquisition of mobile genetic elements. Some of the antibiotics that ESKAPE pathogens have resistance against include oxazolidinones, lipopeptides, macrolides, fluoroquinolones, tetracyclines, β-lactams, β-lactam-β-lactamase inhibitor combinations, and last line of defence antibiotics, such as carbapenems, glycopeptides, and clinically unfavourable polymyxins (De Oliveira *et al.*, 2020). Some mechanisms of resistance shown by ESKAPE pathogens are drug inactivation commonly by an irreversible cleavage catalyzed by an enzyme, modification of the target site where the antibiotic may bind, reduced accumulation of drug either due to reduced permeability or by increased efflux of the drug, and the development of new cell processes that avoid using the target of the antibiotic (**Figure 1.3**) (Centers for Disease Control and Prevention, 2022d; Santajit and Indrawattana, 2016).

The defence strategies used by bacteria and fungi to resist the effects of antibiotics or antifungals are summarized in **Table 1.1** (Centers for Disease Control and Prevention, 2022c). ESKAPE

pathogens also form biofilms that physically prevent the host immune response cells and antibiotics from inhibiting the pathogen. Biofilms are characterized by an enclosed environment that has been created by microbial cells attaching to each other and producing an extracellular polymeric substance (EPS) that forms a protective matrix (Wilkinson and Hardman, 2020; Zhang *et al.*, 2020b; Mihai *et al.*, 2019). It is a significant mechanism of virulence used in the pathogenesis of many medically important bacterial pathogens (Skóra *et al.*, 2021). Additionally, biofilms cause persistent infection and aggravate the occurrence of AMR as they can protect persister cells, which are specialized dormant cells that are tolerant to antibiotics, causing recalcitrant infections that are difficult to treat (Zhang *et al.*, 2020b; Mulani *et al.*, 2019). All the bacteria listed in the WHO list exhibit biofilm formation (Pinto *et al.*, 2020).

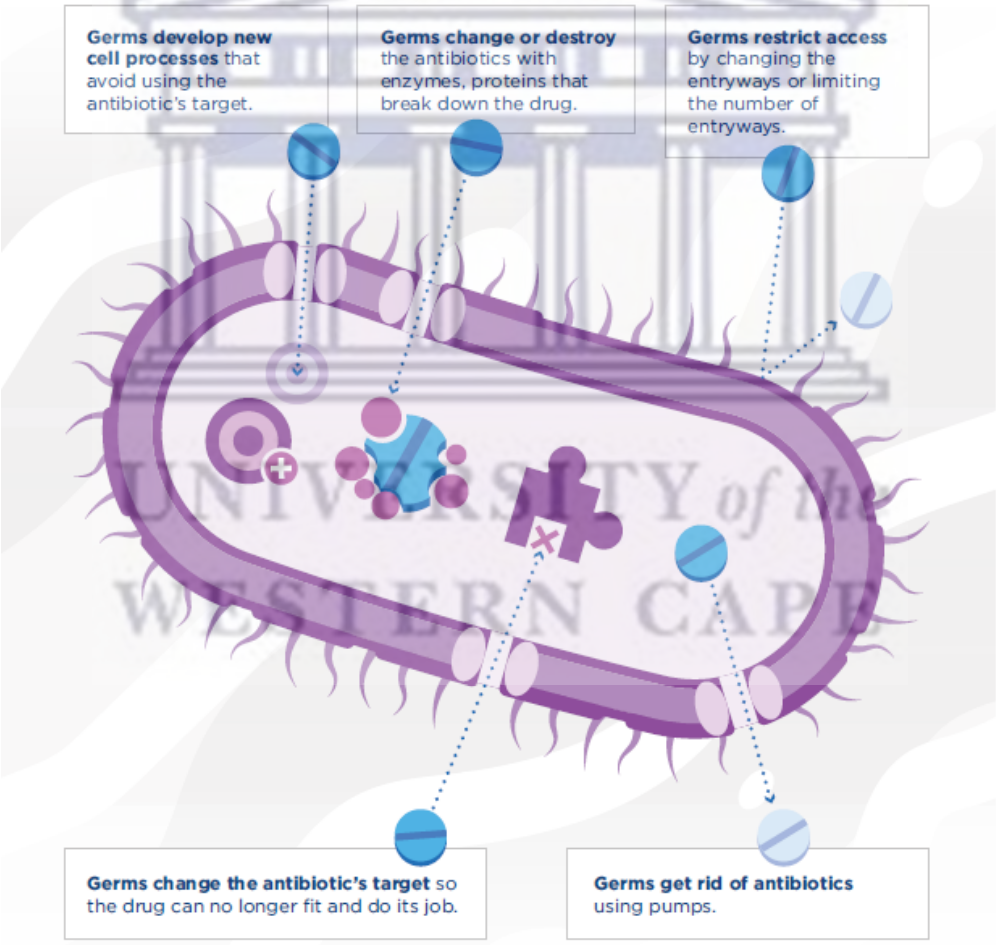

Figure 1.3: Various mechanisms of antibacterial resistance (Adapted from Centers for Disease Control and Prevention, 2022c).

Table 1.1: Defence strategies used by bacteria and fungi to resist the effects of antibacterial agents (Adapted from Centers for Disease Control and Prevention, 2022c)

Resistance Mechanisms	Description
Restrict access of the antibiotic	**Germs restrict access by changing the entryways or limiting the number of entryways.** Gram-negative bacteria have an outer layer (membrane) that protects them from their environment. These bacteria can use this membrane to selectively keep antibiotic drugs from entering.
Get rid of the antibiotic or antifungal	**Germs get rid of antibiotics using pumps in their cell walls to remove antibiotic drugs that enter the cell.** Some *P. aeruginosa* bacteria can produce pumps to get rid of several different important antibiotic drugs, including fluoroquinolones, β-lactams, chloramphenicol, and trimethoprim.
Change or destroy the antibiotic	**Germs change or destroy the antibiotics with enzymes, and proteins that break down the drug.** *K. pneumoniae* bacteria produce enzymes called carbapenemases, which break down carbapenem drugs and most other β-lactam drugs.
Change the targets for the antibiotic or antifungal	**Many antibiotic drugs are designed to single out and destroy specific parts (or targets) of a bacterium. Germs change the antibiotic's target so the drug can no longer fit and do its job.** *E. coli* bacteria with the *mcr*-1 gene can add a compound to the outside of the cell wall so that the drug colistin cannot latch onto it.
Bypass the effects of the antibiotic	**Germs develop new cell processes that avoid using the antibiotic's target.** Some *S. aureus* bacteria can bypass the drug effects of trimethoprim.

Even though *E. coli* has not been formally recognized as part of the ESKAPE pathogens group, AMR *E. coli* has been identified as a major cause of bloodstream and urinary tract infection (UTI) in both community and nosocomial settings across the globe, with *E. coli* UTI frequently manifesting into sepsis. *E. coli* typically acquire resistance genes from members of the Enterobacterales family through horizontal gene transfer. It is the most prevalent gram-negative bacterial species isolated from both blood and urine samples in Australia (De Oliveira *et al.*, 2020). *E. coli* is a common causative agent of infections in surgical wounds, particularly abdominal operations where it is often found mixed with other gut bacteria. However, it can also be found in other postoperative sites. It was previously reported that 46%, 25%, and 21% of *E. coli* isolates from wound infections were resistant to ampicillin, tetracycline, and fluoroquinolones, respectively (Alharbi *et al.*, 2019). According to the WHO, *E. coli* resistance to fluoroquinolone antibiotics is widespread. Fluoroquinolone antibiotics are used for the treatment of UTIs, and many countries have reported that this treatment has become ineffective for more than half of patients suffering from UTIs caused by *E. coli* (World Health Organization, 2021). AMR *E. coli* is presently a major clinical burden negatively impacting both human and animal health. In order not to worsen these challenges further, this pathogen needs to be classified as a critical public health concern (De Oliveira *et al.*, 2020).

Recently, several infections that were under control are now reappearing and new infectious diseases are emerging. An increase in pathogens, such as *S. aureus*, *Enterococcus*, Enterobacteriaceae, and *Candida albicans* has been reported across the globe (Khémiri *et al.*, 2019). In 2019, *E. coli, S. aureus, K. pneumoniae, Streptococcus pneumoniae, A. baumannii,* and *P. aeruginosa*, in that particular order, were the leading cause of death with an astonishing estimate of 3.57 million people dying of AMR associated with these pathogens (Murray *et al.*, 2022). MRSA caused more than 100 000 deaths with MDR bacteria excluding XDR tuberculosis, third-generation cephalosporin-resistant *E. coli*, carbapenem-resistant *A. baumannii*, fluoroquinolone-resistant *E. coli*, carbapenem-resistant *K. pneumoniae*, and third-generation cephalosporin-resistant *K. pneumoniae* each causing 50 000-100 000 deaths (Murray *et al.*, 2022). Hospital-acquired infections are among the deadliest of these AMR infections and new and improved treatments are urgently required (Murray *et al.*, 2022).

It is crucial to gather information about the current magnitude of the burden of AMR, various AMR trends in different geographical locations, and the leading pathogen-drug combinations that contribute to AMR. If the burden of AMR is not addressed, many organisms that pose no serious risk at present may become more lethal in the future through the spread of AMR (Murray *et al.*, 2022). Although AMR affects all people across the globe, the largest threat to human health is posed in LMICs located in Sub-Saharan Africa and south Asia (Murray *et al.*, 2022).

1.2.1.2 AMR: South African Perspective

In SA, there is an increasing burden of IDs mainly of bacterial origin. In a surveillance report by the National Department of Health Republic of South Africa (NDoH-RSA), the most recent available information pertaining to AMR and antimicrobial use (AMU) compiled using data from the National Health Laboratory Service (NHLS) highlighted the burden of ESKAPE bacteria causing bloodstream infections (BSIs) in the public sector (NDoH-RSA, 2022). The total number of blood culture samples tested was 3 610 401, 3 698 756 and 3 805 186 for 2018, 2019, and 2020, respectively (NDoH-RSA, 2022). The increase in the total number of blood culture samples tested indicated a rise in the prevalence of BSIs. Moreover, the percentage of ESKAPE organisms identified from all positive blood culture samples was in the range of 40-41% between 2018 and 2020 (**Figure 1.4**). Interestingly, a previous report by the NDoH-RSA stated that ESKAPE organisms accounted for 33% (n = 22 788) of all positive cultures of blood samples sent to the NHLS from the public sector in 2017 (Chetty, 2021).

Between 2018 and 2020, the most common pathogens isolated from blood cultures from the public sector were *K. pneumoniae* and *S. aureus*, followed by *E. coli* and *A. baumannii* (**Figure 1.5**). For both the public and private sectors, *K. pneumoniae* was the most common organism isolated followed by *S. aureus*, *E. coli*, *P. aeruginosa*, and *A. baumannii* (NDoH-RSA, 2022). Over the past five years, the prevalence of AMR has increased in all ESKAPE organisms cultured by the NHLS, however, AMR in MRSA has shown an unexpected decline from 23% to 18% (NDoH-RSA, 2022).

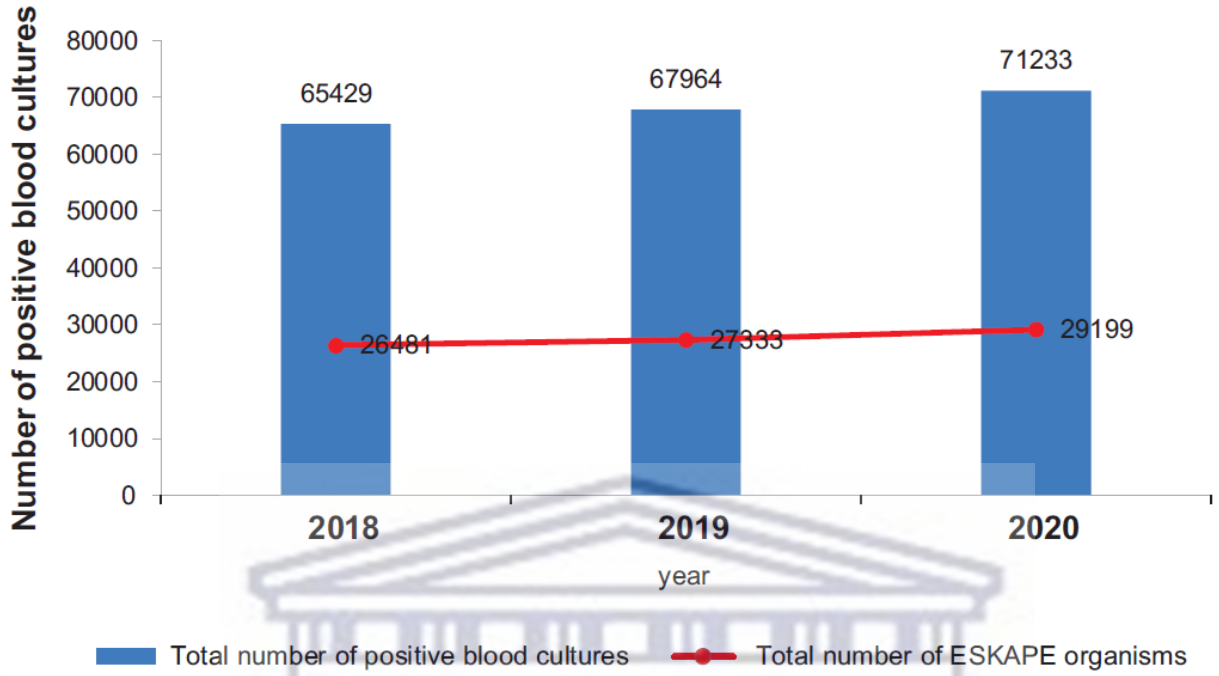

Figure 1.4: Graph displaying the burden of ESKAPE pathogens in the public sector for the period of 2018 to 2020 (Adapted from NDoH-RSA, 2022).

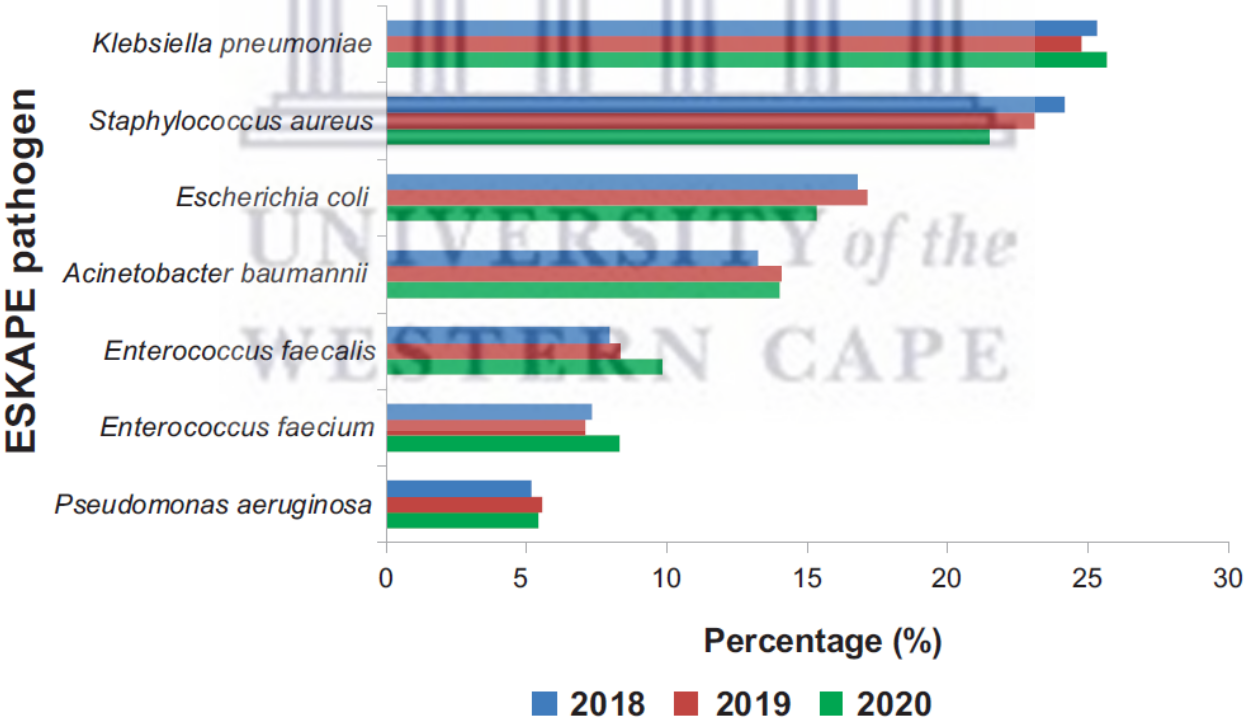

Figure 1.5: Graph displaying the percentage breakdown of ESKAPE pathogens in the public sector for the period of 2018 to 2020 (Adapted from NDoH-RSA, 2022).

Several factors have led to the spread of AMR across the globe, but the abuse of antibiotics is rife in SA where there is an obvious lack of awareness and knowledge regarding AMU. In the most current report on global human AMU compiled in 2015, it was reported that SA's AMU was 9 177 DDD per 1000/population (**Table 1.2**) (NDoH-RSA, 2022). The AMU in SA was alarmingly greater than the AMU in other BRICS countries but lower than what was seen in higher-income countries (HICs) such as USA and Australia (**Figure 1.6**). Broad-spectrum antibiotics are 1.3–3.3 times more likely to be used in SA than in other BRICS countries. SA has 0.8 times higher broad-spectrum AMU than the United Kingdom (UK) or the USA (Chetty, 2021). The real issue is that if the burden of AMR is not urgently addressed in time, it will lead us back to the pre-antibiotic era, where the common cold and minor cuts could be fatal. A potentially gloomy future awaits us, where patients may die of untreatable bacterial infections, which were previously easily managed. Therefore, novel strategies are necessary to tackle the problem of AMR (Hu *et al.*, 2020).

Table 1.2: Global human AMU in SA compared to global levels (Adapted from NDoH-RSA, 2022).

Country	AMU (Defined Daily Dose (DDD) per 1000/population)
South Africa	9 177
Brazil	6 763
Russia	6069
India	4 950
China	3 060
USA	10 298
Canada	7 078
Australia	11 088

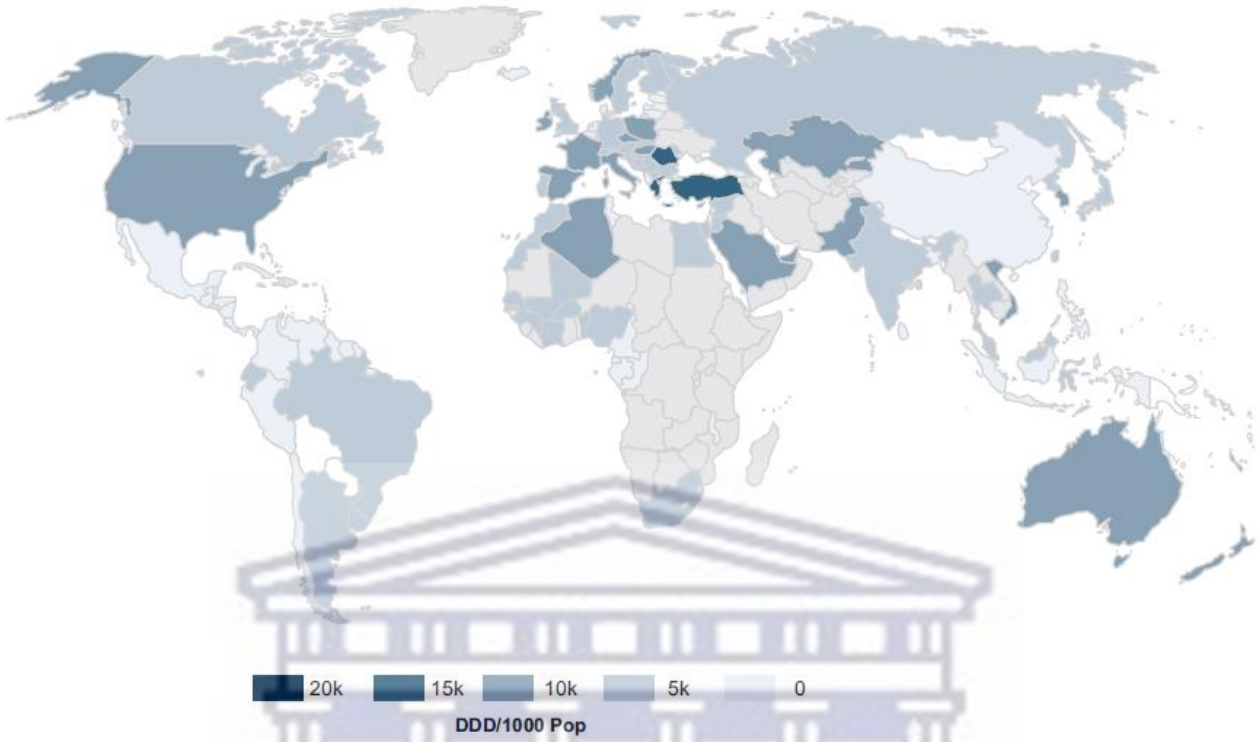

Figure 1.6: Diagram displaying the global human AMU (Adapted from NDoH-RSA, 2022).

1.2.2 Current available treatment to treat AMR infections and their limitations

The current conventional therapy available for bacterial infections and their biofilms is antibiotic therapy. The discovery of antibiotics was undeniably one of the most remarkable breakthroughs for modern medicine, however, the conventional use of antibiotics for the treatment of bacterial infections exhibits some limitations that cannot be ignored any longer. Limitations of available antibiotic therapy include the well-described development of bacterial drug resistance, low bioavailability, narrow antibacterial spectrum, limited infusion to the infection nidus, expensive cost, and major side effects such as nausea, abdominal cramps, and destruction of the normal gut microbiota (Patil and Chandrasekaran, 2020; Yeh *et al.*, 2020; Zhang *et al.*, 2020b; Pizzolato-Cezar *et al.*, 2019; Yang and Yang, 2019).

Conventional therapeutic strategies are often limited due to antibiotic drugs often accumulating intracellularly, being transported out of the bacterial cells (drug efflux) using efflux pumps, and being degraded by bacterial enzymes (e.g., proteases) (Selvarajan *et al.*, 2020; Zhang *et al.*, 2020b). Moreover, when antibiotics are administered to a patient that does not need it, there is no benefit for the patient and they are put at risk for side effects, such as allergic reactions, toxicity resulting

in organ dysfunction, and the potential development of other serious illnesses. Studies have shown that 20% of patients who receive antibiotic treatment have an adverse reaction (Centers for Disease Control and Prevention, 2022c; Patil and Chandrasekaran, 2020). Merchant *et al.* (2018) reported that the use of fluoroquinolones is linked to the development of fluoroquinolone-associated disability (FQAD). The side effects of this antibiotic include damage to muscles and tendons, neuropsychiatric disorders, and mitochondrial toxicity, therefore, extreme caution should be practiced when using this antibiotic as only severe infections should be treated with it (Kumar *et al.*, 2021a; Merchant *et al.*, 2018). Some clinicians administer high dosages of antibiotics and/or increase the frequency of dosages to improve the efficacy of antibiotic treatment, however, this is detrimental as it exacerbates the side effects and toxicity of antibiotic use and leads to the continued development and spread of AMR (Hu *et al.*, 2020; Nilashi *et al.*, 2020).

The overuse of antibiotics may also lead to the overgrowth of the gut bacterium, *Clostridium difficile*, causing *C. difficile* infection (CDI) due to the destruction of the normal gut microbiota which usually provides protection along with the intestinal immune system (Yang and Yang, 2019). A study by Palleja and colleagues showed that the disrupted gut microbiota of half of the healthy participants who were administered a four-day antibiotic (meropenem, gentamicin, and vancomycin) returned to normal after six months but a few microbial species disappeared permanently. This finding indicated that although antibiotics are able to cure infection, they are also able to cause permanent damage to beneficial microorganisms which are usually found in the gut (Yang and Yang, 2019; Palleja *et al.*, 2018).

Certain antibiotic therapies are also inadequate for the safe and effective treatment of biofilms (Zhang *et al.*, 2020b). Infections caused by biofilms usually require highly penetrating antibiotics in high doses to ensure that a sufficient concentration of antibiotics reaches the site of infection, however, with the rise in bacterial resistance to antibiotics, the efficacy of antibiotics has diminished (Zhang *et al.*, 2020b). Studies have shown that combined antibiotic use has better outcomes compared to single antibiotic use. Moreover, the efficacy of antibiotics may be improved when combined with other medicines (Zhang *et al.*, 2020b). Despite the risks involved with antibiotic therapy, it remains the current gold standard practice and it cannot be denied that antibiotics are still effective in most bacterial infection cases at present (Tache *et al.*, 2022; Agarwal *et al.*, 2021; Hu *et al.*, 2020). The proper use of antibiotics such as rational control and

reduction of antibiotic dosages is essential to decrease the harmful impact of AMR and impede AMR development (Hu *et al.*, 2020). Newly developed antibiotics on the market such as ozenoxacin, ceftobiprole, dalbavancin, telavancin, ceftaroline, besifloxacin, tedizolid, omadacycline, oritavancin and delafloxacin are effective against MDR gram-positive bacteria, however, AMR may be developed against them as well. Therefore, the use of non-antibiotic therapies should rather be focused on (Kumar *et al.*, 2021a; Koulenti *et al.*, 2019).

The current alternative non-traditional therapy available for bacterial infections and their biofilms is non-antibiotic therapy. The discovery and development of alternative non-antibiotic therapies that are safe for humans, livestock, and the environment, and effective against AMR infections is important (Kumar *et al.*, 2021a). Non-antibiotic therapeutic strategies include chemical modification of antibiotics, antimicrobial peptides or bacteriocins, bacteriophage therapy, antimicrobial adjuvants, fecal microbiota transplant and competitive exclusion of pathogens through genetically modified probiotics and postbiotics, phototherapy, cationic polymers, nanomaterials and combinational therapy have been used in the fight against antibiotic resistance (Ye and Chen, 2023; Hu *et al.*, 2020; Yeh *et al.*, 2020; Gebreyohannes *et al.*, 2019). Other non-traditional conventional therapies include quorum sensing (QS) system inhibitors, monoclonal antibodies, immunomodulators, microbiome-based therapy, antibiotic potentiators, and antisense nucleic acid approaches (Tache *et al.*, 2022; Hu *et al.*, 2020; Zhang *et al.*, 2020b). Bacteriophages, mutant and bioengineered lytic phages and lytic endolysins alone or in combined use with antibiotics should be considered. Probiotics and phages are able to modify the microbiome to defend against AMR pathogens (Kumar *et al.*, 2021a). Moreover, another alternative strategy that has been under extensive research is the enhancement of antibiotic therapy using various approaches such as increased drug penetration into biofilms, physical destruction of biofilm's EPS, enzymatic degradation of EPS, suppression of QS, and destruction of specific structures of the organism itself (Hu *et al.*, 2020).

Silver products, such as silver nitrate and silver sulfadiazine, have also been extensively used for the treatment of bacterial infections, especially those found in chronic wounds (Mihai *et al.*, 2019). Humankind has been utilizing metals, such as silver and copper, for ages because they exhibited antimicrobial properties (Dawadi *et al.*, 2021). The release of silver ions displays a potent antibacterial effect making these silver products advantageous for application in AMR infections.

The lysis of bacterial cells is caused by silver ions binding to thiol groups of peptidoglycans (Niska *et al.*, 2018). Additionally, silver ions block the respiratory enzyme pathways which lead to the alteration of microbial DNA. Furthermore, silver compounds are efficacious MDR bacteria and bacterial biofilms. On the other hand, tissue toxicity is a concern when making use of silver-derived products (Mihai *et al.*, 2019). Moreover, natural medicines, such as plant-based remedies and herbal therapy, have also been used in the treatment of bacterial infections particularly in combination with antibiotics and other conventional therapies to work in a synergistic manner. Plant-based therapeutics possess antimicrobial and antibiofilm properties and can reduce the symptoms associated with infections as they also possess anti-inflammatory, antipyretic, and analgesic effects. Plant-based remedies used as an alternative to antibiotics are cost-effective, readily available, relatively safe with fewer side effects, and can decrease AMR risks and adverse effects associated with antibiotic use (Tache *et al.*, 2022; Zhang *et al.*, 2020b).

Although, non-antibiotic therapy presents many benefits, they are also associated with limitations which include the possibility of side effects such as nausea, sore throat, abdominal pain, inflammation; the need for prolonged treatment, diagnostic specificity before use and infusion reactions; complicated operation involving complex processes; expensive cost; and many therapies still lack clinical validation (Zhang *et al.*, 2020b; Yang and Yang, 2019). In addition, vaccines are always the first strategy used in the prevention of IDs, however, there are no currently available vaccines against ESKAPE pathogens as those which have been researched thus far have not passed any clinical trials yet (Tache *et al.*, 2022).

Prevention and adequate treatment of AMR infections along with improved accessibility to effective antimicrobials is essential in order to reduce the number of people for whom treatment of AMR infections does not work or who die of AMR infections. Medical procedures requiring surgical measures will become riskier if there are no new interventions to eradicate AMR as postoperative infections will continue to be a cause for concern (World Health Organization, 2021). Measures to improve the use of antibiotics, such as shorter periods of treatment, aligned with the principles of antibiotic stewardship may aid in the preservation of existing antimicrobial agents (Moolla *et al.*, 2021; World Health Organization, 2021). However, existing treatment strategies have not been able to win the fight against AMR infections and are often associated with

many drawbacks, therefore, there is an urgency to develop novel antimicrobial agents to combat bacterial infections and eliminate the burden of AMR.

1.3 Complementary and alternative medicine for AMR infections and its limitations

Complementary and alternative medicine (CAM) refers to any healthcare practice "that does not fall within the realm of conventional medicine." (Monika *et al.*, 2022; Grossman *et al.*, 2018). In certain parts of the world, the terms 'complementary medicine' and 'alternative medicine' are used interchangeably with 'traditional medicine.' The principle of CAM is based on the traditional knowledge of indigenous people and ancient communities that they have been using as healing practices for many years (Monika *et al.*, 2022). Practitioners of "modern" or "western" medicine usually refer to traditional medicine using sceptical terms like "complementary," "alternative," "indigenous," and "non-conventional," when the way "modern" medicine is practiced is not entirely different to the way traditional medicine is practiced (Shedoeva *et al.*, 2019). Before modern or scientifically approved medicine, CAM was the only available option used to treat various diseases and ailments globally (Monika *et al.*, 2022). CAM deals with the use of natural products and/or derivatives of natural products and has relatively good safety profile in comparison to synthetic counterparts (Saka and Chella, 2021; Shedoeva *et al.*, 2019). CAM depends almost exclusively upon natural resources (e.g., plants, animals, minerals, and water). It is widely practiced and valued across the world today with more than half of all available medicines being provided by CAM. A previous study revealed that an estimated 73% of all existing pharmaceuticals included natural product-derived ingredients (Shedoeva *et al.*, 2019). The global herbal remedies market value was estimated at US$62 billion in 2002 which rose to US$131.4 billion in 2018 (Jan *et al.*, 2020). It is anticipated that the herbal drug market will grow to US$5 trillion by 2050 (Nilashi *et al.*, 2020).

The use of natural products such as plant-derived extracts and/or derivatives of natural products has received considerable interest from researchers (Monika *et al.*, 2022). Phytotherapy refers to a form of CAM that makes use of medicinal plants to treat various illnesses and chronic diseases. Approximately 50,000 – 80,000 plant species are utilized for healthcare practices worldwide as reported by the International Union for Conservation of Nature and the World Wildlife Fund (Anand *et al.*, 2017; Chen *et al.*, 2016). Herbal medicines are an important part of therapy in naturopathy and Ayurveda practices (Monika *et al.*, 2022). Medicinally important plant materials

and the herbal medicines derived from them form a significant part of the international medicinal market (Sharma *et al.*, 2021). Herbal remedies are made up of any part of the plant, herbs, mixtures of herbal extracts and materials (i.e., tinctures), and purified herbal products that include an active ingredient called phytochemicals. Phytochemicals are complex and structurally diverse compounds that are naturally bioactive and, thus, have the potential to aid in the eradication of AMR pathogens. The use of medicinal plants is useful in the fight against infections (Monika *et al.*, 2022; Sharma *et al.*, 2021; Chouhan *et al.*, 2017).

Throughout the history of humankind, phytotherapy has been used to cure diseases. For over 5000 years, ancient kingdoms such as the Egyptians and Romans, and indigenous people of Africa, Asia, and the Americas, have used phytotherapy as first-line therapy. At present, there has been an increase in the use of phytotherapy for the management and treatment of various diseases (Zhong *et al.*, 2022). According to the WHO, approximately 80% of the patient population across the world relies on CAM for the treatment of several diseases (Bhatia *et al.*, 2021). In the USA, 70% of the population have used CAM at least once costing $34 billion annually (Nilashi *et al.*, 2020). It has been proven that certain plants have medicinal properties that are beneficial in the treatment of various diseases (Zhong *et al.*, 2022). Sharma and colleagues extensively reviewed a variety of medicinal plants that were found to be effective in the treatment of a variety of illnesses (Sharma *et al.*, 2021). Turmeric (*Curcuma longa* (L.)), Centella (*Centella asiatica*), Aloe (*Aloe vera*), Bay (*Wedelia trilobata*), Neem (*Azadirachta indica*) and Ginseng (*Panax ginseng*) are some medicinal plants which can be used to treat and cure illnesses such as skin infections, inflammation, wounds, ulcers, leprosy, scabies, and venereal disease (Sharma *et al.*, 2021). The use of CAM has also been found to be effective in the treatment of IDs (Nilashi *et al.*, 2020). Moreover, to thwart bacterial resistance to antibiotics, essential oils have commonly been used as alternate non-antibiotic treatment (e.g., incorporation into wound dressings). Essential oils are aromatic oily liquids made up of concentrated extracts (secondary plant metabolites) obtained from plant materials (leaves, buds, fruits, flowers, herbs, twigs, bark, wood, roots, and seeds). Essential oils have significant antiseptic, antibacterial, antiviral, antioxidant, anti-inflammatory, anti-parasitic, antifungal, insecticidal, and regenerative properties. The phospholipid cell membrane of bacteria is destroyed by essential oils leading to the disruption of cellular compartments through the imbalance of pH and cytoplasm outburst. Essential oils may be considered an alternative treatment for AMR infections because they do not cause antimicrobial resistance (Mihai *et al.*, 2019; Chouhan *et al.*,

2017; Orchard and van Vuuren, 2017). A total of 100 plants from 12 countries across Asia, Africa, Europe, North America, and South America that have been proven to show antimicrobial activity against ESKAPE pathogens during the period of 2006–2020 have been tabulated (Bhatia *et al.*, 2021)

Although phytotherapy may be beneficial for the treatment of AMR infections, there are limitations associated with the use of medicinal plant extracts and other naturally derived products (Teoh and Das, 2018). Plant extracts need to be consumed as crude extracts in high quantities to be effective for treatment due to poor oral availability of extracts caused by inadequate solubility and limited permeability. Different plant constituents are naturally pH-sensitive, may degrade in the acidic environment of the gastrointestinal tract, and may be poorly absorbed by the intestine resulting in undesirable outcomes of treatment or even prolonged treatment (Saka and Chella, 2021; Teoh and Das, 2018). In addition, natural compounds may exhibit serious side effects. An anti-fungal antibiotic, amphotericin B, isolated from *Streptomyces nodosus* used to treat meningitis, pneumonia, sepsis and UTIs has exhibited side effects such as anorexia, high fever, dyspnoea, hypotension, chills, cardiac arrhythmias, and damage to major organs (e.g., kidney and liver) (Saka and Chella, 2021).

Additional limitations of phytotherapy are associated with the overharvesting of wild populations of medicinal plants which may lead to increased risks of species extinction and reduction of the diversity among plant species (Jan *et al.*, 2020; Van Wyk and Prinsloo, 2018). However, it is notable to mention that harvesting pressures do not affect all plants of medicinal importance in the same manner. Species rarity (a measure of the extinction risk of plants) can be affected by other factors such as overexploitation, habitat destruction, and deforestation. Overharvesting and habitat destruction of almost 15 000 medicinal plants has resulted in them being at risk of extinction (Jan *et al.*, 2020; Chen *et al.*, 2016). Other challenges associated with CAM include poor access to plant material due to the regulations of different countries which affects the export and import of plant material, the chemical complexity of plant extracts makes it difficult for individual compounds to be isolated as it requires considerable amount of time, resources, and bulk amounts of plant material, and the synergistic pathways of plant-based therapeutic strategies are not fully understood as there are no current technologies developed to elucidate their complete mechanism of synergy (Jan *et al.*, 2020). There is considerable evidence that shows that natural medicines are

favoured over conventional therapeutics for antibacterial antibiofilm therapy, however, there is no effective natural medicine for the elimination of bacterial biofilms. Thus, natural medicines are continuingly being used in conjunction with conventional therapeutics (Zhang *et al.*, 2020b). Moreover, the lack of satisfactory solubility, optimal permeability and stability makes the use of natural compound not a viable source for commercial production (Saka and Chella, 2021). In order to circumvent the limitations associated with the use of phytotherapy in treating AMR infections, novel or improved methods to effectively manage and treat AMR infections are urgently needed.

1.4 Nanotechnology

In recent years, nanotechnology has been considered as the most significant scientific groundbreaking discovery. The introduction of nanotechnology has revolutionized modern medicine through the influence of the global scientific community's efforts to improve human health (Mubeen *et al.*, 2021). The field of nanoscience is interdisciplinary, primarily involving biology, physics, chemistry, computing, material sciences, and engineering (Lozano, 2022), and facilitates the development of novel therapeutic strategies for biomedical and pharmaceutical applications (Parveen *et al.*, 2016). In the 21st century and beyond, many aspects of materials sciences have been transformed since the inception of nanotechnology (Parveen *et al.*, 2016). Nanotechnology refers to the manipulation of particles on an atomic and molecular level for the design, manufacture, and application of new structures, devices, and systems that have size dimensions on the nanometre scale or, in simple terms, nanoscale (Lozano, 2022; Agarwal *et al.*, 2021; Gour and Jain, 2019; Rafique *et al.*, 2017). A schematic representation of the nanoscale is shown in **Figure 1.7**. The word "nano" is derived from the Greek word "dwarf," νᾶννος (nánnos), which means "a billionth." A nanometre is an extremely small unit of measurement, a billionth (10^{-9}) of a meter, which is approximately 10 times the diameter of a hydrogen atom. A single strand of human hair is an estimated 100,000 nm wide (Lozano, 2022; Okkeh *et al.*, 2021; Parveen *et al.*, 2016; Ivanov, 2015).

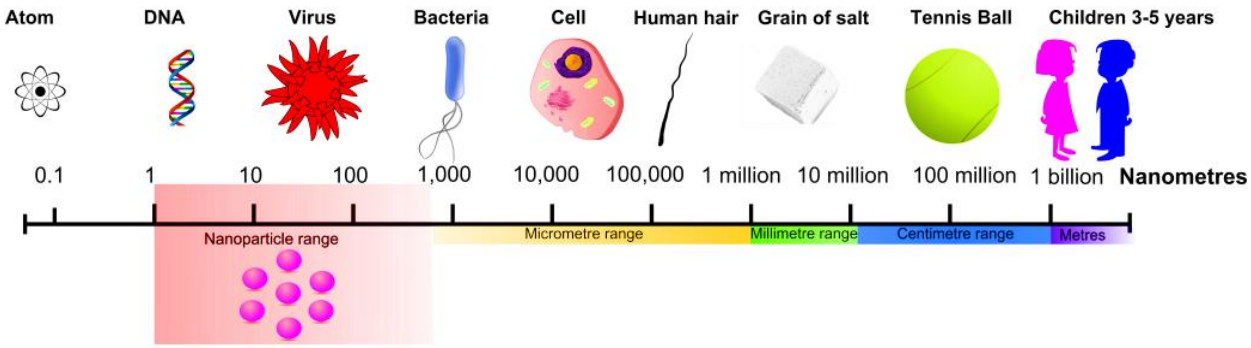

Figure 1.7: Schematic representation of the nanoscale (Adapted from Ivanov, 2015).

Nanomaterials are tiny particles with a range of diameter between 1 and 100 nanometres (nm). At this range, the characteristic properties of these nanomaterials are unique. The physicochemical and structural properties of nanomaterials differ from those of atoms, molecules, and bulk counterparts due to two main factors, namely surface effects, and quantum effects (Joudeh and Linke, 2022; Okkeh *et al.*, 2021; Srikar *et al.*, 2016; Guisbiers *et al.*, 2012). The surface effects of nanomaterials are different compared to the bulk materials owing to the large surface area and high surface area to volume ratio of nanomaterials coupled with an increase in the fraction of atoms at the surface and a decrease in direct neighbours to these atoms at the surface (Joudeh and Linke, 2022). Quantum phenomena are observable in materials with nanoscale dimensions due to the shrinkage in the size of the material. The quantum effects of nanomaterials can directly influence their optical, electrical, thermal, mechanical, magnetic, and catalytic behaviour (Joudeh and Linke, 2022). The properties of nanomaterials (i.e., size, shape, and surface morphology) can impact the intrinsic characteristics of the nanomaterials through the establishment of novel or improved properties (Agarwal *et al.*, 2021; Rafique *et al.*, 2017).

1.4.1 History of nanotechnology

Even though there is evidence that can date the early use of nanotechnology back to ancient times in Egypt, Mesopotamia, India, and the Maya, the birth of nanoscience and nanotechnology concepts is usually associated with the famous lecture of American physicist and Noble Prize laureate, Dr. Richard Feynman from California Institute of Technology in 1959 (Joudeh and Linke, 2022). The visionary lecture titled, "There's plenty of room at the bottom," highlighted the vast possibilities presented by the art of miniaturization and has since become famous as it is believed to have given birth to the concept of nanotechnology long before the term was used. Therefore, Dr. Feynman is commonly referred to as the "father of nanotechnology" (Joudeh and Linke, 2022;

Dawadi *et al.*, 2021; Feynman, 1959). During Dr. Feynman's lecture, he challenged engineers to write all 24 volumes of the Encyclopaedia Britannica on the head of a pin and even mathematically explained how this was possible, however, there was no existing technology at the time that could make it happen. The talk inspired several top-down approaches for the miniaturization of materials (Lozano, 2022). In 1974, Prof. Norio Taniguchi from the Tokyo Science University coined the term, "nanotechnology", when he described it as the manufacturing of nanomaterials with great precision in a paper titled, "On the Basic Concept of 'Nanotechnology", during a scientific conference meeting of the Japan Society of Precision Engineering (Matteucci *et al.*, 2018; Parveen *et al.*, 2016). In 1981, Dr. Kim Eric Drexler, an engineer from the Massachusetts Institute of Technology, wrote a highly ingenious paper in which he proposed the idea of employing a bottom-up approach to build machines where 'molecular assemblers' can be used for the manipulation of individual atoms. Dr. Drexler has been generally regarded to have popularized nanotechnology and founded the field of molecular nanotechnology with the publication of his book titled, "Engines of Creation: The Coming Era of Nanotechnology" in 1986 (Matteucci *et al.*, 2018; Parveen *et al.*, 2016; Drexler, 1981).

The dawn of modern nanotechnology began in 1981 with the invention of the scanning tunnelling microscope which allowed individual atoms to be viewed and manipulated. In 1986, the Nobel Prize in Physics was awarded to International Business Machines (IBM) scientists, Gerd Binnig and Heinrich Rohrer, for their role in the invention of the scanning tunnelling microscope. In 1989, two other IBM scientists, Don Eigler and Erhard Schweizer demonstrated for the first time the wonderful possibilities of nanotechnology and spelled out the acronym "IBM" using only 35 individual atoms of xenon that were rearranged on a substrate of chilled crystal of nickel and it was measured to be three nanometres in length (Lozano, 2022; Picraux, 2022). Over 60 years after Dr. Feynman's visionary talk, nanotechnology has given rise to the field of nanoscience which is an interdisciplinary field that plays a significant role in various scientific fields including chemistry, physics, biology, medicine, computing, materials science, and engineering. The amalgamation of nanoscience and other sciences has given rise to research fields such as nanomedicine and nanobiotechnology which are of particular interest as they have the potential to reshape the world around us by leading to revolutionary breakthroughs in medicine and biotechnology (Picraux, 2022; Dawadi *et al.*, 2021)

Nanomaterials exhibit unique physicochemical properties, such as high surface-area-to-volume ratio and small size, which make them ideal candidates for applications in medical imaging, drug delivery, and disease diagnostics (Okkeh *et al.*, 2021). The most distinctive property of NPs is their large surface-area-to-volume, as an increase in the surface area of NPs leads to an increase in surface energy, and, subsequently, an increase in the biological activity of the NPs. Hence, NPs with smaller sizes and large surface-area-to-volume ratios are more effective even at low concentrations (Geoprincy *et al.*, 2013). The large surface-area-to-volume ratio of NPs also enables a large number of high-affinity ligands to bind, arming NPs with a multivalency in eradicating bacterial cells (Okkeh *et al.*, 2021). The advantages of nanotechnology have been proven particularly within the biomedical and pharmaceutical fields. As the field of nanotechnology continues to advance and more research into the manipulation of structural properties of NPs is conducted, newer NPs with vastly unique characteristics will be developed, the efficacy of already existing NPs will be enhanced, and the potential of nanotechnology to be applied in various fields will be increased (Bhardwaj *et al.*, 2020; Srikar *et al.*, 2016).

1.4.2 Classification of nanoparticles

Nanomaterials may be classified into a variety of classes depending on the type of material(s) used for their synthesis. They may also be classified according to their size, morphology, and physical and/or chemical characteristics (Lozano, 2022; Dawadi *et al.*, 2021; Khan *et al.*, 2019). A vast number of materials are used in nanotechnology to manufacture nanomaterials and a simple classification of nanomaterials is the broad division of NPs into two main categories based on the materials used to produce them: organic and inorganic (**Figure 1.8**) (Martins *et al.*, 2021; Martinelli *et al.*, 2019; Rafique *et al.*, 2017).

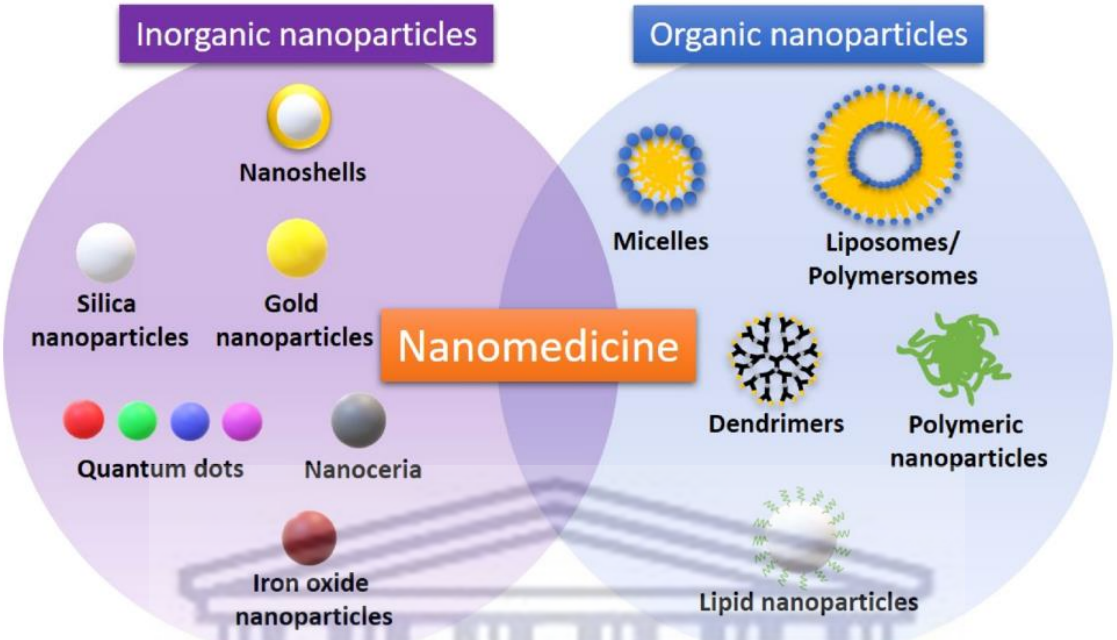

Figure 1.8: Classification of inorganic and organic NPs commonly used in nanomedicine (Adapted from Martinelli *et al.*, 2019).

Organic nanomaterials are composed of organic compounds and encompass carbon nanomaterials such as solid lipid NPs, polymers, fullerenes, and carbon nanotubes. Other organic nanomaterials which are used in drug delivery and bioimaging applications include liposomes/polymersomes, micelles, dendrimers, and polymeric NPs (Khalid *et al.*, 2020; Martinelli *et al.*, 2019). Inorganic nanomaterials are composed of inorganic compounds, like pure metals or metal oxides, and encompass metallic NPs (MNPs) (e.g., silver NPs), magnetic NPs (e.g., iron oxide NPs), and semi-conductor NPs (e.g., quantum dots), and nano shells. Nanobiomaterials are commonly synthesized from inorganic metals or polymers and lipids (Martinelli *et al.*, 2019; Rafique *et al.*, 2017).

MNPs are different from other NPs as their unique physicochemical, electrical, optical, magnetic, thermal, and biological properties make them attractive and favourable for biomedical applications (Khalid *et al.*, 2020; Chahardoli *et al.*, 2018). MNPs are manufactured using various metals precursors including silver (Ag), gold (Au), aluminium (Al), copper (Cu), iron (Fe), titanium (Ti), and platinum (Pt), or combinations of these metals (Khan *et al.*, 2019; Noah, 2019). NPs made from alkali and noble metals such as Cu, Ag, and Au have a broad absorption band in the visible zone of the electromagnetic solar spectrum. Noble metals NPs exhibit a strong UV–visible extinction band that is not present in the spectrum of the bulk metal. This excitation band results

when the incident photon frequency is constant with the collective excitation of the conduction electrons and is recognized as the localized surface plasma resonance (LSPR). Owing to the LSPR characteristics, the noble MNPs possess unique size-dependent optoelectrical properties (Khan *et al.*, 2019).

1.4.2.1 Silver nanoparticles (AgNPs)

For more than 2000 years, the medicinal and preservative qualities of silver have been known (Parveen *et al.*, 2016). Silver has been used in coins, silverware and cutlery, cosmetics, textiles, and medical implants (Park, 2014). Ancient empires, such as the Greeks, Romans, Persians, and Egyptians, have all used silver for the storage of food and water. The use of silver in silverware and cutlery to eat, drink or store food was common as it was believed that silver had antibacterial activity. Therapeutic strategies incorporating silver have been utilized since 1850 B.C. with silver being applied to wounds by the Egyptians and Hippocrates textbooks describing the positive effects of silver in wound healing. It has been documented that silver nitrate was used for ulcer treatment in the 17th and 18th centuries. Interestingly, the antibacterial activity of silver was only elucidated in the 19th century. Moreover, silver was the first choice for antibacterial treatment before antibiotics were discovered in 1940 which led to the use of silver salts being decreased (Paladini and Pollini, 2019; Srikar *et al.*, 2016; Tocco *et al.*, 2012).

Noble metals have received great attention as they can provide NPs with appealing characteristics which makes them suitable to be used in various applications (Rafique *et al.*, 2017). NPs synthesized with noble metals are used in various scientific fields relating to health and biological sciences (Prathna *et al.*, 2011). The enthusiasm for these NPs is due to their superior characteristics (Rafique *et al.*, 2017). Silver is a noble metal that has commonly been used in the synthesis of NPs due to its exceptional properties that provide AgNPs with excellent chemical stability, high electrical and thermal conductivity, catalytic activity, non-linear optical behaviour, and biological properties that make them attractive for applications within the nanobiotechnology field (Skóra *et al.*, 2021; Parveen *et al.*, 2016). The LSPR and physicochemical properties of AgNPs set them apart from other MNPs. AgNPs are used in the diagnostics and treatment of various diseases, biosensors, catalysis, medicine, textiles, cosmetics, and household items. Some of the biological activities of AgNPs include antibacterial, anticancer, antioxidant, and antidiabetic activity (Dawadi *et al.*, 2021; Noah, 2019; Rafique *et al.*, 2017; Ahmed and Ikram, 2016; Balan *et al.*, 2016; Parveen

et al., 2016; Park, 2014; Prathna *et al.*, 2011). The ability of AgNPs to control the colonization of bacteria and bacterial infection in wound healing has been previously demonstrated (Paladini and Pollini, 2019; Skóra *et al.*, 2021). It has also been shown that AgNPs are able to interact with matured biofilm and their high toxicity against bacterial pathogens (Skóra *et al.*, 2021; Kasithevar *et al.*, 2017). Due to their relatively small size, they can penetrate the cell through the cell membrane with ease and serve as a potential antibacterial agent (Dawadi *et al.*, 2021).

1.4.3 Synthesis of NPs

The "Top-down" and "Bottom-up" approaches are the two predominant principles used to synthesize NPs. The "Top-down" approach is based on size reduction as several physical/ mechanical methods are used to fragment bulk material into powder and then into nano-sized particles while the "Bottom-up" approach deals with the synthesis of NPs where atomic-scale particles form clusters/ nuclei and grow into NPs through chemical and biological methods (**Figure 1.9**) (Rafique *et al.*, 2017; Ahmed and Ikram, 2016; Parveen *et al.*, 2016). Various methods including chemical, physical, biological, and hybrid processes have been developed for the synthesis of AgNPs and are entirely dependent on the technology and reducing agents used (**Figure 1.9**) (Dawadi *et al.*, 2021; Skóra *et al.*, 2021; Parveen *et al.*, 2016).

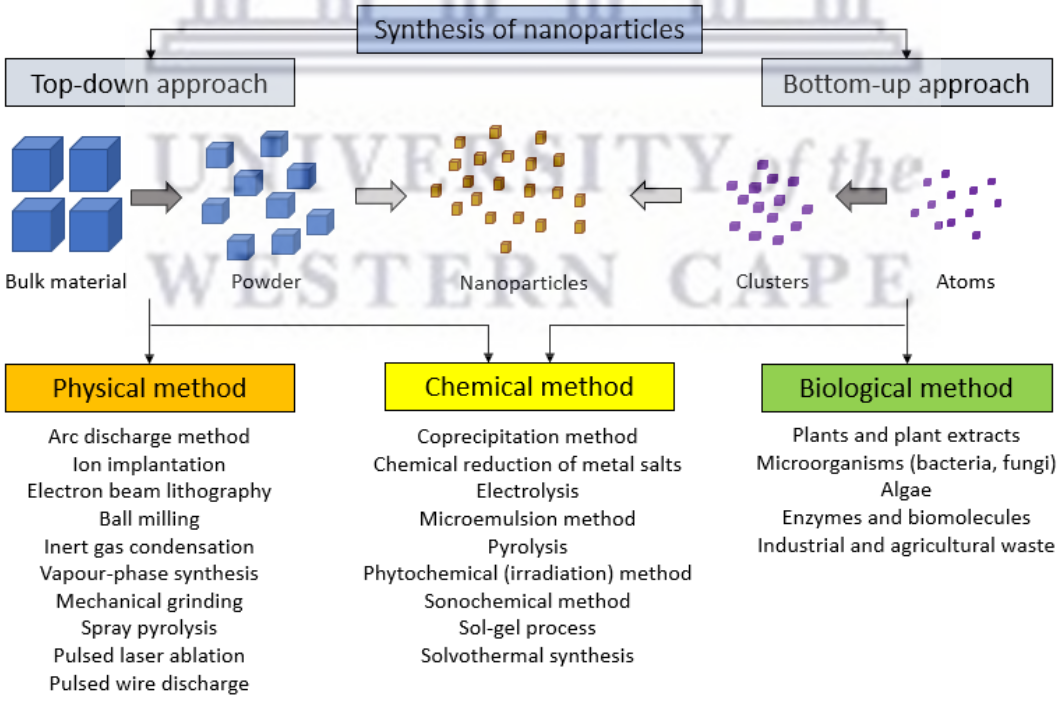

Figure 1.9: Various approaches and methods used in the synthesis of NPs (Adapted from Rafique *et al.*, 2017; Ahmed and Ikram, 2016; Parveen *et al.*, 2016).

1.4.3.1 Physical and chemical methods

Traditional methods of NPs synthesis employ physicochemical approaches which may utilize chemicals, light, laser, electricity, sound, and microwave to produce NPs (Dawadi *et al.*, 2021). Physical methods used to synthesize NPs include arc discharge method, ball milling, ion implantation, thermal evaporation, spray pyrolysis, ultra-thin films, pulsed laser desorption, lithography, sputter deposition, layer-by-layer growth, molecular beam epitasis and diffusion flame synthesis of NPs. Chemical methods used to synthesize NPs include electrodeposition, sol-gel process, chemical solution deposition, chemical vapour deposition, soft chemical method, Langmuir Blodgett method, catalytic route, hydrolysis co-precipitation method, and wet chemical method (**Figure 1.9**) (Rafique *et al.*, 2017; Ahmed and Ikram, 2016; Parveen *et al.*, 2016).

The synthesis of MNPs using physical and chemical methods is linked to severe environmental issues due to toxic and hazardous chemicals being used and released into the environment (Park, 2014). Expensive reagents, high radiation, high voltage, high temperatures and high concentrations of reducing and stabilizing agents that are not environmentally friendly and cause more harm to the environment have been employed in both physical and chemical methods (Parveen *et al.*, 2016). The expensive cost of physical and chemical processes is also a concern. These processes make use of costly machinery that require excessive amounts of energy to function and toxic chemicals that are usually expensive to purchase. Moreover, longer periods are generally required to synthesize NPs in relatively low yields (Rafique *et al.*, 2017; Ahmed and Ikram, 2016).

The main disadvantage of physical methods is the possibility of defects on the surface of the nanomaterial which can negatively impact the properties of MNPs (Soltys *et al.*, 2021). Disadvantages associated with chemical methods of synthesis include the usage of toxic solvents, contamination from chemical precursors, and the formation of hazardous by-products (Chahardoli *et al.*, 2018). Due to issues relating to sustainability, toxicity, and pollution of the environment as a consequence of physical and chemical methods being used for NP synthesis, there is an urgent need for the development of alternative methods of NP synthesis that are environmentally friendly, economical, and sustainable (Park, 2014). Biological methods of NP synthesis may overcome the limitations associated with physical and chemical methods (Dawadi *et al.*, 2021).

1.4.3.2 Biological or green synthesis methods

The biological synthesis of NPs is preferred over physical and chemical methods as it employs sustainable green chemistry principles (Kalantari *et al.*, 2020). The 12 principles of green chemistry were first published by Paul Anastas and John Warner in their book "Green Chemistry: Theory and Practice" in 1998 and provided the global scientific community with a framework to guide them in designing nanomaterials with maximum performance and minimal undesirable implications for the environment and human health. Years of unintentional polluting of the environment and impacts on human health from the production and use of hazardous chemicals could be addressed (Soltys *et al.*, 2021; Gilbertson *et al.*, 2015; Anastas and Warner, 1998). The incorporation of green chemistry principles in the synthesis of NPs has been recommended as it has the potential to reduce the harmful impact of NPs production while also increasing the safety and sustainability of the synthesized NPs (Soni *et al.*, 2022; Noah, 2019; Gilbertson *et al.*, 2015).

The 12 principles of green chemistry have guided researchers across the globe in the development of less hazardous chemical products and by-products (Parveen *et al.*, 2016). Green chemistry accounts for the entire life cycle of nanomaterials and the application of its principles in each stage of the nanomaterials' life cycle is important to help optimize the design framework. A benign target particle or chemical can be developed into a lifesaving therapeutic agent and benefit society, but it may also result in damage and pollution of the environment at the end of its life cycle (Soni *et al.*, 2022) **Figure 1.10** depicts the 12 principles of green chemistry and how each principle is applicable in the life cycle of nanomaterials (Soni *et al.*, 2022; Gilbertson *et al.*, 2015).

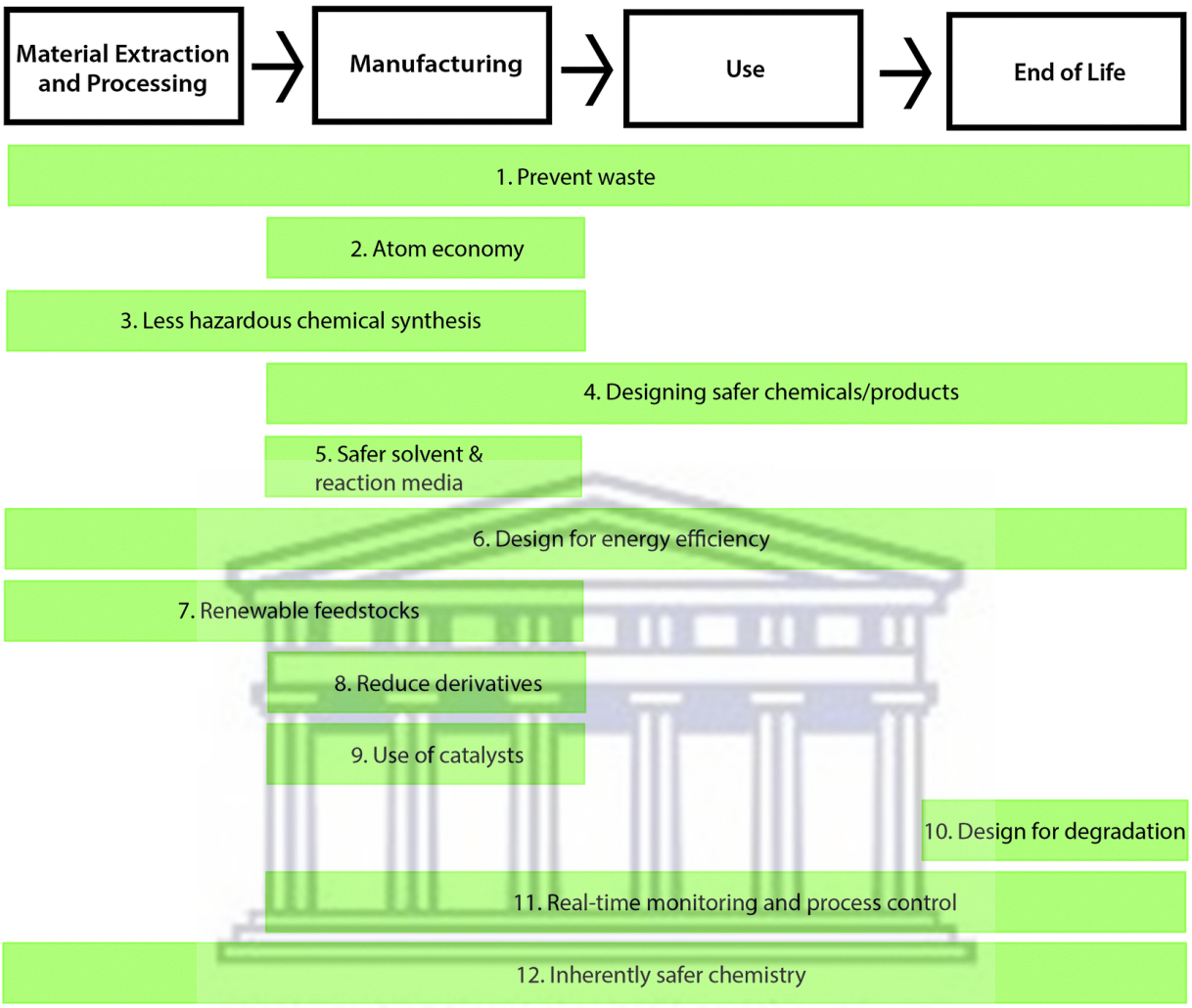

Figure 1.10: Schematic diagram showing the 12 principles of green chemistry and how each principle is applicable in each stage of the life cycle of nanomaterials (Adapted from Soni *et al.*, 2022; Gilbertson *et al.*, 2015).

The practice of green chemistry in the synthesis of NPs brought about green nanotechnology. Green nanotechnology deals with the development of clean nanotechnology that reduce the potential risks to the environment and human health related to the manufacture of nanomaterials. Nanomaterials are synthesized from natural pathways such as microbes, fungi, or plant-based extracts using different biotechnological approaches. Green nanotechnology aims to replace current products with nanoproducts that are environmentally friendly, sustainable, and free from hazardous substances (Soni *et al.*, 2022; Noah, 2019).

Green synthesis of MNPs is a single-step bio-reduction method where a metal salt solution is mixed with a biological entity for the formation of NPs as shown in **Figure 1.11** (Rafique *et al.*, 2017; Park, 2014). It has been proven to be more advantageous than classical chemical approaches as it is a simple one-pot reaction that is easy to scale up, utilizes biological materials, makes use of less energy, and is cost-effective (Parveen *et al.*, 2016; Park, 2014). NPs synthesized via green synthesis techniques are far superior to NPs manufactured with physical and chemical methods because the use of expensive chemicals is eliminated, and environmentally benign products and by-products are generated. Green synthesis of NPs utilizes reagents that are environmentally friendly, non-toxic, and safe to use to synthesize NPs in an eco-friendly manner (Parveen *et al.*, 2016). Various biological entities including microorganisms (bacteria, yeast, fungi, and other prokaryotes), plants and plant extracts, and templates (viral DNA, membranes, and diatoms) can be employed in the synthesis of MNPs as these biological systems can reduce inorganic metal ions into MNPs due to the presence of proteins and metabolites in these organisms which have reducing capabilities (Rafique *et al.*, 2017; Parveen *et al.*, 2016).

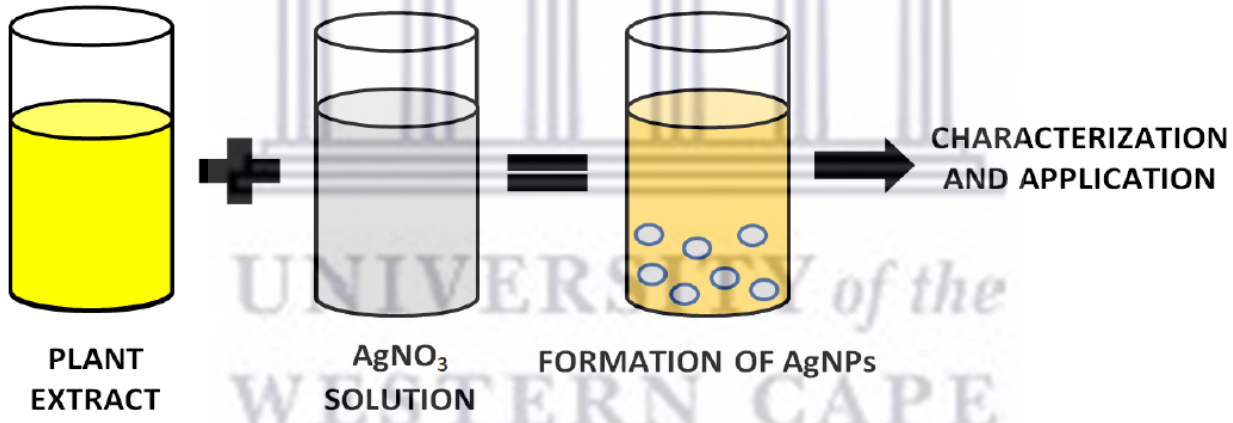

Figure 1.11: One-step method of AgNPs synthesis using plant extract (Adapted from Rafique *et al.*, 2017; Park, 2014).

The synthesis of MNPs using biological entities has received immense interest as these NPs have remarkable optical, chemical, and physical properties (Parveen *et al.*, 2016). As biological techniques are employed in a one-step procedure, NPs have a diverse nature, with greater stability and desirable shapes and sizes (Parveen *et al.*, 2016). Green nanobiotechnology presents a promising alternative route for the synthesis of NPs that are biocompatible and stable (Parveen *et al.*, 2016). The biosynthesis of NPs makes use of a bottom-up approach as synthesis is facilitated by reducing and stabilizing agents (Parveen *et al.*, 2016). When synthesizing NPs using the

biological method, the choice of solvent medium, the choice of eco-friendly and environmentally benign reducing agent, and the choice of non-toxic material as a capping agent to facilitate the stabilization of the synthesized NPs are all considerations to make (Parveen *et al.*, 2016). NPs size and shape can be controlled by specific biomolecules which is favourable for biomedical applications (Kalantari *et al.*, 2020; Parveen *et al.*, 2016). Specific biomolecules present in capping agents provide specific functional groups on the NPs surface which controls the surface chemistry, morphology, and size distribution of the NPs, shields the NPs to prevent agglomeration, and enhances the reduction kinetics of NPs through the formation of complex structures with metallic ions in the precursor salts (Sidhu *et al.*, 2022). Bioactive molecules are renowned for their medicinal properties and can be obtained from various biological organisms (Rigo *et al.*, 2013). These medicinal properties can also be introduced to NPs resulting in the enhancement of biological activities of the NPs (Gnanajobitha *et al.*, 2013). Moreover, the optimization of biological synthesis conditions, focusing on the quantity of metal precursor salts, quantity of reducing and stabilizing agents, temperature, and pH, allows for the easy modulation of shape, size, and distribution of NPs (Zhang *et al.*, 2016).

1.4.3.2.1 Biological synthesis of NPs using microorganisms

Microorganisms are widely used for genetic engineering, bioremediation, and bio-extraction (Soltys *et al.*, 2021). The exploitation of microorganisms in the synthesis of MNPs has been recognized as an efficient and green method. Microorganisms can facilitate the accumulation and detoxification of heavy metals with the aid of various reductase enzymes that can reduce metal salts to MNPs. Various microorganisms of both prokaryotic and eukaryotic origin, such as bacteria, viruses, yeasts, fungi, cyanobacteria, actinomycetes, and microalgae have been used in the production of MNPs either intra- or extracellularly (Bahrolulum *et al.*, 2021; Zhang *et al.*, 2020). These microorganisms can produce organic matter inside their cells and transport it out of the cells. Extracellular synthesis is the preferred method as the extracellular location of the organic material eliminates the need for downstream processing steps that are expensive and complex to recover intracellular NPs. Moreover, extracellular synthesis has higher yields of NPs as compared to intracellular synthesis (Bahrulolum *et al.*, 2021; Zhang *et al.*, 2020b).

The use of microorganisms instead of chemical reagents makes the reaction more environmentally friendly (Skóra *et al.*, 2021). The use of microorganisms in NP synthesis is relatively cheaper, non-

toxic, and does not require much energy in comparison to physical and chemical methods. MNPs synthesized using microorganisms have a wide range of sizes, shapes, compositions, and physicochemical properties. The major limitations associated with microorganism-based synthesis of MNPs include the complicated process of sampling, isolation, culturing, and storage of microorganisms, and downstream processing is essential for the recovery of the NPs (Bahrulolum *et al.*, 2021). Myriad studies have demonstrated the use of microorganisms such as *Bacillus* spp., *Enterobacter cloacae*, *Escherichia coli*, *Lactobacillus* spp., *Fusarium oxysporum*, and *Cylindrospermum stagnale* in the synthesis of AgNPs with varied sizes and morphologies (Soltys *et al.*, 2021; Zhang *et al.*, 2020a; Husain *et al.*, 2015; Ummartyotin *et al.*, 2012; Pugazhenthiran *et al.*, 2009; Sintubin *et al.*, 2009). Moreover, *Saccharomyces cerevisiae* is another nonpathogenic, non-toxic, and generally recognized as safe (GRAS) organism of importance that has been extensively employed in the extracellular synthesis of relatively monodispersed AgNPs with antibiofilm activity and antifungal activity (Skóra *et al.*, 2021; Niknejad *et al.*, 2015).

1.4.3.2.2 Biological synthesis of NPs using whole plants

Whole plant-based synthesis of MNPs makes use of whole plants as bioreactors for the synthesis of MNPs. Whole plants can reduce metal ions both on their surface and in various organs and tissues apart from the ion penetration site (Parveen *et al.*, 2016; Makarov *et al.*, 2014). Plants with strong metal ion hyperaccumulation and high reduction capacity have been used for phytomining. Phytomining is a process where precious metals from land bioaccumulate in plants and are extracted as it would otherwise be economically unjustifiable to mine these metals directly from the land (Makarov *et al.*, 2014).

There are certain restrictions and limitations that should be considered upon industrial application of whole plant-based synthesis of MNPs. Depending on the variations in the content of metal ions in the different tissues of the plant, the localization of the NPs is determined which subsequently controls the size and shape of the NPs. These factors can influence the amount of metal deposition around NPs that have already been synthesized as well as the possibility of new nucleation events which is the initiation of nanoparticle formation. The non-homogeneous nature of the size, morphology, and purity of NPs in whole plants may deter their use in applications where NPs of a particular size, shape, and consistency are required. These limitations prove the inability of whole plant-based synthesis to be tailored for NPs that can be marketed. Moreover, the extraction,

isolation, and purification of NPs from plants is a complicated process associated with many difficulties and low recovery of NPs (Kurhade *et al.*, 2021; Makarov *et al.*, 2014).

A wide variety of plants have been successfully used in the efficient and rapid extracellular synthesis of AgNPs and gold NPs (AuNPs). Alfalfa (*Medicago sativa*), *Chilopsis linearis*, and *Sesbania* seedlings have all demonstrated that synthesis of AuNPs within plants is achievable whereas the sprouts of Alfalfa (*Medicago sativa*) and germinating seeds of *Brassica juncea* can synthesize silver and Ag-Au-Cu alloy NPs (Parveen *et al.*, 2016). Another study also demonstrated the use of *Brassica juncea* (mustard greens) and *Medicago sativa* (alfalfa) for the synthesis of AgNPs. The study demonstrated that the plants were grown on silver nitrate as a substrate and as a result, a large amount of AgNPs with an average size of 50 nm accumulated within the tissues of the plants, making up approximately 13.6% of the plant's total weight (Makarov *et al.*, 2014).

1.4.3.2.3 Biological synthesis of NPs using plant extracts

Although whole plants have shown their potential to be used in the synthesis of NPs, plant extracts have been also used successfully in the synthesis of several MNPs, such as silver, copper, cobalt, gold, platinum, palladium, zinc oxide, and magnetite (Parveen *et al.*, 2016). Biologically active compounds found in plant extracts also referred to as phytochemicals, are responsible for the bio-reduction of metal ions due to their ability to act as reducing and stabilizing agents (Soltys *et al.*, 2021; Bhardwaj *et al.*, 2020; Rigo *et al.*, 2013). Various parts of the plant like leaves, stems, seeds, fruits, roots, and latex can be used to extract phytochemicals (Kurhade *et al.*, 2021). Numerous primary and secondary metabolites of plants such as polyphenols, tannins, alkaloids, terpenoids, saponins, vitamins, polysaccharides, glycosides, proteins, flavonoids, amino acids, and enzymes possess the ability to act as reducing and stabilizing agents (**Figure 1.12**) (Soltys *et al.*, 2021; Ahmed and Ikram, 2016). The processes involved in the reduction and stabilization of metal ions to NPs are rapid, can often be easily conducted at ambient temperatures and pressure, are easy to scale up, are cost-effective, are environmentally friendly, and are deemed safe for biomedical research. Making sure that the reducing and stabilizing agents used in NPs synthesis results in a process that saves energy, is cost-efficient, improves safety, and reduces waste adheres to the green chemistry principles (Noah, 2019).

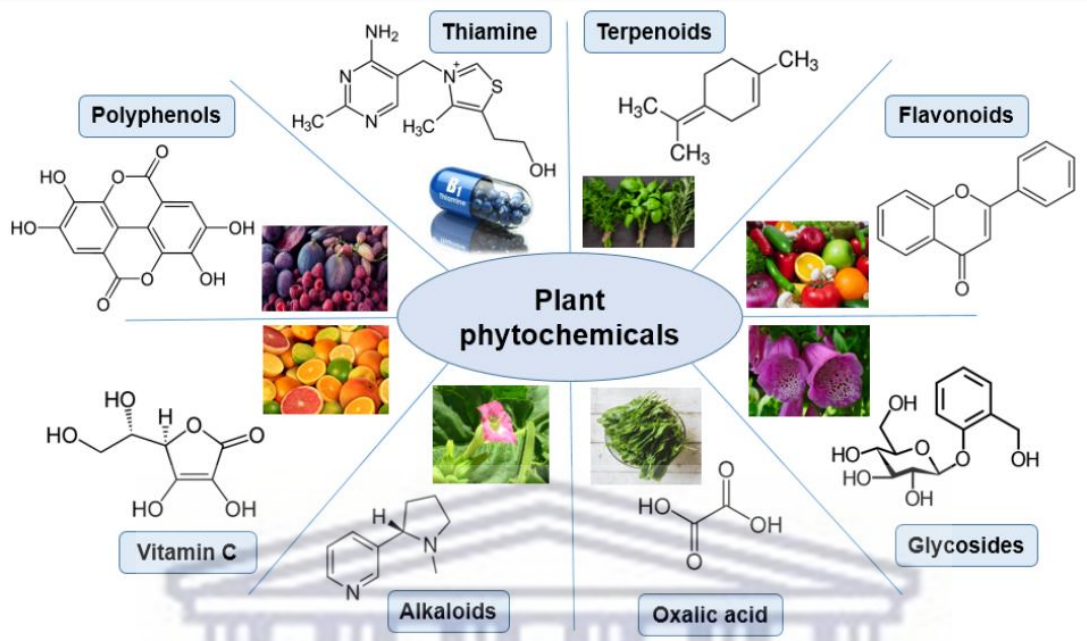

Figure 1.12: Some biologically active compounds found in plants (phytochemicals) (Adapted from Soltys *et al.*, 2021).

The utilization of plant extracts is generally preferred over microorganisms as the rate of synthesis appears to be quicker. Bioactive compounds found in plants can reduce metal ions much faster than bacteria or fungi due to the presence of functional groups. The method involving plant extracts can also be modified with ease due to the single-step, non-pathogenic, and eco-friendly nature of the method. Moreover, the utilization of plant extracts instead of microorganisms eradicates the biohazardous risks (i.e., pathogen activity) and costs and labour of the isolation and maintenance of large cultures and purification of NPs, and slowness of the synthesis process (Soni *et al.*, 2022; Soltys *et al.*, 2021; Rafique *et al.*, 2017; Ahmed and Ikram, 2016). Plants are also extensively distributed, readily available, and relatively safe to handle (Geoprincy *et al.*, 2013). Generally, NPs that have been synthesized using leaf extracts have well-defined morphological features in comparison to NPs that have been synthesized using extracts from plant tissues, bark, and whole plant (Srikar *et al.*, 2016).

Several studies have demonstrated that plant extracts can act as potential precursors for nanomaterial synthesis (Parveen *et al.*, 2016). The leaf extracts of *Cymbopogon flexuosus* (lemongrass), *Cinnamommum camphora*, *Azadirachta indica* (neem), *Aloe vera*, and *Tamarindus indica* (tamarind) have been able to reduce silver nitrate to Ag^0 in the formation of AgNPs,

respectively (Parveen *et al.*, 2016). Green-synthesized AgNPs may possess antibacterial and antifungal properties and therefore may aid in the reduction or prevention of infections (Shalaby *et al.*, 2022). AgNPs synthesized from leaf extracts of *Cestrum nocturnum* have shown significant antibacterial activity (Rigo *et al.*, 2013). AgNPs synthesis using plant extracts is beneficial as it is eco-friendly, economical, and energy-efficient, thus, a healthier workplace for humans with less waste production and more safety is provided (Shalaby *et al.*, 2022; Kalantari *et al.*, 2020).

1.4.3.3 Mechanism involved in green synthesis of NPs

There are two main requirements in the green synthesis of AgNPs using plant extracts, namely, silver metal ion solution and plant extract. The plant extract acts as a reducing, stabilizing, and capping agent in a simple one-step bioreduction reaction (**Figure 1.13**). The Ag^{+} ions can be obtained from a variety of water-soluble salts of silver (e.g., aqueous silver nitrate ($AgNO_3$)), and the plant extracts can be obtained from a plethora of flora found globally. For green nanotechnology, the preferred solvent for the extraction of reducing agents from plants is water. Water is the cheapest and most available solvent and has been employed in the synthesis of various NPs (Soltys *et al.*, 2021; Bhardwaj *et al.*, 2020; Srikar *et al.*, 2016). Using this approach, the use of high temperatures and pressure, high consumption of energy, and harmful chemicals are avoided (Rafique *et al.*, 2017).

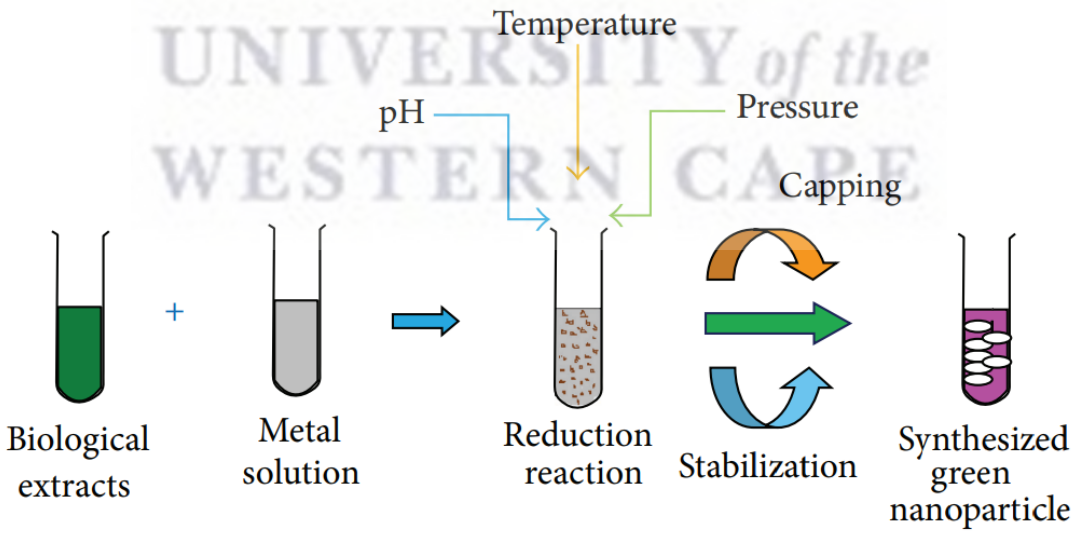

Figure 1.13: Biological synthesis of NPs using green nanotechnology (Adapted from Patra and Baek, 2015).

The biological synthesis of AgNPs is facilitated by the donation of electrons from organic chemicals which play a role in the reduction of Ag^+ ions to Ag^0. The reducing agent is the active ingredient found within the biological entity and it usually differs according to the choice of biological entity used for the NPs synthesis. The mechanism involved in the formation of AgNPs is displayed in **Figure 1.14** (Gamboa *et al.*, 2019). Overall, there are three main steps in the mechanism of NP formation through plant extracts: (i) activation stage: metal ions are reduced and the zerovalent metal atoms in the solution (in this case, Ag^0) become supersaturated, nucleation takes place and nuclei/ clusters start to form, (ii) growth phase: each cluster acts as a foundation for the growth of each nanoparticle which occurs by the diffusional capture of other zerovalent metal atoms in solution which have not formed nuclei so metal atoms coalesce to form larger particles, and (iii) termination phase: the final shape of the NP is determined in this stage and is dependent on the length of the growth phase (Kurhade *et al.*, 2021; Makarov *et al.*, 2014; Prathna *et al.*, 2011). Moreover, the capping agent plays a pivotal role in the synthesis of NPs. The functionalization and stabilization of the synthesized NPs are achieved using capping agents which provide the synthesized NPs with properties by controlling the size and shape of the NPs and protecting the NP surface to prevent aggregation of the NPs. The coating of bioactive molecules on the NP's surface makes them biocompatible as compared to the NPs prepared using chemical methods (Sharma *et al.*, 2019).

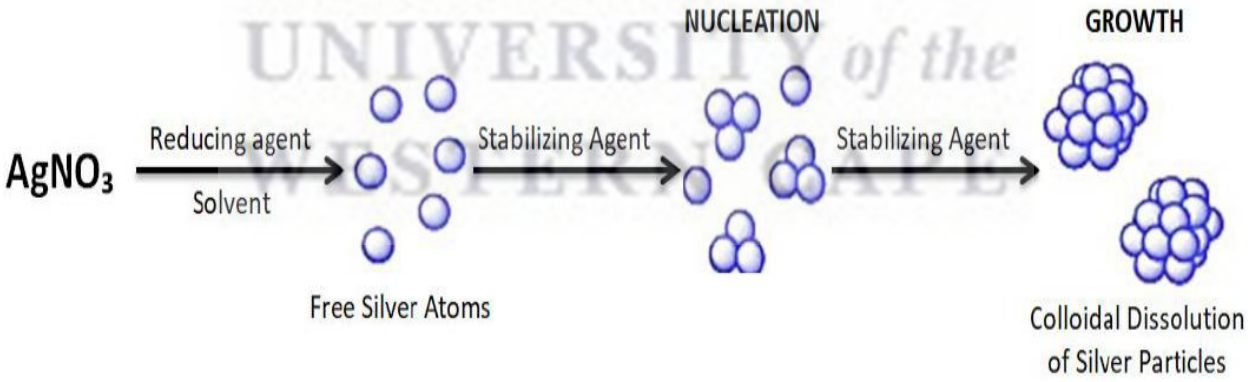

Figure 1.14: Schematic diagram displaying the steps involved in the formation of AgNPs (Adapted from Gamboa *et al.*, 2019).

1.4.3.4 Parameters affecting the synthesis of NPs

In the synthesis of NPs, careful consideration of several reaction conditions is required due to the potential influence on the overall synthesis of NPs, the rate at which NPs are produced, the yield and stability of NPs formed, and various physicochemical characteristics of NPs which may affect the morphology of the NPs as well (Soltys *et al.*, 2021; Ahmed *et al.*, 2016a). More importantly, reaction parameters can also influence the potential application of NPs (Srikar *et al.*, 2016). In the biogenic synthesis of NPs using plant extracts, a range of factors which may have an influence on the size, shape, and surface morphology of NPs include pH, temperature, pressure, mixing speed, reaction time, metal salt concentration, and the type and concentration of plant extract. The ratio of the metal salt to plant extract is another crucial factor to consider (Soltys *et al.*, 2021; Rafique *et al.*, 2017; Srikar *et al.*, 2016; Makarov *et al.*, 2014; Park, 2014).

When the pH of the reaction mixture is adjusted, the charges of the functional groups of secondary metabolites or biomolecules present in the plant extract are also adjusted (Reyes *et al.*, 2020). The change in the charges of the functional groups is due to protonation and deprotonation taking place on the surface of the biomolecules depending on the pH being acidic or basic. This leads to changes in the local surface charge of NPs in the nucleation and growth stages of NP synthesis (Patil and Chandrasekaran, 2020; Barisik *et al.*, 2014). This change in the pH of plant extract affects how the biomolecules interact with the metal ions present in the reaction mixture and subsequently affects how the NPs are capped and stabilized, hence, the growth of the NPs is affected as well. Changes to the pH affects the shape, size, and yield of NPs produced (Lade and Shanware, 2020; Zhang *et al.*, 2020a; Makarov *et al.*, 2014; Park, 2014).

Under basic conditions, the increased levels of OH- species may aid in the deprotonation of functional groups such as the carboxyl group (from -COOH to -COO-). Biomolecules with carboxyl groups have been reported to have better reduction potential under basic pHs (Miranda *et al.*, 2022). The deprotonation of functional groups present in the biomolecules allows for the adsorption of Ag^+ ions by electrostatic attraction or affinity interaction resulting in the AgNPs with small size and well-dispersed distribution (Miranda *et al.*, 2022). It has been reported that an acidic reactant may cause prolonging of the reaction time therefore indicating that acidic medium is not ideal for NP synthesis. Moreover, NPs synthesized under acidic conditions resulted in NPs with a greater size as compared to NPs synthesized under basic conditions (Lade and Shanware, 2020).

NPs formed at basic pHs are not only smaller in size but are formed in higher yields as well (Miranda *et al.*, 2022; Reyes *et al.*, 2020).

When the temperature and mixing speed of the reaction is increased then the rate of reaction and rate of particle formation is increased as well. Moreover, when the reaction is allowed to run for longer periods, changes in the size and shape of synthesized NPs can be observed (Zhang *et al.*, 2020a; Makarov *et al.*, 2014; Park, 2014). Generally, the synthesis of NPs using green technology requires temperatures less than 100 ℃ or ambient temperature (Patra and Baek, 2015). Previous studies have shown that MNPs can be synthesized at room temperature within a short amount of time (Rafique *et al.*, 2017). The pressure of the reaction medium influences the shape and size of the synthesized NPs. The rate of reduction of metal ions is much faster at ambient pressure conditions in the green synthesis of NPs (Patra and Baek, 2015). The concentrations of metal salt and plant extract, and the proportions at which they are mixed in the reaction, have a direct effect on the shape, size, and yield of the synthesized NPs (Zhang *et al.*, 2020a; Srikar *et al.*, 2016; Park, 2014).

1.4.3.5 Purification of NPs

The purification process of the synthesized NPs is essential because the applicability of the NPs is dependent on their purity (Martins *et al.*, 2021). Purification of NPs aids in the understanding of their physical properties (i.e., size and shape) and reduces their variability in biological applications (Robertson *et al.*, 2016). There are various methods used to purify NPs, such as density gradient centrifugation, membrane filtration, selective precipitation, liquid extraction, chromatography, electrophoresis, separation by hydrodynamic forces, and magnetic-based techniques (Martins *et al.*, 2021). The choice of purification method used can influence NP quantity and quality (Patra and Baek, 2015). Certain methods can alter the physicochemical properties of NPs, often resulting in the disintegration of the NPs, making them impractical for their further use, therefore, the choice of method is restricted (Martins *et al.*, 2021).

Although the benefits and shortfalls of various purification methods were extensively reviewed by Martins and colleagues, it was concluded that it is impossible to choose one standard method for the purification of all NPs. The most appropriate method is dependent on the type of NPs and their intended application for which it is vital that the integrity of the NPs is maintained (Martins *et al.*,

2021). Nevertheless, centrifugation is a cheap, straightforward, and suitable method for the recovery and purification of AgNPs, especially to remove contaminants and/or residues from freshly synthesized suspensions. Centrifugation allows for the successful separation of NPs by size and shape based on gravitational force and ensures that their physicochemical properties are preserved making them ideal for their intended application (Martins *et al.*, 2021; Park, 2014). A previous study by Sholikhah *et al.* (2020) carried out experiments on the separation of AgNPs using size exclusion chromatography (SEC) and centrifugation methods to determine which method is more effective. The findings of the study demonstrated that centrifugation had better homogeneity than the SEC method (Sholikhah *et al.*, 2020).

1.5 *Manihot esculenta* (cassava)

M. esculenta, commonly known as cassava, manioc, yuca, tapioca, mandioca, shushu, muk shue, cassave, manioc, tapioca, imanoka, maniba, kasaba, katela boodin, sweet potato tree, or Brazilian arrowroot, is a plant belonging to the Euphorbiaceae family which has great importance as a global agro-industrial crop (Jampa *et al.*, 2022; Bahekar and Kale, 2013). In tropical and subtropical parts of the world, cassava is grown as an annual crop and is one of the largest sources of carbohydrates along with rice and maize (Syafiuddin *et al.*, 2017; Ferraro *et al.*, 2016; Ogola and Mathews, 2011). It is native to Central and South America; however, it can be found widely distributed across southeast Asia and Africa (Burns *et al.*, 2012; Zakaria *et al.*, 2006). It is a woody, perennial shrub with compound leaves, small green flowers, and large, brown roots that have chalk-white or yellow flesh inside (Mountain Herb Estate, 2022). An image of the cassava leaves used in this study is shown in **Figure 1.15**.

Figure 1.15: Image of *Manihot esculenta* (cassava) leaves used in this study.

Cassava offers a massive opportunity as a food, feed, and industrial crop (Amelework *et al.*, 2021). It is generally grown for its enlarged tuberous roots which are rich in starch (Zakaria *et al.*, 2006; El-Sharkawy, 2004). The various parts of cassava are consumed as part of the human diet to provide energy and nutrition in the form of carbohydrates, and other macronutrients, minerals, and vitamins, respectively (Zakaria *et al.*, 2006). Although both roots and leaves are consumed, the roots are the primary food source and cassava leaves are often a leftover co-product (Jampa *et al.*, 2022). Nearly 70% of the global cassava root production is used for human consumption, either after cooking or in processed forms while the remaining 30% is used for animal feed and other industrial products such as starch, glucose, and alcohol (Marie-Magdeleine *et al.*, 2010; El-Sharkawy, 2004). Cassava has also been used as feedstock to produce biofuel in Brazil and China (Amelework *et al.*, 2021; Narina and Odeny, 2011; Ogola and Mathews, 2011).

Cassava is grown in over 105 countries with Nigeria, Thailand, the Democratic Republic of Congo, Indonesia, and Brazil being the leading producers of the crop (Amelework *et al.*, 2021; Oghenejoboh *et al.*, 2021). In 1961, the total global cassava production was 78.5 million tons grown on 9.6 million hectares which 44% was contributed by Africa. In 2017, the total global cassava production skyrocketed to 322 million tons grown on 26 million hectares of land (Amelework *et al.*, 2021). Nigeria earns approximately US$3 billion per year by exporting the crop and related products (Ogola and Matthews, 2011).

Over 800 million people living in developing tropical countries, including 45% of Sub-Saharan Africans, consider cassava as a staple food crop (Burns *et al.*, 2012; Ogola and Matthews, 2011). In developing regions such as Africa, Asia Pacific, and South America, food security is maintained through the manufacturing of cassava as a food product. The key role of cassava in the maintenance of food security is attributed to its ease of cultivation, high resistance to drought and tolerance to low soil fertility, low rainfall, and high temperatures which is especially important as climate change has negatively affected global crop production (Jampa *et al.*, 2022; Burns *et al.*, 2012).

The roots and leaves of cassava are a good source of carbohydrates, minerals, and vitamins; however, the roots have low amounts of protein, and all parts of the plant are toxic as cyanogenic glycosides (α-hydroxynitrile glucosides) are present. Cyanogenic glycosides release toxic cyanide (HCN) when broken down through the processing of the plant tissue as the cells are disrupted (Burns *et al.*, 2012). Cassava needs to be processed adequately before consumption as it may cause

serious illness or death (Burns *et al.*, 2012). There are thousands of cultivars of this crop as breeding by farmers and scientists have promoted their development. All cultivars contain the cyanogenic glycosides linamarin and lotaustralin (Burns *et al.*, 2012; Marie-Magdeleine *et al.*, 2010). The highest concentrations are present in the peel of the roots and leaves, with the flesh of the roots being less cyanogenic. The potential for poisoning is further exacerbated as the content of cyanide within cassava varies with environmental conditions such as drought, which may lead to increased cyanogenic potential, and soil nutrient supply. Another important variable is the low concentration of other key nutrients present, for example, there are low concentrations of the sulfur-containing amino acids methionine and cysteine in cassava which are essential in the detoxification of cyanide that has been ingested (Burns *et al.*, 2012).

1.5.1 Medicinal importance of cassava

The pharmacological potency and health benefits of cassava leaves can be attributed to their nutritional, mineral, and phytochemical contents which include carbohydrates, essential amino acids (methionine and phenylalanine), dietary fibres, β-carotene, vitamins, phenolics, anthocyanins and flavonoids (Essien *et al.*, 2022; Jampa *et al.*, 2022). Many phytochemical studies of cassava have shown that the biomedical activities of the plant are due to the presence of several metabolites (Lima *et al.*, 2017). Vitamin A, B1, calcium, calories, phosphorus, protein, fat, carbohydrate, and iron can be found in the leaves of *M. esculenta* which is often discarded during harvest (Essien *et al.*, 2022). Flavonoids, tannins, ascorbic acid, alkaloids, and saponins found in *M. esculenta* have displayed antimicrobial, antioxidant, and anti-inflammatory activities (Lima *et al.*, 2017). The leaves also contain free quercetin, which is an antioxidative, anti-inflammatory, renal protective, and venotonic flavonoid. Other biomolecules found in the leaves are vitamin C, flavonol glucosides, alkanes and sulfhydric acid, and condensed tannins (Marie-Magdeleine *et al.*, 2010). Rutin, a flavonoid compound, has been proposed as the bioactive constituent involved in the antioxidative property of cassava leaves (Jampa *et al.*, 2022). Moreover, chlorophyll present in the leaves serves as an antioxidant and anticancer agent (Essien *et al.*, 2022). The chemical composition of *M. esculenta* is shown in **Table 1.3**.

Table 1.3: Chemical composition of *M. esculenta* (Adapted from Syafiuddin *et al.*, 2017; Ferraro *et al.*, 2016).

Proximate	Mineral	Vitamin
Caloric content	Calcium	Ascorbic acid
Water	Copper	Niacin
Protein	Iron	Riboflavin (vitamin B2)
Lipid	Magnesium	Thiamin
Carbohydrates	Manganese	Vitamin A
Fiber	Phosphorus	
Ash	Potassium	
	Sodium	

In various parts of the world, cassava is recognized for its medicinal value in the treatment of various ailments. In the Caribbean, the leaf is used as a cure for headaches, and its antifungal, anthelmintic, and antihemorrhagic properties. It has been previously reported that ethanolic extracts of cassava had antiviral and antimycobacterial properties, with the fresh leaf inhibiting protein synthesis (Marie-Magdeleine *et al.*, 2010). In traditional practices of Suriname medicine, the brown juice obtained during processing is used for burns while a decoction made from *M. esculenta* can be used as an anthelminthic. *M. esculenta* has also been used in folk medicine for the treatment of abscesses, boils, conjunctivitis, diarrhoea, dysentery, flu, hernia, inflammation, prostatitis, snakebite, sores, spasms, and swellings (Zakaria *et al.*, 2006). Moreover, *M. esculenta* has also been recognized for its efficacy in treating asthma, coughs, wounds, skin rashes, tuberculosis (TB), backache, chest pain, sweating, stomachache, and medicinal anaesthesia. Cassava leaves can also be used to treat measles, smallpox, chickenpox, fevers and headaches, colds, constipation, tumours, rheumatism, haemorrhoids, ringworm infection, conjunctivitis, sores, and abscesses (Essien *et al.*, 2022; Jampa *et al.*, 2022; Zakaria *et al.*, 2006).

Previous literature has shown that cassava leaves have antimicrobial, antioxidant, anti-inflammatory, analgesic, antipyretic, anthelminthic, anticancer, larvicidal, and wound-healing activities (Amado-Cornejo *et al.*, 2020; Laya and Koubala, 2020; Mustarichie *et al.*, 2020; Anwar and Bohari, 2019; Bahekar and Kale, 2013; Bokanisereme and Okechukwu, 2013; Al-Rofaai *et al.*, 2012; Marie-Magdeleine *et al.*, 2010). Phytochemical studies have confirmed the presence of biomolecules such as proteins, enzymes, polysaccharides, amino acids, and vitamins in cassava

leaves (Syafiuddin *et al.*, 2017; Chung *et al.*, 2016; Bahekar and Kale, 2013). A study demonstrated the antibacterial activity of the ethanolic extract of *M. esculenta* leaves as it proved to be effective against clinical isolates of *Staphylococcus epidermidis* and *Propionibacterium acnes (*Mustarichie *et al.*, 2020). The aqueous leaf extract of *M. esculenta* had better antibacterial activity against *Bacillus cereus* than the aqueous leaf extracts of *Carica papaya* and *Morinda citrifolia* in a study conducted by Syafiuddin and colleagues. The aqueous leaf extract of *M. esculenta* exhibited antibacterial activity against *B. cereus, E. coli, S. aureus,* and *P. aeruginosa* (Wattimena *et al.*, 2022; Syafiuddin *et al.*, 2017; Ramesh *et al.*, 2013). Additionally, *M. esculenta* extract has also been shown to be effective against *Corynebacterium diphtheriae, Listeria monocytogenes, Vibrio cholera, Shigella flexneri,* and *Salmonella typhi* (Zakaria *et al.*, 2006).

Furthermore, AgNPs synthesized using *M. esculenta* displayed larvicidal activity against mosquito species, *Aedes aegypti* and *Culex quinquefasciatus,* which are known to carry deadly diseases such as Zika, Dengue fever, and Japanese encephalitis (Velayutham *et al.*, 2016). Moreover, it was discovered that 200 µg/mL of *M. esculenta* aqueous leaf extract coupled with therapeutic ultrasound at a specific dose of 3 MHz, 300 mWatt/cm^2, 50% for 5 min have the potential to accelerate the wound healing process of cells *in vitro* (Anwar and Bohari, 2019). In a study by Meilawaty, it was shown that *M. esculenta* leaves play a role in accelerating the process of wound healing by decreasing inflammation (Meilawaty, 2013). The biomolecules present in *M. esculenta* leaves do not only have direct health benefits but possess the ability to reduce metal ions to form AgNPs in solution (Syafiuddin *et al.*, 2017; Chung *et al.*, 2016). With the antibacterial activity of *M. esculenta* leaves being previously proven, the exploration of the leaf extract to facilitate in the synthesis of AgNPs as a reducing, capping, and stabilizing agent is attractive for further research (Syafiuddin *et al.*, 2017).

1.5.2 Cassava production in South Africa and the valorisation of cassava biowaste

Despite the long history of cassava in Africa and other parts of the world, cassava is not regarded as a traditional commodity crop in SA. There has been limited cassava production in the country with smallholder farmers growing cassava as a minor crop for home consumption in the north-eastern parts of SA (Amelework *et al.*, 2021, Ogola and Mathews, 2011). Recently, cassava has been recognized by the Southern African Development Community (SADC) as one of the potential industrial crops for SADC farmers (Amelework *et al.*, 2021). A study revealed that SA imports

more than 66 000 tons of various starches each year, of which 33% is cassava starch (19 800 tons). The importing of starch costs SA an estimated value of more than R40 million per annum, with cassava starch accounting for R6.8 million of the total import costs, therefore, it is evident that there is the availability of a local market (Amelework *et al.*, 2021).

Intriguingly, SA has recently developed an interest in the large-scale cultivation of cassava to produce high-quality industrial starch (Amelework *et al.*, 2021). The fleshy part of the cassava root is used to produce industrial starch, and the rest of the cassava plant (leaves, stems, peels, pulp, and rhizomes) is often discarded as biowaste (Amelework *et al.*, 2021; Kowsalya *et al.*, 2021). The growing demand for cassava production and processing will lead to an increase in cassava biowaste accumulation. Cassava biowaste poses a considerable risk to the environment as its organic content is a source of pollution which leads to the contamination of soil and groundwater if not disposed of properly. Degradation of the environment by cassava biowaste can have detrimental implications for human health, ecosystems, and the economy (Oghenejoboh *et al.*, 2021; Olukanni and Olatunji, 2018; Ghimire *et al.*, 2015). A major environmental challenge facing both agricultural and industrial production is the management of waste from farming and manufacturing practices. The proper management of cassava biowaste can alleviate the burden of environmental pollution and lead to environmental, human health, and socio-economic benefits (Hadzi-Nikolova *et al.*, 2021; Oghenejoboh *et al.*, 2021; Ghimire *et al.*, 2015).

The management of biowaste plays a key role in ensuring the sustainability of the bioeconomy (Ortega *et al.*, 2022). Biowaste forms part of the circular bioeconomy as a valuable resource. It has been reported in literature that the creation of a circular bioeconomy based on the effective use of biomass (including biowaste) is of utmost importance (Hadzi-Nikolova *et al.*, 2022). A shift towards the valorisation of biowaste can help to create a sustainable, biobased society and circular economy (Ortega *et al.*, 2022). The discarding of cassava biowaste provides an opportunity for it to be transformed from "trash to treasure." The upcycling of cassava biowaste in the manufacturing of new high-value biobased products indicates that the valorisation of cassava biowaste is achievable. Previous literature has reported on the valorisation of cassava biowaste (Amelework *et al.*, 2021; Oghenejoboh *et al.*, 2021; Olukanni and Olatunji, 2018). The potential of cassava biowaste as a source of bioethanol, biogas, and organic fertilizer has been extensively explored worldwide (Amelework *et al.*, 2021; Oghenejoboh *et al.*, 2021; Ekop *et al.*, 2019; Itoba-Tombo *et*

al., 2019). Other value-added products such as pharmaceuticals, biofuels, ethanol, adhesives, tires, livestock feeds, cold meats, and alcohol, can also be manufactured from cassava biowaste (Amelework *et al.*, 2021). Moreover, numerous studies have shown that the phytochemicals extracted from cassava biowaste, particularly tuber peels and leaves, can reduce $AgNO_3$ to synthesize AgNPs with antimicrobial properties (Kowsalya *et al.*, 2020; Syafiuddin *et al.*, 2017).

1.6 Application of AgNPs with antibacterial activity

Nanotechnology has received great attention due to the versatile physicochemical properties of nanomaterials which make them favourable to be utilized in various applications in diverse fields such as the medical, pharmaceutical, and food sectors; water treatment; cosmetics ingredients; and antimicrobial textiles, and many more (Rosli *et al.*, 2021). In recent years, nanotechnology has been deemed as the most scientific breakthrough as its introduction revolutionized the field of modern medicine and played a leading role in the improvement of global human health (Mubeen *et al.*, 2021). Due to the failure of traditional drugs and antibacterial agents to eradicate resistant bacteria and biofilms, there is a necessity to develop new tools (Okkeh *et al.*, 2021). Nanotechnology is a significant tool that can treat and prevent infections with various advantages over standard-of-care procedures (Shalaby *et al.*, 2022). Nanotechnology-based therapeutic strategies can aid in the eradication of the AMR burden and improve the therapeutic outcomes of current available treatment for bacterial infections associated with AMR by overcoming their limitations (Saka and Chella, 2021).

Based on the antibacterial properties and low toxicity profile of MNPs (i.e., silver, gold, and zinc), MNPs are ideal candidates for antibacterial therapy (Mihai *et al.*, 2019). MNPs have significant beneficial use in dermatology by aiding in the prevention and treatment of infections as well as the process of wound healing process with the application of NPs in wound dressings. Literature has shown that antimicrobial wound dressings can be viewed as an alternative approach to reduce the bacterial colonization and infection in wound healing (Rosli *et al.*, 2021; Mihai *et al.*, 2019). Besides wound healing, NPs have also found potential use in tissue engineering, bone cement, urinary catheters, dental implants, food packaging and wastewater treatment due to their antimicrobial activity (**Figure 1.16**) (Rosli *et al.*, 2021).

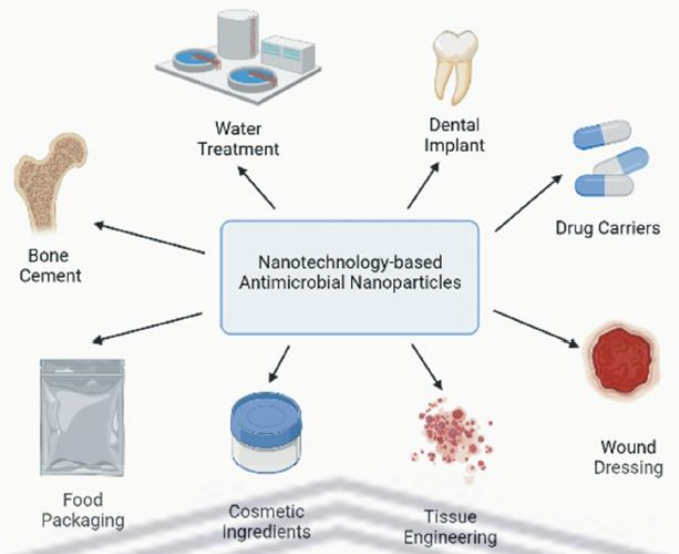

Figure 1.16: Practical applications of nanotechnology-based products due to their antimicrobial activity (Adapted from Rosli *et al.*, 2021).

Several studies investigating the antibacterial effects of MNPs have exhibited promising results in both gram-positive and gram-negative bacteria (**Table 1.4)** (Patil and Chandrasekaran, 2020; Sánchez-López *et al.*, 2020; Rigo *et al.*, 2013). Silver and AgNPs (AgNPs) are deemed optimal candidates for the treatment of pathologies that have previously been treated with conventional antibiotics (Boateng and Catanzano, 2020). However, AgNPs may overcome the limitations of standard silver compounds due to their increased surface-to-volume ratio as AgNPs are more potent at lower concentrations, hence, reducing toxicity (Kumar *et al.*, 2018; Hamdan *et al.*, 2017). Moreover, AgNPs has shown exciting potential to be used as an effective antibacterial agent as their distinctive unusual physicochemical properties as well as their broad-spectrum antibacterial activity make them ideal for the treatment of infections caused by AMR bacteria (Hu *et al.*, 2020; Rigo *et al.*, 2013).

Table 1.4: Antibacterial activity of MNPs (Adapted from Patil and Chandrasekaran, 2020).

NPs	Source	Bacteria	Gram reaction	Reference
AgNPs	*Erythrina suberosa (Roxb.)*	*S. aureus*	+	(Mohanta *et al.*, 2017)
		P. aeruginosa	-	
		E. coli	-	
		B. subtilis	+	
AuNPs	*Ziziphus zizyphus*	*E. coli*	-	(Aljabali *et al.*, 2018)
ZnONPs	*Albizia lebbeck*	*S. aureus*	+	(Umar *et al.*, 2019)
		E. coli	-	
		K. pneumonia	-	
		S. typhi	-	
		B. cereus	+	
IONPs	*Acacia nilotica*	*E. coli*	-	(Da'na *et al.*, 2018)
		Salmonella	-	
		S. aureus	+	
SeNPs	*Emblica officinalis*	*E. coli*	-	(Gunti *et al.*, 2019)
		S. aureus	+	
		E. faecalis	-	
		L. monocytogenes	-	
NiNPs	*Monsonia burkeana*	*E. coli*	-	(Kganyago *et al.*, 2018)
		P. aeruginosa	-	

In order for nanomaterials to be applicable for biomedical purposes, nanomaterials need to be biocompatible, well-characterized, and stable *in vivo* (Martinelli *et al.*, 2019). The biological efficiency of NPs is determined by their physicochemical properties (e.g., size and shape) (Mihai *et al.*, 2019). Through the variation of material, size, morphology and electrical charge of the NPs, their biochemical features such as interaction with biological targets, hydrophobicity, and deeper levels of tissue penetration may be simply altered (Hamdan *et al.*, 2017). Numerous studies have shown that diverse types of nanomaterials have displayed promising results concerning antibacterial activity. The use of nanomaterials to overcome microbial drug resistance has been claimed as one of the most promising strategies (Okkeh *et al.*, 2021).

In an attempt to gain a better understanding of the bacterial infection and to assess new prevention and treatment protocols, experimental models have been established. *In vitro* experimental models are laboratory-based tests that provide valuable tools that are essential for drug development (Da

Costa Mousinho, 2013). Researchers can simulate specific events that occur at cellular and molecular levels using *in vitro* techniques which enable the rapid assessment of a multitude of test substances under controlled conditions providing useful information regarding how cells are affected by these test substances. Significant preliminary results obtained from *in vitro* models lead to the design of subsequent investigations (Kalantari *et al.*, 2020; Masson-Meyers *et al.*, 2020; Wilhelm *et al.*, 2017; Da Costa Mousinho, 2013). The process of *in vitro* testing is relatively easy, rapid, inexpensive, and does not require a lot of material in comparison to *in vivo* testing. These benefits show the value of *in vitro* testing in the initial stages of the development of potential therapeutic materials (Kalantari *et al.*, 2020; Da Costa Mousinho, 2013).

Several *in vitro* and *in vivo* studies have demonstrated the antimicrobial effects of AgNPs synthesized from different biological sources. Some examples of green synthesized AgNPs and their practical applications are: AgNPs synthesized with *M. esculenta* aqueous leaf extract exhibited antibacterial activity against *B. cereus*, *E. coli S. aureus,* and *Pseudomonas aeruginosa* (Wattimena *et al.*, 2022; Syafiuddin *et al.*, 2017; Ramesh *et al.*, 2013). Another study showed that AgNPs synthesized using *M. esculenta* had larvicidal activity against mosquito species, *Aedes aegypti* and *Culex quinquefasciatus* (Velayutham *et al.*, 2016). The extract of *Prosopis juliflora* was used to synthesize AgNPs and displayed antibacterial activity against *E. coli* and *P. aeruginosa*, and anti-biofilm activity against *B. subtilis* and *P. aeruginosa* (Arya *et al.*, 2019). The AgNPs synthesized using *Persicaria odorata* leaf extract showed a dose-dependent inhibition of *Staphylococcus epidermidis* and MRSA. Moreover, the *P. odorata*-AgNPs were non-toxic to normal cells and displayed wound healing potential as cell migration was enhanced in comparison to non-treated cells (Lubis *et al.*, 2022). In a study conducted by Sood *et al.*, *Ocimum sanctum*-AgNPs were incorporated into a carbopol gel base and showed antibacterial inhibition similar to commercial products against *S. aureus* and *P. aeruginosa*. Additionally, the nanomaterial was also able to promote wound closure by 96.2% over a period of 14 days (Sood and Chopra, 2018). Tannic acid modified AgNPs have demonstrated their antibacterial properties against a wide range of bacteria, such as *P. aeruginosa*, *E. coli,* and *S. aureus* (Orlowski *et al.*, 2018). AgNPs synthesized from leaf extracts of *Cestrum nocturnum* have shown significant antimicrobial activity against *V. cholera*, *Enterococcus faecalis*, *S. typhi*, *E. coli*, *Proteus vulgaris*, and *Citrobacter* sp. (Keshari *et al.*, 2020).

Some green synthesized AgNPs have been assessed using *in vivo* models. In a previous study, AgNPs prepared with the extracts of *Catharanthus roseus* and *Azadirachta indica* were effective against multidrug-resistant bacteria and enhanced excision wound healing in mice (Shalaby *et al.*, 2022; Lakkim *et al.*, 2020). Stable AgNPs using the *Orchidantha chinensis* fungus successfully treated multistrain-infected wounds in the Sprague Dawley rats (Wen *et al.*, 2016). A recent *in vivo* investigation on wound healing in dogs showed that Ag-incorporated coatings promoted wound healing and hindered microbial colonization at the wound site (Mihai *et al.*, 2019; Mihai *et al.*, 2018). In another study, AgNPs were integrated into mesoporous silica NPs to form biodegradable Ag-MSNs with strong adhesive properties. The Ag-MSNs demonstrated rapid and efficient healing of wounds, excellent antibacterial activity and low toxicity effects in comparison to sutures or MSNs in a mouse skin wound model (Mihai *et al.*, 2019; Lu *et al.*, 2018).

To reduce the side effects of AgNPs, they can be used in low doses along with antibacterial drugs to achieve increased efficiency (Mihai *et al.*, 2019). In a study where AgNPs were combined with tetracycline, an acceleration in wound healing was achieved which was hallmarked by a decrease in bacterial load in both superficial and deep tissue layers in a mouse model (Ahmadi and Adibhesami, 2017). These findings support the use of AgNPs in conjunction with traditional antibacterial agents or dressings to treat infected wounds with efficiency. The functionalization of biocellulose with AgNPs was used as an antibacterial coating for open wounds and was proven to have bactericidal effects against gram-negative pathogens (Pal *et al.*, 2017). Polyester-nylon dressings coated with AgNPs were able to interfere with the colonization of bacteria and biofilm synthesis whilst maintaining a low toxicity profile (Radulescu *et al.*, 2016). Due to the considerable surface energy of AgNPs, they tend to agglomerate resulting in decreased antibacterial activity. However, loading AgNPs on a solid support system may be a solution (Dawadi *et al.*, 2021). Evidence from a study where nanocrystalline Ag dressings were used showed that bacterial levels and chronic inflammatory responses were reduced, thus promoting wound healing. Similarly, healing of chronic venous leg ulcers was linked to the reduction in bacteria and neutrophilic inflammation (Rosique *et al.*, 2015; Sibbald *et al.*, 2007).

The advantages of nanomaterials in wound healing such as their antibacterial effects, stimulation of wound healing, and role in preventing abnormal scarring make a good argument for their use in clinical practice (Mihai *et al.*, 2019). AgNPs have been investigated in numerous clinical trials for

wound therapy, particularly in burns and chronic wounds such as diabetic ulcers (Mihai *et al.*, 2019; Boroumand *et al.*, 2018). There is a growing market for nanotechnology-based products, especially for AgNPs. Since the discovery of the antimicrobial activity of MNPs, AgNPs have taken the lead since they were marketed for the first time in 2016. The market for AgNPs is expected to exceed US$3 billion in 2024 (Sánchez-López *et al.*, 2020). Due to the broad-spectrum antibacterial capacity of silver and AgNPs, silver-based creams and ointments and AgNPs-based biomedical products (e.g., wound dressings) are commercially available (Paladini and Pollini, 2019). There is currently a high commercialization of AgNPs, with 55.4% of the total nanomaterial-based consumer products available on the market (313 out of 565 products) incorporating AgNPs in some way (Paladini and Pollini, 2019). Examples of commercially available AgNPs wound healing products that have been approved by the U.S. FDA include Acticoat™, Bactigras™, Aquacel™, PolyMem Silver™, and Tegaderm™ (Paladini and Pollini, 2019). Some of the properties of Acticoat™ wound dressing that have been observed by patients include wound healing, reduction of infection at the wound site, and reduction in pain. Acticoat™ wound dressing is still under investigation for its use in the therapy of burns. It was concluded in a clinical trial that Acticoat™ wound dressing can prevent infections in burns when used in combination with silver sulphadiazine and chlorhexidine digluconate cream (Mihai *et al.*, 2019; Fong *et al.*, 2005). Other AgNPs-incorporated materials which have shown promising results for wound healing include modified cotton, bacterial cellulose, chitosan, and sodium alginate (Paladini and Pollini, 2019).

1.7 Mechanism of antibacterial effect of AgNPs

It has been proposed that nanomaterials exert their antibacterial effects using several mechanisms (Dawadi *et al.*, 2021). The mechanisms that nanomaterials make use of are: (1) direct contact with the bacterial cell wall; (2) inhibition of biofilm formation; (3) elicitation of both innate and acquired host immune responses; (4) reactive oxygen species (ROS) production; and (5) initiation of interactions with intracellular components such as DNA and/or proteins. Nanomaterials do not possess the same mechanisms of action as antibiotics, therefore are promising candidates which can be extremely useful in eradicating MDR bacteria. Additionally, a single nanomaterial may make use of more than one way to act on MDR bacteria which has an immense impact on the fight against MDR bacteria (Dawadi *et al.*, 2021; Okkeh *et al.*, 2021).

The antibacterial mechanism of AgNPs in diverse biological systems remains perplexing and is an area of research that is not yet fully understood (Dawadi *et al.*, 2021; Paladini and Pollini, 2019). It has been proposed that their mechanisms of action are like that of silver ions. Silver ions act by adhering and destructing the cell wall or membrane; interacting and disrupting biomolecules such as nucleic acids and enzymes; and generating ROS and free radicals which cause oxidative stress in the cells. Silver ions bind non-specifically to various targets affecting the metabolism and structure of bacteria simultaneously which is more advantageous than antibiotics which usually target a specific aspect of bacteria limiting their capabilities (Dawadi *et al.*, 2021; Paladini and Pollini, 2019).

The proposed antibacterial mechanisms of action of AgNPs are depicted in **Figure 1.17**. Due to the nanometric size and increased surface area, it has been proposed that: (1) AgNPs adhere to the surface of the microbial cell resulting in membrane damage and altered transport activity; (2) AgNPs penetrate the microbial cells and interact with cellular organelles; (3) AgNPs increase the ROS inside the cells leading to cell damage; (4) AgNPs cause direct damage to the DNA and disrupt cellular signals (Dawadi *et al.*, 2021; Paladini and Pollini, 2019). AgNPs act on biofilms by destroying bacteria in existing biofilms and dismantling the ability of the bacteria to synthesize exopolysaccharides, thus preventing further biofilm formation (Dawadi *et al.*, 2021; Paladini and Pollini, 2019).

Another mechanism through which AgNPs reduce biofilm formation is by interrupting QS. QS is a bacterial gene expression system controlled by small-signaling molecules (Paladini and Pollini, 2019). AgNPs synthesized using the extract from *S. anacardium* and *B. retusa* successfully displayed antibiofilm activity against numerous clinically relevant human pathogens and altered the development and structure of the biofilm present (Dawadi *et al.*, 2021; Mohanta *et al.*, 2020). Moreover, the main antibacterial mechanism of AgNPs is the creation of sulfuric bonds with either the proteins in the bacterial cell membrane or thiol groups of different enzymes resulting in apoptosis (Vijayakumar *et al.*, 2019). AgNPs may interfere with DNA synthesis during cell division due to the presence of sulfurous and phosphorous bonds leading to the multiplication of bacteria being inhibited (Mihai *et al.*, 2019; Vijayakumar *et al.*, 2019).

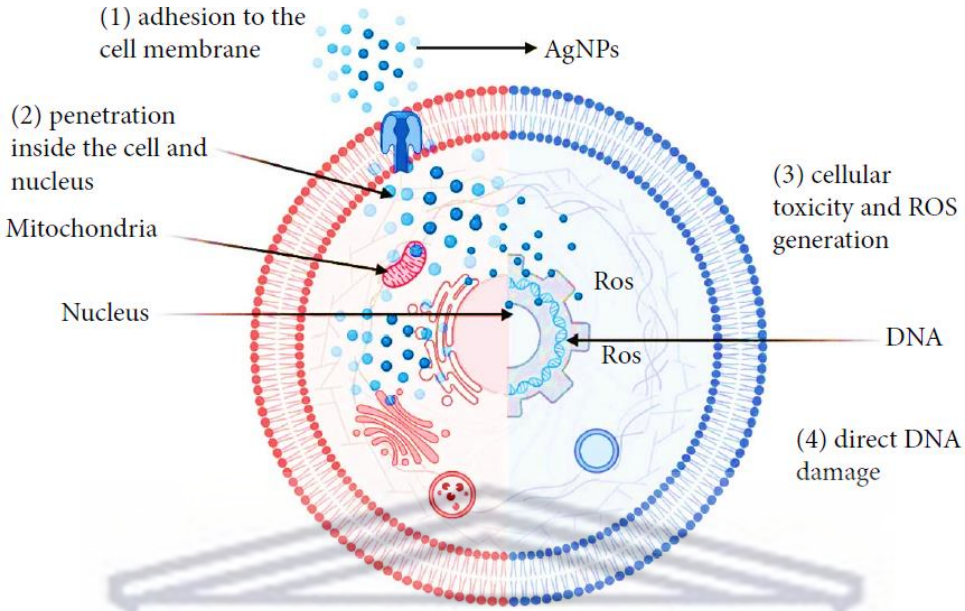

Figure 1.17: Graphical representation of the proposed mechanisms of action of AgNPs in bacterial cells (Adapted from Dawadi *et al.*, 2021).

1.8 Detailed research proposal

1.8.1 Problem statement

Antimicrobial resistance (AMR) has emerged as a significant global health threat that demands urgent multisectoral action. AMR affects human, animal and environmental health, and is therefore considered as a 'One Health' problem. The burden of AMR is mainly due to the misuse of antibiotic therapeutics which is further compounded by the failure of traditional drugs and antimicrobial agents to eradicate multidrug-resistant bacteria along with a reduced drug discovery rate of novel antibiotics. The latest global health threat, the emergence of the COVID-19 pandemic, also exacerbated the spread of AMR due to the incorrect early administration of antibiotics to treat bacterial coinfections in COVID-19 hospitalized patients as a strategy to reduce morbidity and mortality which led to an escalation in the abuse and misuse of antibiotics. Recalcitrant bacterial infections are frequently caused by AMR bacteria which leads to longer length of hospital stays and increased healthcare costs. Longer hospital stays are often associated with a greater risk of contracting nosocomial infections which may result in severe adverse events such as sepsis and death. The current therapeutic strategies available to treat bacterial infections are associated with various limitations (e.g., side effects, poor efficacy, and expensive cost) and largely do not provide a good clinical outcome due to AMR. Therefore, there is an urgent need to develop novel

antimicrobial agents to combat bacterial infections and eliminate the burden of AMR. Green silver nanotechnology can revolutionize the field of AMR by providing alternative novel or improved therapeutic strategies that are promising, cost-effective, and environmentally safe. Biogenic AgNPs with antibacterial efficacy may be employed as an alternative strategy to treat bacterial infections with AMR.

1.8.2 Aims and objectives

The main aim of this study is to investigate the antibacterial effects of biogenic silver nanoparticles (AgNPs) synthesized using *Manihot esculenta* (cassava) aqueous leaf extract.

The specific objectives of this research are as follows:

1. Prepare an aqueous plant extract from the *Manihot esculenta* (cassava) leaves
2. Evaluate the effect of temperature, pH, extract concentration, silver nitrate concentration, and reaction time on the synthesis of AgNPs using the cassava leaf extract (CLE)
3. Synthesize AgNPs using all the optimized conditions for CLE-AgNPs synthesis
4. Characterize the biogenic CLE-AgNPs
5. Determine the stability of the CLE-AgNPs in media
6. Assess the antibacterial activity of CLE and CLE-AgNPs against ESKAPE pathogens

1.8.3 Primary research question

The primary research question for this study is, "Do biogenic silver nanoparticles (AgNPs) synthesized using an aqueous leaf extract from *Manihot esculenta* (cassava) possess antibacterial properties?"

1.8.4 Hypothesis

The hypothesis that will be tested is: "Phytochemicals present in the aqueous leaf extract from *Manihot esculenta* (cassava) may act as reducing, stabilizing, and capping agents in the formation of AgNPs with antibacterial properties."

CHAPTER 2: MATERIALS AND METHODS

2.1. Materials – Reagents, Equipment, and Suppliers

Table 2.1: Materials and reagents used and their suppliers.

Materials and reagents used	Supplier	Company location
AlamarBlue™ cell viability reagent	Thermo Fisher Scientific	Massachusetts, United States of America (USA)
Bovine serum albumin (BSA)	Roche	Basel, Switzerland
Cell culture flasks (25 cm^2 and 75 cm^2)	SPL Life Sciences	Kyonggi-do, South Korea
Ciprofloxacin	Sigma-Aldrich	Missouri, USA
Conical tubes (15 ml and 50 ml)	SPL Life Sciences	Kyonggi-do, South Korea
Disposable cuvette (DTS0012)	Malvern Instruments	Worcestershire, United Kingdom (UK)
Disposable folded capillary cell (DTS1070)	Malvern Instruments	Worcestershire, UK
Folin-Ciocalteu (FC) reagent	Sigma-Aldrich	Missouri, USA
Gallic acid	Sigma-Aldrich	Missouri, USA
Hydrochloric acid (HCl)	Merck	New Jersey, USA
Millipore 0.45-micron filter paper	Sigma-Aldrich	Missouri, USA
Millipore Ultra-purified distilled water (18.2 MΩ cm at 25 °C)	Thermo Fisher Scientific	Massachusetts, USA
Mueller Hinton agar	Sigma-Aldrich	Missouri, USA
Mueller Hinton broth	Sigma-Aldrich	Missouri, USA
Sodium carbonate (Na_2CO_3)	Sigma-Aldrich	Missouri, USA
Nitric acid (HNO_3)	Kimix	Cape Town, Republic of South Africa (RSA)
Phosphate buffered saline (PBS)	Lonza	Basel, Switzerland
Polystyrene 96-well microtiter™ plates	Greiner Bio-One (Lasec)	Cape Town, RSA

Silver nitrate ($AgNO_3$)	Sigma-Aldrich	Missouri, USA
Sodium hydroxide (NaOH)	Sigma-Aldrich	Missouri, USA
Sterile cotton swabs	Lasec	Cape Town, RSA
Sterile loops	Lasec	Cape Town, RSA
Whatman No. 1 filter paper	Sigma-Aldrich	Missouri, USA

Table 2.2: Equipment used and their suppliers.

Equipment	**Supplier**	**Company location**
Analytical weighing balance	Ohaus Adventurer	New Jersey, USA
Blender	Panasonic	Osaka, Japan
Centrifuge 5415D	Eppendorf	Hamburg, Germany
Desiccator	Thomas Scientific	New Jersey, USA
High-Resolution Transmission Electron Microscope (FEI Tecnai G2 20 FEG)	Thermo Fisher Scientific	Massachusetts, USA
IncoTherm Oven	Labotec	Cape Town, RSA
Incubator	Thermo Fisher Scientific	Massachusetts, USA
Fourier-Transform Infrared Spectrophotometer Perkin Elmer Spectrum 400	Perkin Elmer	Waltham, USA
Laminar flow hood	Thermo Fisher Scientific	Massachusetts, USA
pH meter – Crison Basic 20	Lasec	Cape Town, RSA
POLARstar Omega Plate Reader	BMG Labtech	Ortenberg, Germany
Sorvall Lynx 6000 Centrifuge	Thermo Fisher Scientific	Massachusetts, USA
Stuart Heat-Stir CB162 Hot Plate	Lasec	Cape Town, RSA
Thermomixer Comfort	Eppendorf	Hamburg, Germany
Vacuum Filtration System	KNF Labotech	Cape Town, RSA
Varian 710-ES Inductively Coupled Plasma Optical Emission Spectrometer	Varian	California, USA
VirTis freeze dryer - BenchTop Pro with Omnitronics	SP Scientific	Pennsylvania, USA
Zetasizer – Nano-ZS90 System	Malvern Instruments	Worcestershire, UK

Table 2.3: Bacterial strains and their suppliers.

Bacterial strain	ATCC number	Gram reaction	Supplier
Staphylococcus aureus	25923	gram-positive	ATCC*
Methicillin-resistant *Staphylococcus aureus*	33591	gram-positive	ATCC
Escherichia coli	35218	gram-negative	ATCC
Pseudomonas aeruginosa	27853	gram-negative	ATCC
Klebsiella pneumoniae	13883	gram-negative	ATCC
Acinetobacter baumannii	19606	gram-negative	ATCC

*The bacterial strains used in this study were acquired from American Type Culture Collection (ATCC) (Virginia, USA) and used as representative bacterial strains for the testing of the antibacterial activity of the CLE-AgNPs.

2.2 Research Methodology

2.2.1 Preparation of aqueous *Manihot esculenta* (cassava) leaf extract

Fresh leaves of the *Manihot esculenta* (cassava) plant were harvested during summer (February 2021) by Prof. Abram Madiehe in Kuilsriver, Cape Town, SA. The leaves were thoroughly washed with deionized distilled water (ddH_2O) and dried in an oven for 72 hrs at 50 – 55 °C. After drying, the plant material was homogenized using a blender. One hundred grams (100 g) of plant material was added to 1 L of boiling sterile ddH_2O with stirring using a magnetic stirrer. The mixture was allowed to cool down to room temperature (RT). The 0.1 % (w/v) mixture was left to macerate by magnetic stirring for 24 hrs at RT. The mixture was vacuum filtered through glass wool to remove the bulk plant material, and the filtrate was centrifuged at 9 000 rpm for 20 mins at 4 °C**.** The supernatant was vacuum filtered through Whatman No. 1 filter paper and further micro-filtered using Millipore 0.45 µm filter paper. The filtrate was frozen overnight at – 80 °C and freeze-dried for 3 days. Organoleptic observation of the cassava leaf extract (CLE) was conducted before the CLE was weighed and stored at RT in a desiccator with silica gel beads in the dark until further use. Schematic diagram of the preparation of aqueous CLE is depicted in **Figure 2.1**.

Figure 2.1: Schematic diagram of the preparation of aqueous CLE.

2.2.2 Optimization and synthesis of CLE-AgNPs

CLE and 1 mM $AgNO_3$ were mixed in a volume ratio of 1:10 (v/v) in a final reaction volume of 400 µl, and mixed in an Eppendorf thermomixer for the optimization of synthesis conditions. To investigate the influence of various reaction parameters, namely, pH, temperature, the concentration of CLE, and the concentration of $AgNO_3$, on the synthesis of CLE-AgNPs, these parameters were altered for each set of reactions, and the optimum conditions for CLE-AgNPs

synthesis were determined. To prevent photoactivation of $AgNO_3$, the CLE-AgNPs were protected from light during synthesis by covering the samples with aluminium foil. A colour change from light yellow to brown indicated the successful synthesis of CLE-AgNPs.

2.2.2.1 Effect of pH vs. temperature on CLE-AgNPs synthesis

A stock of 125 mg/ml CLE was prepared in sterile ddH_2O and adjusted to a range of pH values. Firstly, the biological pH of the CLE was determined (pH 5.87), then the pH was adjusted to pH 4 and 5 using 0.1 M HCl and pH 6, 7, 8, 9, and 10 using 0.1 M NaOH. The final concentration of all newly prepared samples was 12.5 mg/ml. The CLE samples were centrifuged at 13 200 rpm for 10 min and the pellet was discarded. The supernatants were used in the synthesis of the CLE-AgNPs. Subsequently, 40 µl of 12.5 mg/ml CLE concentration at the various pH values were mixed with 360 µl of 1 mM $AgNO_3$ in 2 ml tubes, respectively. The samples were transferred to the Eppendorf thermomixer comfort and subjected to shaking at 500 rpm for 1 hr at 100 °C. After synthesis, the samples were cooled to RT and centrifuged for 15 min at 13 200 rpm. The supernatants were removed, and the pellets were resuspended in 400 µl of sterile ddH_2O. The procedure was repeated for the following temperatures: 90, 80, 70, 60, 50, 37, and 25 °C.

2.2.2.2 Effect of CLE concentration on CLE-AgNPs synthesis

Various concentrations (1.56, 3.125, 6.25, 12.5, 25, 50 and 100 mg/ml) of CLE (40 µl) at pH 10 were mixed with 360 µl of 1 mM $AgNO_3$ in 2 ml tubes, respectively. The samples were transferred to the Eppendorf thermomixer comfort and subjected to shaking at 500 rpm for 1 hr at 100 °C. After 1 hr, the CLE-AgNPs were cooled to RT and centrifuged for 15 min at 13 200 rpm. The supernatants were removed, and the pellets were resuspended in 400 µl of sterile ddH_2O. The experiment was performed in triplicate.

2.2.2.3 Effect of $AgNO_3$ concentration on CLE-AgNPs synthesis

Forty microlitres (40 µl) of CLE (6.25 mg/ml, pH 10) was mixed with 360 µl of $AgNO_3$ at various concentrations (0.25, 0.5, 0.75, 1, 2, 3, 4, and 5 mM) in 2 ml tubes, respectively. The samples were transferred to the Eppendorf thermomixer comfort and subjected to shaking at 500 rpm for 1 hr at 100 °C. After 1 hr, the CLE-AgNPs were cooled to RT and centrifuged for 15 min at 13 200 rpm.

The supernatants were removed, and the pellets were resuspended in 400 µl of sterile ddH_2O**.** The experiment was performed in triplicate.

2.2.2.4 Effect of reaction time on CLE-AgNPs synthesis

One hundred microlitres (100 µl) of CLE (6.25 mg/ml, pH 10) was mixed with 900 µl of 3 mM $AgNO_3$. The samples were transferred to the Eppendorf thermomixer comfort and subjected to shaking at 500 rpm at 100 °C. The UV-vis spectra were measured after 5, 10, 15, 30, 45, 60, 120, 180, 240, 300, 360, 720, 1440, 2880, and 4320 min.

2.2.2.5 Effect of reaction time vs. CLE concentration on CLE-AgNPs synthesis

Forty microlitres (40 µl) of CLE (pH 10) at various concentrations (3.125, 6.25, 12.5 and 25mg/ml) were mixed with 360 µl of 3 mM $AgNO_3$, respectively. The samples were transferred to the Eppendorf thermomixer comfort and subjected to shaking at 500 rpm for 72 hrs at 25 °C. After 72 hrs, the CLE-AgNPs were centrifuged for 15 min at 13 200 rpm. The supernatants were removed, and the pellets were resuspended in 400 µl of sterile ddH_2O**.** The experiment was performed in triplicate.

2.2.3 Upscaling of CLE-AgNPs synthesis

The synthesis of the CLE-AgNPs was upscaled to a final volume of 50 ml for further characterization, stability assays, and biological applications using the optimum conditions of pH (pH 10), temperature (25 °C), CLE concentration (12.5 mg/ml), $AgNO_3$ concentration (3 mM), reaction time (72 hrs) and shaking at 500 rpm for synthesis. After synthesis, the CLE-AgNPs samples were washed by centrifugation at 13 200 rpm for 15 min and the pellet was resuspended in sterile ddH_2O to a final volume of 50 ml. The experiment was performed in triplicate.

2.2.3 Characterization of CLE-AgNPs

Various analytical techniques, such as Ultraviolet-Visible (UV-vis) Spectroscopy, Dynamic Light Scattering (DLS), High-Resolution Transmission Electron Microscopy (HR-TEM), and Fourier-Transform Infrared (FTIR) Spectroscopy, were employed in the characterization of the CLE-AgNPs.

2.2.3.1 Ultraviolet-visible spectroscopy

Ultraviolet-visible (UV-vis) spectroscopy was used to confirm the formation of CLE-AgNPs by observing the surface plasmon resonance (SPR) properties of the biogenic AgNPs. The presence of CLE-AgNPs was confirmed using a POLARstar Omega microplate reader, by monitoring the reduction of silver ions. The absorbance spectra readings were measured in a wavelength (λ) range of 300 to 800 nm. The CLE-AgNPs samples were diluted in a 1:10 (v/v) ratio with sterile ddH_2O in a final volume of 300 µl in a 96-well flat-bottom microtiter plate. The data obtained were analysed using Omega Mars and Microsoft Excel software.

2.2.3.2 Dynamic Light Scattering

The hydrodynamic size, size distribution, polydispersity index (PDI), and zeta potential (ζ-potential) of the CLE-AgNPs were analysed using a Malvern Zetasizer Nano ZS90. To determine the hydrodynamic size and PDI, the CLE-AgNPs samples were diluted in a 1:10 (v/v) ratio with sterile ddH_2O and transferred into a 10 mm optical density square polystyrene cuvette. The CLE-AgNPs solution was analysed at 25 °C and 90° angle using DLS. For ζ-potential measurements, 0.7 ml of the diluted sample of CLE-AgNPs was transferred into a disposable folded capillary cell and analysed at a voltage of 4 mV at 25 °C and 90° angle.

2.2.3.3 High-resolution transmission electron microscopy

High-resolution transmission electron microscopy (HR-TEM) was used to characterize the core size and morphology of the synthesized CLE-AgNPs. The samples were prepared by placing one drop of sample onto a carbon-coated copper grid, which was then allowed to dry under a xenon lamp for 10 min before being analysed and viewed using an FEI Tecnai G2 20 field-emission gun HR-TEM microscope. The microscope was operated in a bright field mode at an accelerating voltage of 200 kV. Micrograph images were taken and used to estimate the core size of the CLE-AgNPs using ImageJ analysis software (National Institute of Health, USA) and OriginPro 2021 software.

2.2.3.4 Fourier-transform infrared spectroscopy

FTIR analysis was performed to determine the possible compounds responsible for CLE-AgNPs synthesis. Freeze-dried CLE and CLE-AgNPs were individually mixed and ground with potassium

bromide (KBr) in a pestle and mortar. The powdered mixtures were pressed into a pellet and analysed on an Attenuated Total Reflectance (ATR) element using a Perkin Elmer Spectrum 400 FTIR spectrometer. Pressed pure KBr was used for background correction. The data was analysed using Spectrum and OriginPro 2021 software.

2.2.3.5 Induced coupled plasma optical emission spectrometry

Induced coupled plasma optical emission spectrometry (ICP-OES) was used to determine the concentration of silver in the CLE-AgNPs. A Varian 710-ES ICP Optical Emission Spectrometer (Varian) was used for this analysis. Argon gas was used for the excitation of silver atoms. Before the ICP-OES quantification of silver occurred, acid digestion of the CLE-AgNPs was performed. An aliquot of 1 ml of CLE-AgNPs was centrifuged at 13 200 rpm for 15 mins at 25 °C. The concentrated pellet of CLE-AgNPs was transferred to a clean glass vial. Two ml of freshly prepared aqua regia (3 HCl:1 HNO_3) solution was mixed with the CLE-AgNPs in the glass vial and incubated at 90 °C for 24 hrs. After incubation, the remaining solution was diluted to 10 mL with 2% HCl. The experiment was performed in triplicate. The samples were sent to the Chemistry Department at the University of the Western Cape for further analysis. The values reported were based on a calibration curve using a silver ICP standard (Sigma-Aldrich). The formula below was used to calculate the concentration of silver in the sample:

$$Concentration\ of\ silver\ \left(\frac{\mu g}{ml}\right) = Amount\ of\ silver\ detected \times dilution\ factor$$

2.2.4 Further analysis of CLE and CLE-AgNPs

2.2.4.1 Determination of total phenolic content (TPC) of CLE and CLE-AgNPs

To estimate and compare the phenolic content of CLE and CLE-AgNPs, the total phenolic content (TPC) was determined according to a reported method with slight modifications (Ghosh *et al.*, 2012). Standard solutions of gallic acid (15.13, 31.25, 62.5, 125, 250, and 500 ug/ml) were prepared and 25 µl of each concentration of gallic acid standards, 1% CLE and CLE-AgNPs were added to a 96-well plate, respectively. Twenty-five µl of ddH_2O was added to a well as the blank control. This step was followed by the addition of 125 µl of 7.5 % Na_2CO_3 and 125 µl of 10 % Folin-Ciocalteu (FC) reagent to all wells. The 96-well plate was incubated at RT for 20 min and the absorbance was measured at 760 nm using a spectrophotometer (POLARstar Omega

microplate reader, BMG Labtech, Germany). A standard gallic acid curve was used to determine the total phenolic content of the CLE and CLE-AgNPs. The experiment was performed in triplicate.

2.2.4.2 Stability analysis of CLE-AgNPs

This study evaluated the stability of the CLE-AgNPs in MHB, dH_2O, and ddH_2O. In 15 ml Greiner tubes, MHB, dH_2O, and ddH_2O were mixed with CLE-AgNPs in a 1:10 (v/v) ratio in a final volume of 1 ml, respectively. The samples were placed in an incubator at 37 °C. Aliquots of 100 µl were plated in a 96-well plate after 0, 3, 6, and 24 hrs to take UV-vis spectra measurements in a range of 300-900 nm, and the stability of the CLE-AgNPs was determined by observing any changes in the UV-vis spectra (POLARstar Omega microplate reader, BMG Labtech, Germany). The experiment was performed in triplicate.

2.2.5 Antibacterial activity of CLE-AgNPs

2.2.5.1 Bacterial strains

Staphylococcus aureus (*S. aureus*, ATCC 25923), Methicillin-resistant *Staphylococcus aureus* (MRSA, ATCC 33591), *Escherichia coli* (*E. coli*, ATCC 35218), *Pseudomonas aeruginosa* (*P. aeruginosa*, ATCC 27853), *Klebsiella pneumoniae* (*K. pneumoniae*, ATCC 13883), and *Acinetobacter baumannii* (*A. baumannii*, ATCC 19606) were acquired from American Type Culture Collection (ATCC) (Virginia, USA) and used as representative bacterial strains for the testing of the antibacterial activity of the CLE-AgNPs.

2.2.5.2 Standardization of microbial tests using MacFarland turbidity standard

The antibacterial tests were standardized by making use of the MacFarland turbidity standard. The standard was used as a reference to adjust the turbidity of the bacterial suspensions so the number of bacteria to be used in the assay fell within a particular range. Bacterial strains were individually cultured onto Mueller Hinton agar (MHA) plates and incubated at 37 °C for 24 hrs. Single colonies from the individual bacterial cultures were inoculated in 2 ml of Mueller Hinton broth (MHB) and incubated for 2 hrs at 37 °C in a shaking incubator at 200 rpm. Subsequently, the optical density (OD) of the bacterial suspensions was measured at a wavelength of 600 nm using the

spectrophotometer. The OD value was adjusted to 0.08-0.12 which is the equivalent to the 0.5 MacFarland turbidity standard (~ 1.5×10^8 CFU/ml).

2.2.5.3 Determination of antibacterial activity using agar well diffusion method

The agar well diffusion method was used to study the antibacterial activity of the CLE and CLE-AgNPs. The bacterial suspensions at 0.5 MacFarland turbidity standard were uniformly spread onto MHA plates using sterile cotton swabs, respectively. After 5 min of pre-incubation, seven wells (6 mm in diameter) were punched into the MHA plates using a sterile P200 yellow tip. The wells were then filled with 50 µl of five different concentrations of CLE and CLE-AgNPs, respectively. For the negative control, 50 µl of MHB was added to the well. For the positive control, 50 µl of 15 ug/ml Ciprofloxacin was added to the well, except for E. coli where 10 ug/ml Ciprofloxacin was added to the well. The MHA plates were allowed to dry for 1 hr before being inverted and incubated at 37 °C for 24 hrs. The diameter of the zone of inhibition was measured using a ruler to evaluate the antibacterial activity of the CLE and CLE-AgNPs. The experiment was performed in triplicate.

2.2.5.4 Determination of minimum inhibitory concentration

The microdilution assay was used to determine the minimum inhibitory concentration (MIC) of the CLE-AgNPs. Microbial cultures were prepared to a MacFarland turbidity standard as described in 2.2.6.2. The bacterial suspensions were further diluted in a 1:150 (v/v) ratio with MHB and 50 µl of the bacterial suspensions was added to a Greiner Bio-One 96-well flat-bottom polystyrene microtiter™ plate followed by the addition of 50 µl of CLE-AgNPs (serially diluted in sterile ddH_2O) with decreasing concentrations (100, 50, 25, 12.5, 6.25, 3.125, 1.56 and 0.78 %). For the negative control, 50 µl of MHB was added to the well. For the positive control, 50 µl of 15 ug/ml Ciprofloxacin was added to the well, except for *E. coli* where 10 ug/ml Ciprofloxacin was used instead. The plates were sealed and incubated at 37 °C for 24 hrs. After incubation, 10 µl of AlamarBlue™ was added to each well and the plate was covered in foil and incubated for 4 hrs. The non-fluorescent AlamarBlue™ dye (resazurin) is reduced to resofurin, a highly fluorescent pink compound, in the presence of viable bacteria, and, thus, it is used as a colourimetric indicator of viable/non-viable bacteria. Moreover, the intensity of the pink colour and fluorescence is proportional to the number of viable cells present. The MIC was determined as the lowest

concentration where no microbial growth was observed in the wells as well as by spectrophotometry (POLARstar Omega microplate reader, BMG Labtech, Germany) at an absorbance wavelength of 570 nm (reference wavelength at 600 nm) and a fluorescence excitation/emission wavelength of 530-560/590 nm, respectively. The experiment was performed in triplicate.

2.2.5.5 Determination of minimum bactericidal concentration

The minimum bactericidal concentration (MBC) was determined by subculturing the bacterial culture/CLE-AgNPs mixture from the wells that showed no microbial growth (wells that had no colour change) in the microdilution assay onto MHA plates. The plates were incubated at 37 °C for 24 hrs. The MBC was recorded as the lowest concentration at which no growth was observed on the culture plates. The experiment was performed in triplicate.

CHAPTER 3: RESULTS AND DISCUSSION

In recent years, green synthesis of MNPs has received great attention from researchers (Beyene *et al.*, 2017). It has been established as a cost-effective, energy-efficient, and environmentally friendly method that adheres to the sustainable green chemistry principles and makes use of natural reducing and capping agents, making it the preferred method of NP synthesis (Bold *et al.*, 2022; Soltys *et al.*, 2021; Bhardwaj *et al.*, 2020; Chung *et al.*, 2016; Rigo *et al.*, 2013). The use of plant extracts in the synthesis of MNPs is advantageous due to the biocompatibility of phytochemicals present in the extracts and their ability to facilitate the formation of MNPs by acting as reducing and capping agents. The biocompatibility of phytochemicals is conferred onto the synthesized MNPs as the phytochemicals coat the surface of the MNPs (Sharma *et al.*, 2019). The functionalization and stabilization of MNPs are also achieved by using capping agents which also controls their size and shape and protects the NP surface to prevent aggregation (Chinnasamy *et al.*, 2021; Sharma *et al.*, 2019; Noruzi, 2015). Medicinal plants, such as cassava, are rich in phytochemicals that should be further explored for their potential benefits in MNPs synthesis (Bold *et al.*, 2022). The medicinal properties of phytochemicals can be introduced to NPs resulting in the enhancement of biological activities of the NPs (Gnanajobitha *et al.*, 2013). Moreover, recent literature reports on the utilization of biodegradable food waste for the manufacturing of NPs (Sharma et al., 2019). The proper management of biowaste plays a key role in ensuring the sustainability of the bioeconomy (Ortega *et al.*, 2022). Thus, the use of cassava biowaste as a source of phytochemicals to be employed in AgNPs synthesis is an opportunity for the valorisation of cassava biowaste, manufacturing of new high-value biobased products and ensuring a sustainable bioeconomy (Amelework *et al.*, 2021; Oghenejoboh *et al.*, 2021; Olukanni and Olatunji, 2018).

The use of noble metals in MNPs synthesis is appealing as MNPs are endowed with characteristics that make them favourable for various applications in medicine, biology, material science, physics, and chemistry (Rafique *et al.*, 2017; Chung *et al.*, 2016). Silver is predominantly used in nano-based therapies mainly due to its inherent antimicrobial properties (Chinnasamy *et al.*, 2021; Chung *et al.*, 2016). Generally, AgNPs are of particular interest due to their unique physicochemical properties and LSPR which set them apart from other MNPs (Burdușel *et al.*, 2018). The characteristics of AgNPs make them relevant for medical and pharmaceutical

applications where they may function as antimicrobial agents for the efficient prevention and/or treatment of infections (Bruna *et al.*, 2021; Chung *et al.*, 2016). Previous literature has proven that AgNPs are beneficial in wound-healing largely due to their antimicrobial activity. AgNPs are also used in cosmetics, electronics, optics, catalysis, and Raman scattering due to their catalytic, anticancer, antioxidant, anti-inflammatory, and antiviral activity for which they are also well-known (Sharma *et al.*, 2020; Simões *et al.*, 2020; Chung *et al.*, 2016).

The biological properties of AgNPs are usually influenced by their physicochemical properties which are impacted by various reaction parameters of AgNPs synthesis. The intended application of AgNPs should be considered when performing the optimization of the reaction parameters as it is based on the biological properties they exhibit after synthesis with optimized conditions (Bruna *et al.*, 2021; Singh *et al.*, 2020; Ahmed *et al.*, 2016a). The optimization of biosynthesis reaction conditions namely, pH, temperature, the concentration of plant extract, and the concentration of metal precursor salt on the synthesis of AgNPs, enables simple alteration of shape, size, surface chemistry and distribution of AgNPs (Sidhu *et al.*, 2022; Chung *et al.*, 2016; Zhang *et al.*, 2016). It is essential that high yields of stable AgNPs with good monodispersity (uniform size and shape) are synthesized. Hence, performing the characterization of AgNPs during and after the optimization of reaction parameters of AgNPs synthesis is paramount to understand the potential of the synthesized AgNPs (Bruna *et al.*, 2021; Singh *et al.*, 2020). Since AgNPs display variable antibacterial activity based on their physicochemical properties, the production of AgNPs with desirable antibacterial efficacy can be achieved through modifications of the reaction parameters to produce a promising antibacterial agent with optimized properties (Bruna *et al.*, 2021).

This chapter reports and discusses the results of the green synthesis and characterization of biogenic AgNPs and the investigation of their *in vitro* antibacterial effects. In this study, biogenic AgNPs were synthesized using an aqueous CLE, and the synthesized CLE-AgNPs were characterized using UV-vis spectroscopy, DLS, ζ-potential, HR-TEM, and FTIR. The *in vitro* antibacterial effects of the biogenic CLE-AgNPs were tested against six human pathogenic bacteria associated with AMR namely, *S. aureus*, MRSA, *E. coli*, *P. aeruginosa K. pneumoniae*, and *A. baumannii*, using conventional microbiological testing methods such as agar well diffusion, microdilution assay to obtain the minimum inhibitory concentration (MIC), and minimum bactericidal concentration (MBC).

3.1 Visual observation of synthesis of CLE-AgNPs

AgNPs were synthesized using a green synthesis method in which an aqueous plant extract (CLE) mediated the synthesis of AgNPs as the reducing agent and $AgNO_3$ as the silver (Ag^+) ion precursor. The bioreduction reaction was visually observed for a visible change in the colour of the CLE-$AgNO_3$ mixture solution **(Figure 3.1)**. The CLE had a golden-brown hue before being mixed with the clear $AgNO_3$ solution to give a slightly darker golden-brown hue CLE-$AgNO_3$ mixture. An evident colour change which intensified over time from golden-brown to dark brown was observed, indicating the formation of AgNPs from the Ag^+ ion precursor. The colour change can be attributed to the surface plasmon resonance (SPR) and bioreduction of Ag^+ by phytochemicals present in the CLE (Dada *et al.*, 2019). Moreover, the colour change has been previously reported to preliminary confirm the formation of AgNPs as it is expected that AgNPs have a characteristic brown colour (Tenderwealth *et al.*, 2018). Another study by Bold *et al.* (2022) showed that the colour change from pale yellow to colloidal dark brown as a function of time is an indication that AgNPs have been successfully synthesized (Bold *et al.*, 2022). It is characteristic of several types of MNPs to exhibit distinct colours in solution due to their optical properties. The colour exhibited by AgNPs is due to their LSPR properties. The strong absorption and scattering of light properties of AgNPs give rise to strong interactions between light at definite wavelengths in the visible region of the electromagnetic spectrum and the conductive electrons in the metal surface leading to different colouring absorbed and reflected (Al Azad *et al.*, 2017).

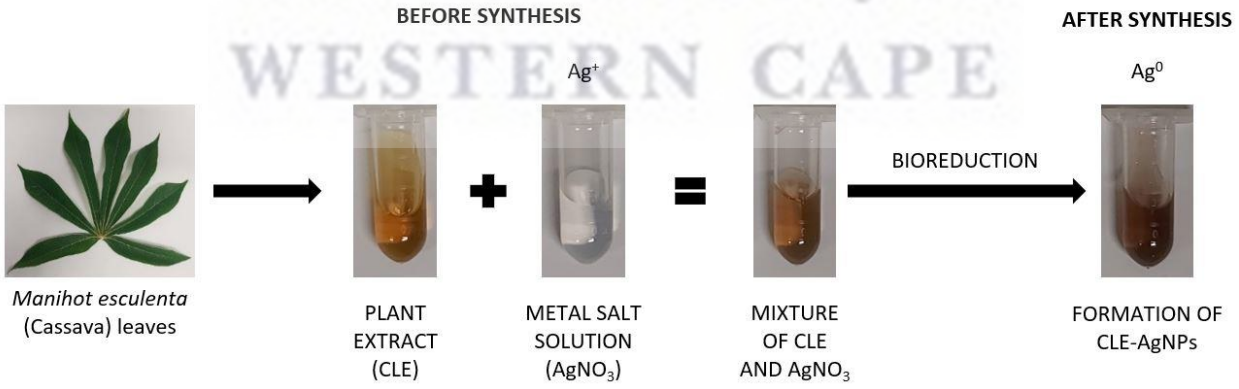

Figure 3.1: Schematic diagram of CLE-mediated synthesis of AgNPs.

3.2. Characterization of synthesized CLE-AgNPs

3.2.1. UV-vis spectroscopy of CLE-AgNPs

Various reaction conditions such as pH, temperature, extract, and silver nitrate concentration may affect the physicochemical properties of the CLE-AgNPs which influences their application (Singh *et al.*, 2020). Consequently, the intended application needs to be considered when optimizing reaction parameters as it is often important that high yields of stable AgNPs with good monodispersity (uniform size and shape) are synthesized. For further confirmation of the successful synthesis of CLE-AgNPs, UV-vis spectroscopy was used to monitor the SPR band of CLE-AgNPs.

3.2.1.1. Effect of pH vs. temperature on CLE-AgNPs

Figure 3.2 displays the effect of varying pH and temperatures on the formation of CLE-AgNPs. The presence of the SPR peak in the UV-vis absorption spectra along with a colour change of the reaction mixture as previously mentioned indicates the successful formation of AgNPs. The colour change is due to the SPR of the synthesized NPs (Dube *et al.*, 2020; Ahmed *et al.*, 2016b). According to literature, the SPR band of AgNPs is normally observed in the range of 380 to 450 nm (Lee and Jun, 2019). Other studies have reported that the SPR band of AgNPs can also be found between 400-500 nm (Bold *et al.*, 2022). The intensity of the SPR absorbance peak or 'maximum absorbance' (λmax) provides information regarding the size and concentration of the synthesized NPs (Dube *et al.*, 2020). Another study reported that the change of the colour from transparent to yellowish-brown took place gradually and it correlated to the formation of AgNPs synthesized with *M. esculenta*. The process of nucleation is associated with the change of the colour as once the formation of NPs stops, the colour also stops changing and stays constant (Wattimena *et al.*, 2022).

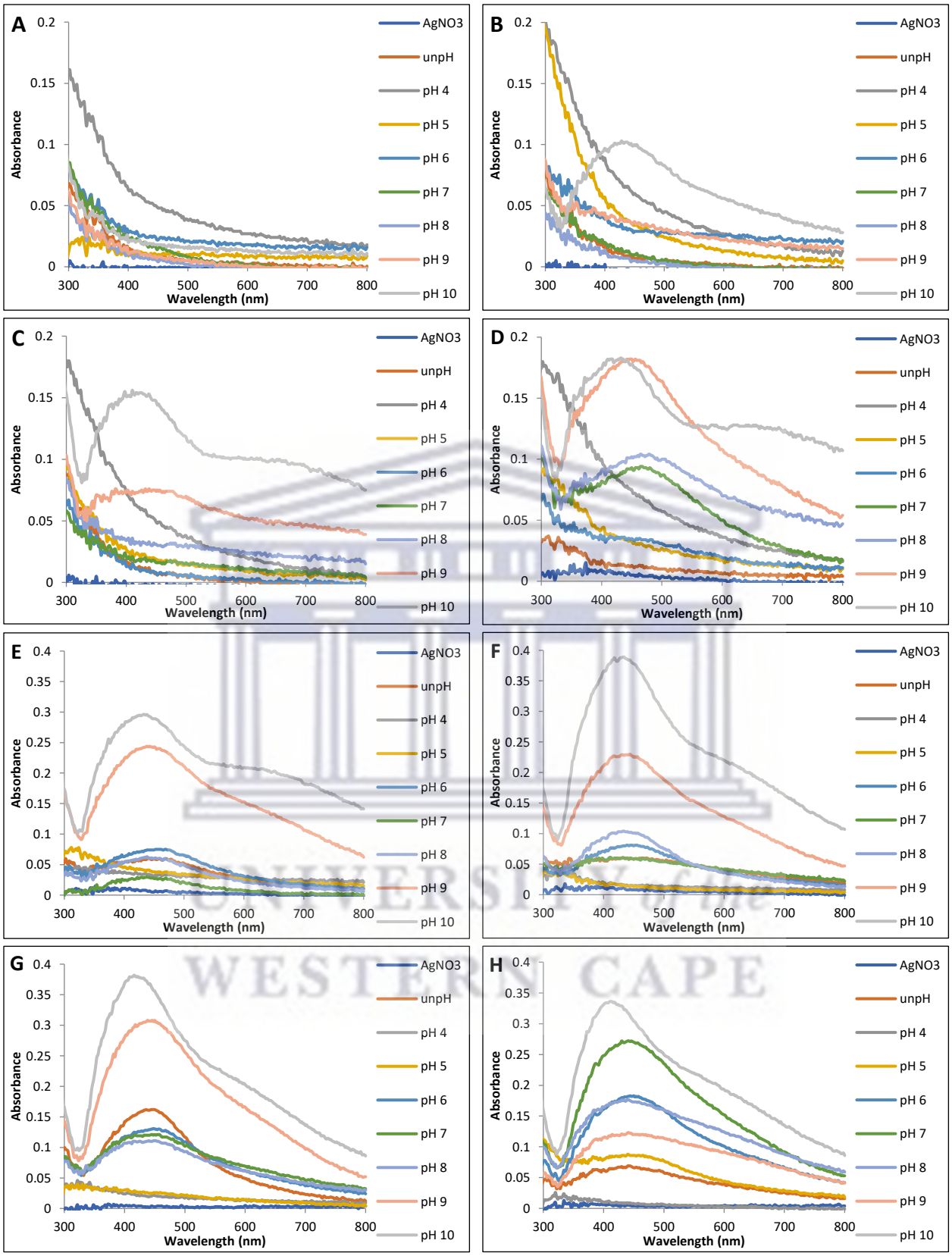

Figure 3.2: UV-vis absorption spectra for various reactions showing the effect of varying pH and temperatures on the formation of CLE-AgNPs (A: 25, B: 37, C: 50, D: 60, E: 70, F: 80, G: 90 and H: 100 °C).

Figure 3.2. A show that there was no significant reduction of the Ag^+ to AgNPs at 25 °C for any of the pH conditions, as no SPR peaks nor any change in colour of reaction mixtures were observed. In previous studies, the absence of a colour change and characteristic SPR peaks indicated that the synthesis of NPs was a failure (Philip *et al.*, 2011). This may be due to a lack of strong reducing phytochemicals in the CLE and/or the existing phytochemicals demands the use of higher temperatures to initiate the reduction reaction (Tyavambiza *et al.*, 2021). Moreover, the CLE was incubated with $AgNO_3$ for only 1 hr and the reaction may have required longer periods of incubation to initiate the reduction process of Ag^+ to Ag^0 by the CLE at low temperatures. When the temperature of the reaction is increased then the rate of reaction and rate of particle formation is increased as well. Moreover, when the reaction is allowed to run for longer periods, changes in the size and shape of synthesized NPs can be observed (Zhang *et al.*, 2020a; Makarov *et al.*, 2014; Park, 2014).

Figure 3.2. B shows that the reduction of the Ag^+ to Ag^0 occurred at 37 °C as there was a broad SPR band observed for pH 10. No SPR peaks were observed for the remaining pH values indicating that CLE-AgNPs were only formed at pH 10 when incubated at this particular temperature. The CLE-AgNPs synthesized at pH 10 had a λmax at 428 nm and OD value of 0.103. This may have occurred due to the fact that adjustments made to the pH results in a change in the charge of the phytochemicals present in the extract. Previous studies have displayed that synthesis of NPs at this pH could be due to the dissociation of NaOH in water which generates negatively charged hydroxide ions (OH-) which enhances the complete reduction of Ag^+ ions into AgNPs (Traiwatcharanon *et al.*, 2016). The deprotonation of functional groups present in the biomolecules allows for the adsorption of Ag^+ ions by electrostatic attraction or affinity interaction resulting in the AgNPs with small size and well-dispersed distribution (Miranda *et al.*, 2022).

Figure 3.2. C shows that two broad SPR bands were observed for pH 9 and 10 indicating CLE-AgNPs synthesis at 50 °C. No SPR peaks were observed for the remaining pH 4-8 indicating that there was no synthesis of CLE-AgNPs at the pH values within this range. The absence of SPR peaks at low pH values demonstrates that acidic conditions are not favourable for the synthesis of AgNPs. It is possible that the biomolecules that facilitate the bioreduction process of Ag^+ ions into AgNPs may have been protonated under acidic conditions, therefore, the synthesis of NPs did not occur (Omran *et al.*, 2018). The CLE-AgNPs synthesized at pH 9 had a λmax at 382 nm and an

OD value of 0.076 and the CLE-AgNPs synthesized at pH 10 had a λmax at 398 nm and an OD value of 0.155. The peak for pH 10 at 50 °C had an OD value higher than the peak for pH 10 at 37 °C. The difference in the values of λmax and OD signifies the differences in the NP size and concentration (Tripathy *et al.*, 2010). Moreover, it has been demonstrated that increased temperatures increase the rate at which AgNPs synthesis are formed. Sankar and colleagues (2013) showed that AgNPs synthesised with aqueous leaf extract of *Origanum vulgare* at 60 °C had a conversation rate of Ag^{+} ions to AgNPs of 45% whilst the conversation rate at 90 °C was 100% (Sankar *et al.*, 2013). The temperature of the reaction influences the rate at which AgNPs grow, thus, an increase in temperature results in the faster growth of AgNPs (Dawadi *et al.*, 2021; Venugopal *et al.*, 2017).

Figure 3.2. D shows the successful synthesis of CLE-AgNPs at 60 °C, four broad SPR peaks were observed for pH 7, 8, 9 and 10. There were no SPR peaks observed for pH 4-6. The CLE-AgNPs synthesized at pH 7, 8, 9 and 10 had λmax at 466, 472, 449, and 432 nm with OD values of 0.094, 0.104, 0.182, and 0.183, respectively. At this temperature, the peaks for pH 9 and 10 had slightly higher OD values than the peaks for the same pH values at 50 °C. Broader bands may be due to the insufficient number of biomolecules required for capping and stabilizing of the synthesized NPs (Dube *et al.*, 2020; Philip *et al.*, 2011).

Figure 3.2. E shows CLE-AgNPs were successfully synthesized at all pH values besides pH 4 and 5 at 70 °C with broad SPR bands at pH 6-10. The SPR bands for pH 6, 7, 8, 9, and 10 had λmax at 461, 438, 438, 440, and 435 nm, with OD values of 0.075, 0.03, 0.063, 0.244, and 0.296, respectively. The SPR peaks for pH 9 and 10 had higher OD values than pH 6, 7, and 8. The SPR bands for pH 6, 7, and 8 were quite broad and relatively flat. At this temperature, an increase of more than 0.1 in the OD values for pH 10 was observed as compared to the peak for the same pH value at 60 °C.

Figure 3.2. F shows that the same findings observed at 70 °C was observed at 80 °C, CLE-AgNPs were successfully synthesized at all pH values besides pH 4 and 5 with broad SPR bands at pH 6-10. The SPR bands for pH 6, 7, 8, 9, and 10 had λmax at 447, 421, 433, 444, and 432 nm, with OD values of 0.081, 0.061, 0.104, 0.23, and 0.389, respectively. The SPR peak for pH 10 was significantly higher than the peaks for the rest of the pH values that were able to facilitate the

synthesis of CLE-AgNPs. This finding further confirms that AgNPs synthesis is favoured by basic conditions.

Figure 3.2. G shows that the same phenomenon that occurred at 70 and 80 °C was observed at 90 °C with the CLE-AgNPs being successfully synthesized at all pH values besides pH 4 and 5. SPR bands were observed for pH 6-10. The SPR bands for pH 6, 7, 8, 9, and 10 had λmax at 448, 451, 446, 444, and 416 nm, with OD values of 0.131, 0.121, 0.111, 0.308, and 0.382, respectively. The SPR bands were broad with a low OD for pH 6, 7, and 8, indicating high polydispersity and low concentration as compared to the SPR bands of pH 9 and 10 which were broad with a higher OD indicating higher concentrations of CLE-AgNPs being produced.

Figure 3.2. H shows that CLE-AgNPs were synthesized at all pH values besides pH 4 at 100 °C. SPR peaks were observed for pH 5-10. The SPR bands for pH 5, 6, 7, 8, 9, and 10 had λmax at 440, 447, 438, 440, 441, and 412 nm, with OD values of 0.088, 0.183, 0.272, 0.177, 0.123, and 0.336, respectively. The SPR peak for pH 10 had the highest OD value indicating that more CLE-AgNPs were synthesized at this pH as compared to the other pH values. The SPR bands showed an increase in the SPR peaks from pH 5 to 7 before decreasing at pH 8 and 9 indicating that the temperature was not favourable for the optimal synthesis of CLE-AgNPs at the latter pH values. The SPR band for pH 10 (λmax at 412 nm) showed that the CLE-AgNPs were blue-shifted which indicated that CLE-AgNPs of small size were produced. Numerous studies have proven that NPs synthesized using plant extract-mediated methods produce larger NPs at acidic pHs (pH 2–4) in comparison to basic pHs. Reyes and colleagues (2020) reported that NPs formed at basic pHs are smaller in size and are generally formed in higher yields (Miranda *et al.*, 2022; Reyes *et al.*, 2020). In another study, it was shown that NPs at pH 3 were greater than NPs at pH 8 indicating that alkaline conditions are more favourable for NP synthesis (Lade and Shanware, 2020).

Notably, AgNPs were only synthesized at 70, 80, 90, and 100 °C with CLE at biological pH (pH 5.87) and CLE at pH 6 also only synthesized AgNPs at these temperatures. The AgNPs synthesized at these pH values had similar SPR peaks in the range of 442 – 461 nm with OD values in a range of 0.06 – 0.183. It has been previously reported that a change in pH results in a change in the charge of polyphenols present in the extract. Studies have shown that NP synthesis occurs at high pH due to the dissociation of NaOH in water which results in negatively charged hydroxide ions (OH^-) being produced and encourages the complete reduction of Ag^+ into AgNPs

(Traiwatcharanon *et al.*, 2016). Low SPR peaks were observed at low pH ranges with no peak being observed at pH 4 for any of the temperatures. Thus, it is shown that acidic conditions are not favourable for the synthesis of AgNPs. Under acidic conditions, the phytochemicals which play a role in the bioreduction of Ag^+ ions may become protonated and negatively affect the synthesis of NPs (Omran *et al.*, 2018). A previous study also reported that an alkaline environment enhanced the reduction and stabilization capacity of the antioxidants present in hot water olive leaf extract used to synthesise AgNPs (Dawadi *et al.*, 2021; Khalil *et al.*, 2014).

There was an overall increase in absorbance with increasing temperatures which indicated higher synthesis yields. In this study, none of the pH or temperatures had OD values above 1. Although pH 10 had the highest SPR peaks at lower wavelengths, there were also absorption tails towards longer wavelengths (~ 500 nm) which indicated the aggregation of AgNPs. Altering the extract and silver concentration may allow for the synthesis of stable, monodispersed AgNPs which are desirable. The optimum temperature and pH chosen for synthesis were 100 °C and pH 10, respectively.

Moreover, elevated temperatures facilitate the synthesis of NPs and play a role in determining the size, shape and yield of NPs synthesized using plant extracts (Tyavambiza *et al.*, 2021; Shah *et al.*, 2015; Liu *et al.*, 2011). In this study, it was shown that with increasing temperature from 37 to 100 °C, a blue-shift of the λmax of the CLE-AgNPs synthesized at pH 10 was observed showing that the CLE-AgNPs produced became smaller as temperature were increased. Another study also described that basic pH conditions (pH 8-10) leads to improvements in the yield of the synthesised AgNPs and the production of smaller sized NPs. In contrast, at acidic pH conditions, precipitation of Ag^+ ions occurs and the synthesis of AgNPs is hardly observed (Sánchez-López *et al.*, 2020; Jang *et al.*, 2018). The results of this study are in agreement with literature that states that the addition of –OH groups assist in the reduction process of metal ions (Feng *et al.*, 2007).

AgNPs synthesised at ambient temperatures adheres to the green chemistry principles (Dahl *et al.*, 2007). However, it has been reported that an increase in temperature leads to an increase in the average kinetic energy of molecules present in the reaction (Myers, 2003). Previous studies have demonstrated that more uniform and smaller-sized NPs were synthesized at a faster rate with the use of higher temperatures as compared to lower temperatures (Rajeshkumar *et al.*, 2017; Mountrichas *et al.*, 2014).

3.2.1.2. Effect of CLE concentration on CLE-AgNPs synthesis

Figure 3.3 displays the effect of varying CLE concentrations on the formation of CLE-AgNPs. AgNPs were successfully synthesized with all CLE concentrations except 1.56 mg/ml. At a low concentration of extract, there are fewer phytochemicals present in the reaction for the reduction of Ag^{+} ions to Ag^{0}. The SPR band for 6.25 mg/ml had a λmax at 432 nm and the highest OD value (0.371) of all the CLE concentrations used indicating the highest yield of CLE-AgNPs. This was followed by the SPR band for 12.5 mg/ml that had a λmax at 416 nm and an OD value of 0.334. Moreover, the SPR bands for the concentrations of 3.125, 12.5, 25, 50, and 100 mg/ml were broader than the SPR band of 6.25 mg/ml, and absorption tails towards longer wavelengths were present which showed aggregation of the AgNPs at these CLE concentrations. Although, the CLE-AgNPs synthesized with 12.5 mg/ml were relatively smaller in size as compared to 6.25 mg/ml, there was an absorption tail toward the longer wavelengths that indicate the presence of larger AgNPs which may be due to aggregation. Therefore, the optimum concentration for CLE was determined to be 6.25 mg/ml.

In a previous study, AgNPs were synthesized using various concentrations of tea leaf extract and silver nitrate in order to control the size of the resulting AgNPs. It was observed that with an increase in the extract concentration, the SPR peak got sharper with a blue shifting of colour which indicated that there was a reduction in AgNPs diameter (Moulton *et al.*, 2010). Low concentrations of extract are able to reduce Ag^{+} ions, however, they cannot protect spherical AgNPs from agglomeration as there is too little biomolecules to act as capping agents. The number of biomolecules present in higher concentrations of extract is able to reduce and stabilize AgNPs as well as play a key role in the formation of spherical AgNPs (Dawadi *et al.*, 2021). It has been reported that extremely high concentrations of plant extract may negatively affect the formation of NPs (Tyavambiza *et al.*, 2021). In another study, it was also reported that an increase in the concentration of the plant extract results in the formation of NPs with sharper absorbance peaks (Benakashani *et al.*, 2016). This observation agrees with the observation made in this study, where an increase in the CLE (from 1.56 to 6.25 mg/ml) resulted in the enhancement of the formation of CLE-AgNPs.

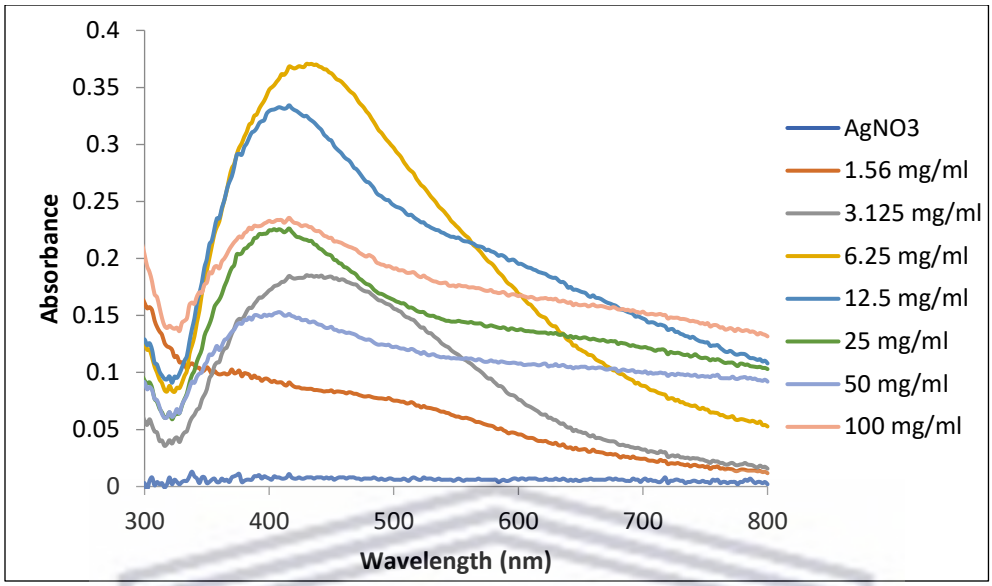

Figure 3.3: UV-vis absorption spectra showing the effect of varying CLE concentration on the formation of CLE-AgNPs. The experiment was performed in triplicate (n=3) and the graphs are presented as average results.

3.2.1.3. Effect of $AgNO_3$ concentration on CLE-AgNPs synthesis

Figure 3.4 displays the effect of varying $AgNO_3$ concentration on the formation of CLE-AgNPs. AgNPs were successfully synthesized at all the $AgNO_3$ concentrations used indicated by the presence of SPR bands. The SPR bands of the AgNPs showed that with increasing $AgNO_3$ concentration, there was an increase in the OD values. The SPR bands of 0.25, 0.5, 0.75, 1, 2, 3, 4, and 5 $AgNO_3$ had λmax at 390, 414, 426, 428, 448, 434, 434, and 436 nm, respectively. The SPR bands of 0.25, 0.5, 0.75, 1, and 2 mM $AgNO_3$ were broad with a low OD indicating that the AgNPs were polydispersed at a greater degree as compared to the other concentrations of $AgNO_3$. The OD values for these concentrations were all below 0.3 while the OD values for 3, 4, and 5 mM $AgNO_3$ were 0.583, 0.7, and 0.801, respectively. It has been previously reported that NPs synthesized with higher metal salt concentrations are prone to destabilization (Omran *et al.*, 2018). The initial concentration of metal ions is also directly related to the average size of NPs, therefore, an increase in the initial metal ion concentration may lead to an increase in the size of NPs (Htwe *et al.*, 2019). In this study, 3 mM $AgNO_3$ was chosen as the optimum $AgNO_3$ concentration.

The findings of this study are in agreement with the findings of a previous study which reported on the synthesis of AgNPs synthesized with *M. esculenta* leaf extract using $AgNO_3$ at

concentrations of 0.5 and 1 mM. The SPR peaks observed for the reactions using 0.5 and 1 mM $AgNO_3$ had λmax at 422 nm and 426 nm, respectively (Velayutham *et al.*, 2016). A previous study investigated the effect of $AgNO_3$ on synthesis of AgNPs with the concentrations of 1 and 3 mM $AgNO_3$, which are commonly used in the synthesis of AgNPs as reported in the literature. The AgNPs synthesized with 3 mM $AgNO_3$ gave sharper absorbance peaks and formed a larger quantity of AgNPs (Tyavambiza *et al.*, 2021).

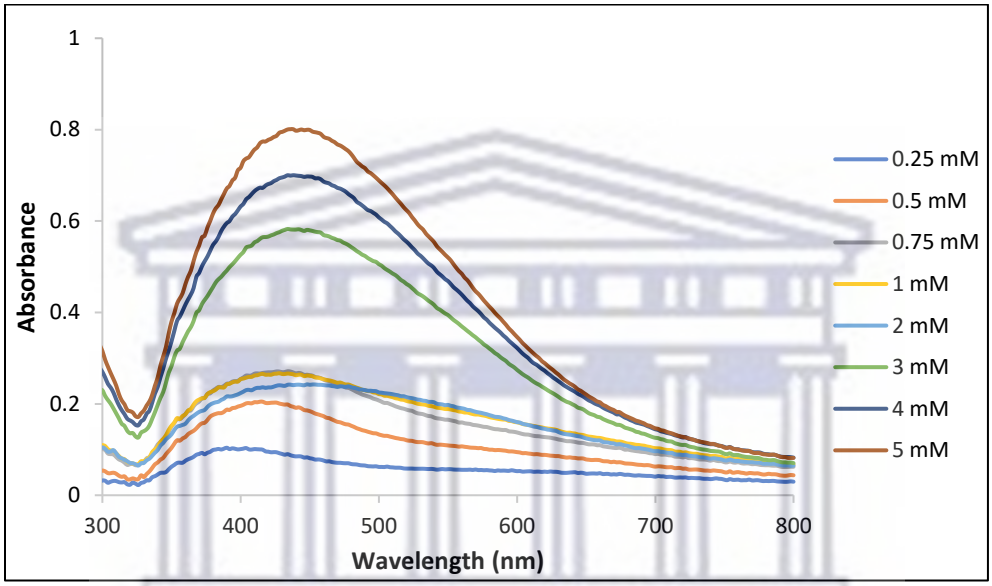

Figure 3.4: UV-vis absorption spectra showing the effect of varying $AgNO_3$ on the formation of CLE-AgNPs. The experiment was performed in triplicate (n=3) and the graphs are presented as average results.

3.2.1.4. Effect of CLE concentration vs. 3mM $AgNO_3$ on CLE-AgNPs synthesis

Due to the broadness of the SPR band at 3 mM $AgNO_3$ concentration in the previous experiment, synthesis with 3 mM $AgNO_3$ and varying concentrations of CLE (3.125, 6.25, 12.5, and 25 mg/ml) at 25 °C for a longer period (72 hrs) was performed to determine whether more monodispersed CLE-AgNPs with more desirable SPR properties could be synthesized. The decision to reduce the temperature of the reaction and increase the reaction time was based on the fact that in a preliminary study, CLE-AgNPs were synthesized at RT and UV-vis spectra were measured after 24, 48 and 72 hrs. Synthesis of CLE-AgNPs was observed after 24 hrs, however, the OD was too low at 24 and 48 hrs indicating a low yield of CLE-AgNPs (data not shown) which was not desirable in this study therefore the reaction was allowed to run for 72 hrs which gave satisfactory

results for the CLE-AgNPs synthesis. Previous studies have shown the synthesis of AgNPs is achievable at RT but over a longer period of time (Siddiqi *et al.*, 2018).

Figure 3.5 displays the effect of varying CLE concentration on the formation of CLE-AgNPs at 25 °C for 72 hrs. CLE-AgNPs were successfully synthesized at all concentrations of CLE with an increase in OD being observed for CLE concentrations of 3.125, 6.25, and 12.5 mg/ml. Interestingly, a decrease in the OD was seen for 25 mg/ml CLE. The SPR bands for each concentration became narrower with increasing CLE concentration from 3.125-12.5 mg/ml. AgNPs synthesized at a CLE concentration of 12.5 mg/ml had a λmax at 429 nm and an OD value of 0.597 indicating the highest synthesis yield of all CLE concentrations. Therefore, the optimum conditions for concentration of CLE and temperature were determined to be 12.5 mg/ml and 25 °C with a reaction time of 72 hrs. A previous study reported that on the synthesis of AgNPs with different concentrations of yellow exotic oysters mushroom (*Pleurotus cornucopiae* var. *citrinopileatus*) extract and 1 mM $AgNO_3$ at 25 °C for 24, 48, and 72 hrs. A colour change from yellow to yellowish-brown was observed and the SPR peak had a λmax between 420 and 450 nm, characteristic of AgNPs. The width of the SPR band suggested that the NPs were polydispersed in nature (Siddiqi *et al.*, 2018; Owaid *et al.*, 2015).

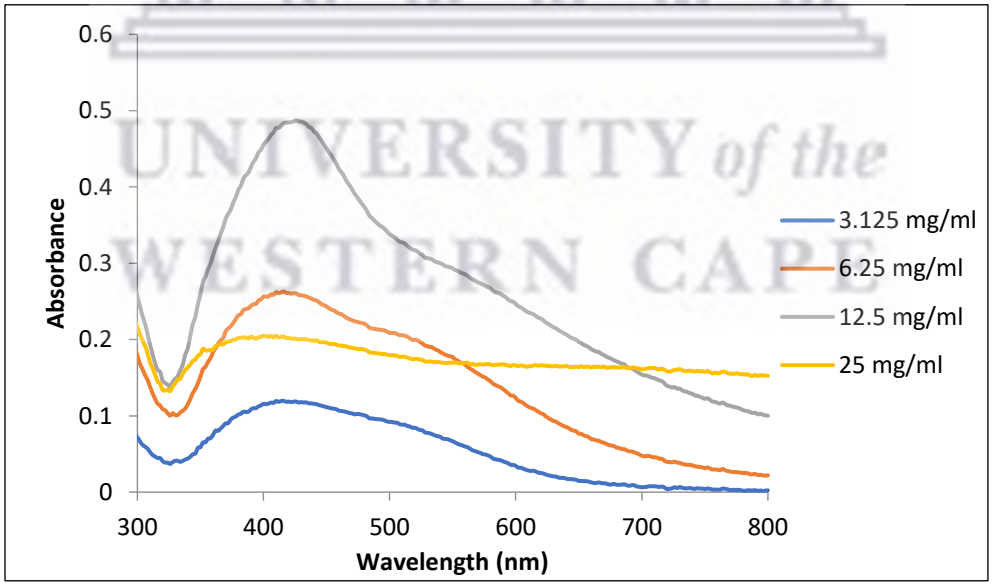

Figure 3.5: UV-vis absorption spectra showing the effect of varying CLE concentration on the formation of CLE-AgNPs at 25 °C for 72 hrs using 3 mM $AgNO_3$. The experiment was performed in triplicate (n=3) and the graphs are presented as average results.

3.2.1.5. Upscaled synthesis of CLE-AgNPs with all optimum synthesis conditions

Figure 3.6 displays the UV-vis absorption spectra of CLE-AgNPs synthesized using all optimum synthesis conditions – CLE concentration: 12.5 mg/ml, $AgNO_3$ concentration: 3 mM, temperature: 25 °C, pH 10, time of reaction: 72 hrs, shaking at 500 rpm – in a final reaction volume of 50 ml. There was a single SPR peak observed on the UV-vis spectra which confirmed the synthesis of the spherical CLE-AgNPs. The synthesized CLE-AgNPs had a λmax at 432 nm with an OD of 0.511. The CLE-AgNPs were subjected to further characterization to determine the size, shape, polydispersity index, and zeta potential. These findings are in agreement with those found in previous literature (Wattimena *et al.*, 2022; Syafiuddin *et al.*, 2017). In previous studies, leaves of *M. esculenta* have been used to synthesize AgNPs. A previous study synthesized AgNPs using *M. esculenta* leaf extract and observed a λmax at 356 nm with a single SPR peak in the UV-vis spectrum. A single peak in the UV-vis spectrum is associated with spherical NPs and two or more peaks correspond with irregular shaped AgNPs, dependent on their symmetry (Syafiuddin *et al.*, 2017). Another study showed *M. esculenta*-AgNPs synthesized from the leaf extract had a λmax at 430 nm whilst the tuber extract had a λmax at 415 nm (Wattimena *et al.*, 2022). The observations made in this study are also in agreement with a study where AgNPs were synthesized with *Cotyledon orbiculata* aqueous leaf extract, which had a λmax around 420 nm, characteristic of AgNPs (Tyavambiza *et al.*, 2021). Another study reported that the medicinal plant *Rhodiola rosea* facilitated the synthesis of AgNPs and revealed that the AgNPs had a λmax around 430 nm with a single narrow SPR peak indicating that the AgNPs were spherical and monodispersed (Bold *et al.*, 2022). The optimization of the synthesis of AgNPs with *Azadirachta indica* was conducted in another study and the optimized reaction parameters (addition of 5 mL of AI-extract (pH 7) to 45 mL of 1 mM $AgNO_3$ and incubated at 25 °C in dark at 200 rpm for 18 hrs) were used to synthesise stable *A. indica*-AgNPs (Chinnasamy *et al.*, 2021)

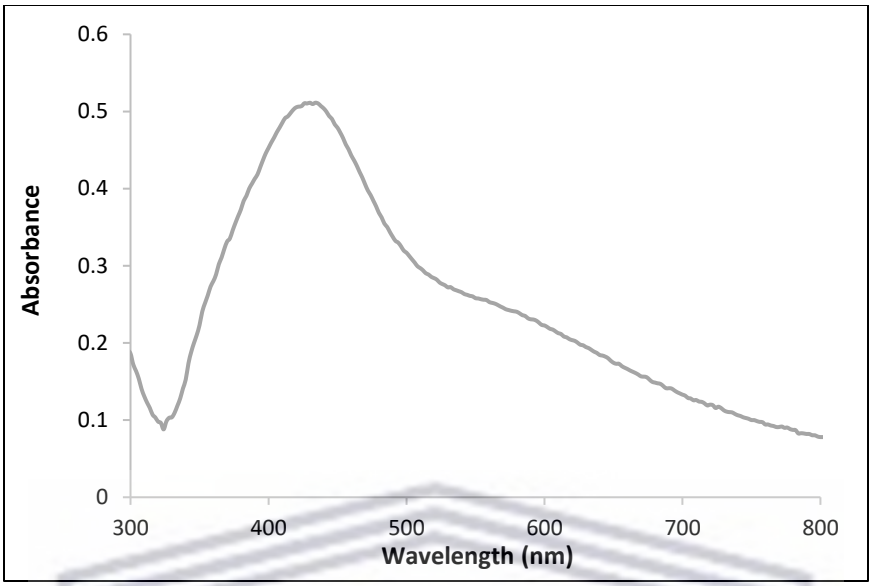

Figure 3.6: UV-vis absorption spectra showing the upscaled synthesis of CLE-AgNPs using all optimum conditions. (CLE concentration: 12.5 mg/ml, $AgNO_3$ concentration: 3 mM, temperature: 25 °C, pH 10, time of reaction: 72 hrs, shaking at 500 rpm). The experiment was performed in triplicate (n=3) and the graphs are presented as average results.

3.2.2. Dynamic light scattering analysis of CLE-AgNPs

The hydrodynamic size of the CLE-AgNPs was measured by DLS. DLS is one of the preferred analytical methods used in the characterization of AgNP size (Omran *et al.*, 2018). **Figure 3.7** displays the hydrodynamic size distribution of the biogenic CLE-AgNPs. The biogenic CLE-AgNPs had a Z-average hydrodynamic diameter of 44.49 ± 0.55 nm based on the cumulants analysis. According to distribution analysis, the size distribution by intensity was 84.8 % of the CLE-AgNPs suspension had a hydrodynamic diameter of 91.5 ± 50.82 nm, and 15 % of the CLE-AgNPs suspension had a hydrodynamic diameter of 12.18 ± 4.042 nm. Two distinct peaks in the hydrodynamic size distribution can be seen in **Figure 3.**7. The hydrodynamic diameter is dependent on the size of the particle "core" and the surface structure as well as the type and concentration of any ions in the medium (Maguire *et al.*, 2018).

The PDI, a dimensionless measure of the broadness of the size distribution, of the CLE-AgNPs was determined as 0.52 ± 0.014 which indicated slight polydispersity which may be attributed to the two distinct peak sizes of the CLE-AgNPs. Previous literature has reported that a PDI of 0.7 indicates a broad size distribution of AgNPs while a PDI between 0.001 and 0.5 indicates a good

monodispersity of the AgNPs (Tarannum *et al.*, 2019). Therefore, the results indicated that the biogenic CLE-AgNPs were within the nanoscale range but were larger in size and relatively polydisperse. This observation is in agreement with observations reported by Dube *et al.* (2020) where polydispersed SAL-AgNPs and SF-AgNPs had PDI values of 0.63 ± 0.03 nm and 0.612 ± 0.02 nm, respectively (Dube *et al.*, 2020). In another study, the leaf extract of *Enicostemma axillare* was used to synthesize AgNPs and yielded NPs with sizes ranging between 25 to 80 nm and a PDI of 0.412 (Raj *et al.*, 2018). A previous study specified that the Z-average hydrodynamic diameter could only be considered as an accurate measurement of the hydrodynamic size if the NPs in the sample are monomodal and/ or monodispersed (Lim *et al.*, 2013).

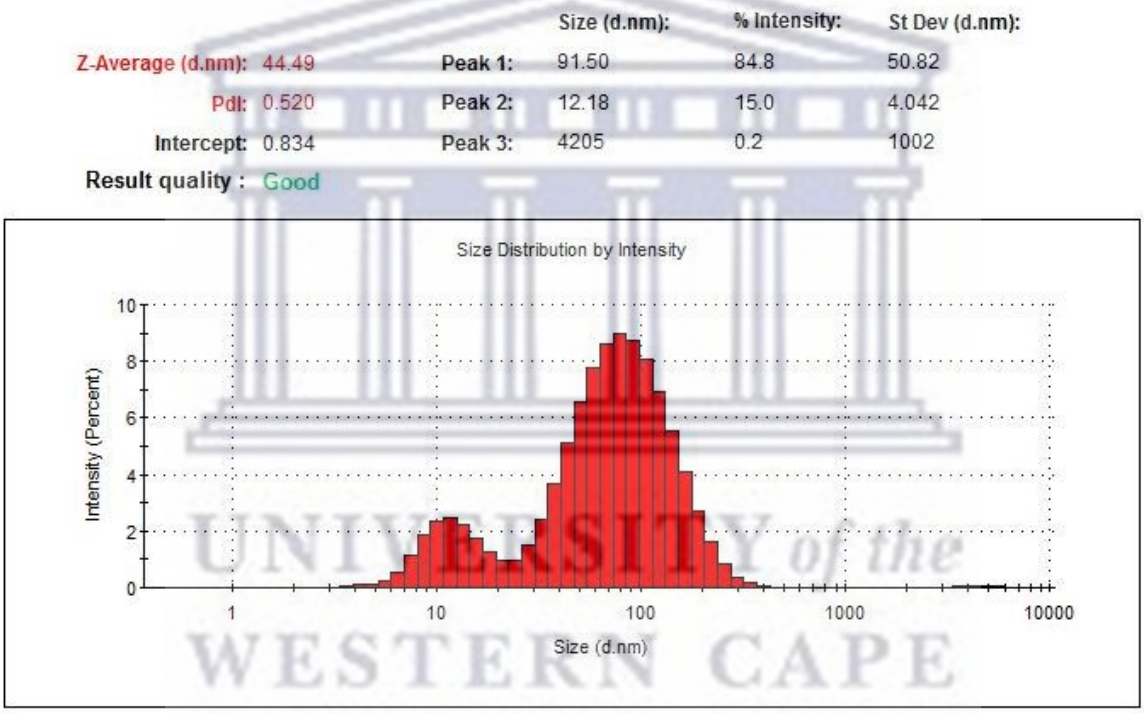

Figure 3.7: Hydrodynamic size distribution of the biogenic CLE-AgNPs.

3.2.3. ζ-potential analysis of CLE-AgNPs

ζ-potential analysis was used to determine the stability of the synthesized CLE-AgNPs (**Figure 3.8**). The ζ-potential value is defined as the measurement of the electrostatic potential at the electrical double layer surrounding an NP in liquid suspension or simpler terms, electrostatic charge on the surface of the NPs (Khorrami *et al.*, 2018). NPs with a ζ-potential between -10 and +10 mV are considered neutral. NPs with a ζ-potential greater than +30 mV or less than -30 mV

are strongly cationic or strongly anionic, respectively (Clogston and Patri, 2011). The CLE-AgNPs showed a ζ-potential of – 21.7 ± 11.3 mV which indicated that the synthesized CLE-AgNPs were partially stable and anionic in nature. The *E. axillare*-AgNPs synthesized by Raj and colleagues (2018) had a ζ-potential of -24.6 nm informed by DLS which was reported as a high electrical charge on the surface of the AgNPs that could cause a strong repellent force among the NPs to prevent agglomeration (Raj *et al.*, 2018). Oxidized pullulan-mediated AgNPs had a high negative ζ-potential which increased their stability due to the repulsion among the particles (Coseri *et al.*, 2015). The ζ-potential values of NPs can either be positive or negative, however, it is commonly negative because of the presence of biomolecules present in the extract bound to the surface of the NPs as they act as capping agents (Sánchez-López, 2020). In the study where *R. rosea*-AgNPs were synthesised, it was reported that the AgNPs had a negative ζ-potential implying that the AgNPs were capped and stabilized by an electronegative compound which may be the biomolecules present in the *R. rosea* extract (Bold *et al.*, 2022).

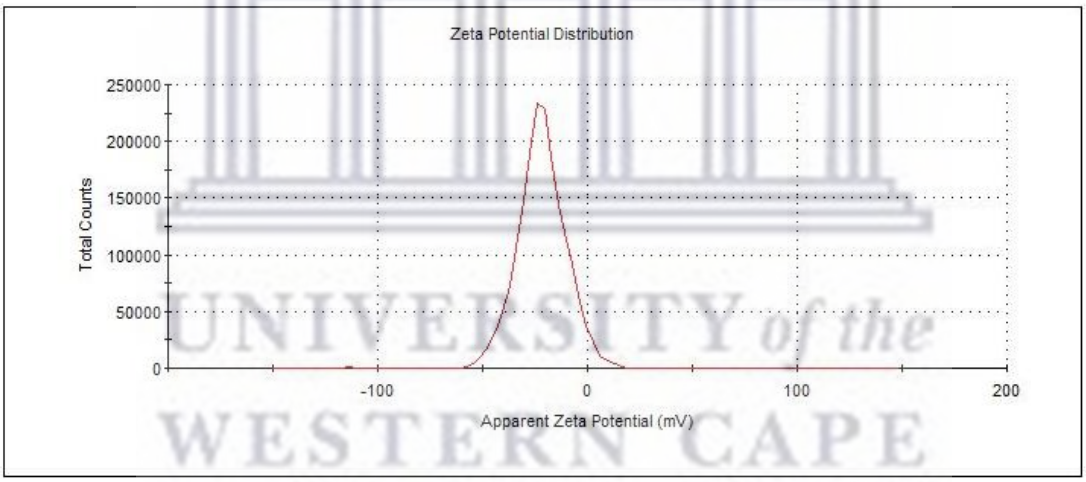

Figure 3.8: ζ-potential distribution curve of the biogenic CLE-AgNPs.

3.2.4. High-resolution transmission microscopy analysis of CLE-AgNPs

HR-TEM was used to analyse the shape, size, and morphology of the biogenic CLE-AgNPs. **Figure 3.9** displays the micrograph and size distribution of the CLE-AgNPs which indicates that reaction conditions yielded CLE-AgNPs that were anisotropic (i.e., different shapes and sizes), but mostly spherical, which is in agreement with the single SPR band and PDI value reported for the synthesised CLE-AgNPs in this study. To determine the average core size of the synthesized CLE-

AgNPs, 55 individual NPs were selected from the HR-TEM micrograph image and measured using ImageJ software. The average core size was estimated to be 16.11 ± 10.6 nm in diameter. Notably, the average size derived from HR-TEM is relatively smaller compared to the hydrodynamic size obtained from DLS. This discrepancy is explainable as DLS measures the hydrodynamic radius which is not a true size of the NP because it includes the surrounding organic layer (i.e., hydration layer around the NPs where the capping and stabilizing agents are present) whereas HR-TEM measures the size of the inorganic core (Tyavambiza *et al.*, 2021).

The observation of this study correlates with those in literature that have reported on the geometrical and size variation of biogenic NPs which has been linked to the phytochemical profile of the plants used in the synthesis of NPs (Dube *et al.*, 2020; Kumar *et al.*, 2017). Previously synthesized AgNPs from *M. esculenta*, *Carica papaya*, and *Morinda citrifolia* leaf extracts, respectively, were also reported to be spherically shaped. The *M. esculenta*-AgNPs size was in the range of 13-38 nm with an average of 23 nm which is in agreement with the findings of this study (Syafiuddin *et al.*, 2017). In a study where *M. esculenta*-AgNPs were synthesized with tuber and leaf extracts the NPs were spherically shaped with mean diameters of 31 ± 9.9 nm and 8.5 ± 4.7 nm, respectively (Wattimena *et al.*, 2022). Another study reported that the synthesis of AgNPs using the plant extracts of *Ocimum sanctum* (basil) produced smaller-sized NPs, with 10 ± 2 nm for the root extract and 5 ± 1.5 nm for the stem extract (Ahmad *et al.*, 2010).

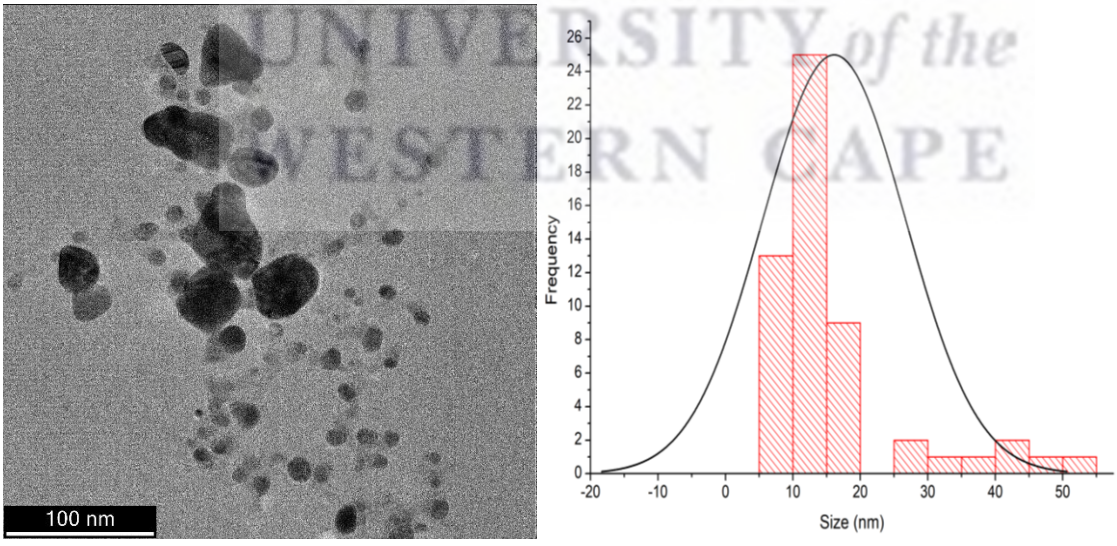

Figure 3.9: HR-TEM analysis of the biogenic CLE-AgNPs showing their morphology and size. A) Micrograph of CLE-AgNPs and B) Size distribution of CLE-AgNPs.

3.2.5. Fourier-transform infrared spectroscopy of CLE and CLE-AgNPs

FTIR spectroscopy was used to identify the structural composition of the CLE and CLE-AgNPs. The structural composition may provide information that aids in the identification of the major functional groups in the plant extract and their potential involvement in the synthesis of AgNPs as reducing and capping agents (Jalani *et al.*, 2018). This information may also aid in identifying the actual phytochemicals responsible for the AgNPs synthesis. Previous literature has shown that various phytochemicals play a key role in the plant-mediated synthesis of AgNPs (Shaikh *et al.*, 2021). The FTIR spectrum is made up of absorption peaks or bands that correspond to the frequencies of vibration between the bonds of atoms in the nanoparticle (Torres-Rivero *et al.*, 2021). The functional groups are identified based on peak values in the region of infrared radiation (Jini and Sharmila, 2020). The IR spectrum is split into three wavenumber regions, namely, far-IR spectrum (<400 cm^{-1}), mid-IR spectrum (400-4000 cm^{-1}), and near-IR spectrum (4000-13000 cm^{-1}). The mid-IR spectrum is the region that provides the most detail and is often focused on identifying the functional groups within a sample. The mid-IR spectrum is split into two major regions: the functional group region and the fingerprint region. The functional group region is positioned between 4000 – 1500 cm^{-1} and is divided into three sub-regions: (1) the single bond region (2500 – 4000 cm^{-1}), (2) the triple bond region (2000 – 2500 cm^{-1}), and (3) the double bond region (1500 – 2000 cm^{-1}). The rest of the mid-IR spectrum is the fingerprint region (600-1500 cm^{-1}) and the functional groups present in this region are specific, unique, and attributable to a specific compound (Nandiyanto *et al.*, 2019). The peaks in the fingerprint region are dependent on complex vibrations involving the entire molecule and it is highly unlikely that more than one compound will have the exact IR spectrum (Nandiyanto *et al.*, 2019; Coates, 2000).

In this study, FTIR was used to identify the bioactive compounds in the CLE which may have been responsible for the reduction of Ag^{+} to Ag^{0}, and the capping and stabilizing of the synthesized CLE-AgNPs. **Figure 3.10** displays the FTIR spectra of both the CLE and CLE-AgNPs. The FTIR spectrum of the CLE-AgNPs was similar to the spectrum of the CLE which was the plant extract used to synthesize the AgNPs. Peaks between the two spectra were transmitted at similar wavelengths which indicates that the phytochemicals present in the extract can be found on the surface of the AgNPs, however, certain peaks between the CLE and CLE-AgNPs spectra were slightly shifted. The shifts between the spectra can be expected due to the influence of the metal

based on its proximity to the corresponding functional groups and may further confirm the involvement of the corresponding functional groups in the synthesis of the CLE-AgNPs (Elia *et al.*, 2014). The FTIR spectra peak values, peak shifts, and their possible corresponding functional groups/ assignments are tabulated (**Table 3.1**).

A strong broad absorption band at 3351.62 cm^{-1} in the CLE shifted to 3422.35 cm^{-1} in the AgNPs and was assigned to the stretching vibration of intermolecular polymeric bonded O-H groups or N-H groups which are characteristic of alcohols, phenols, and aliphatic primary or secondary amines. A band of similar frequency (3314 cm^{-1}) in FTIR spectra of cassava leaves extract was identified and attributed mainly to carbohydrates and sugars, such as cellulose and lignin, or cellulose glycosidic bonds (Cruz *et al.*, 2021). The broadness of the band may be due to intra- and intermolecular hydrogen bonds that were formed (Kusuma *et al.*, 2022; Kumar *et al.*, 2020). The strong absorption band at 1603.6 cm^{-1} in the CLE shifted to 1613.24 cm^{-1} in the AgNPs and was assigned to the vibrations of N-H bending due to the presence of primary amines. The strong sharp absorption band at 1407.39 cm^{-1}in the CLE which shifted to 1382 cm^{-1} in the AgNPs was assigned to O-H bending vibration of phenolic compounds or tertiary alcohol (Nandiyanto *et al.*, 2019). The weak absorption band at 1122.65 cm^{-1} in the CLE shifted to 1113.58 cm^{-1} in the AgNPs and was assigned to the stretching vibrations of C-O groups which could indicate the presence of alcohols, carboxylic acids, esters, or ethers (Nandiyanto *et al.*, 2019). The presence of the weak absorption band at 1045.57 cm^{-1} in the CLE which shifted to 1042.85 cm^{-1} in the AgNPs may be assigned to the vibrations of a C-H stretch and C-F stretch of aliphatic amines and fluoro compounds, respectively. The peak at 1042.85 cm^{-1} may indicate the presence of phosphate ions (Nandiyanto *et al.*, 2019) which is in accordance with the results of a study on cassava leaves conducted where IR bands found in the range of 1042-1084 cm^{-1} were characterized as phosphorous compounds (Syafiuddin *et al.*, 2017). It has been previously reported that peaks at 1113 cm^{-1} and 1051 cm^{-1}, respectively, were attributed to -C-OC linkages and -C-O bonds which represent the presence of flavonoids and terpenoids found in most plant extracts (Jalani *et al.*, 2018; Ahmed *et al.*, 2016b). The weak absorption band at 667.42 cm^{-1} in the CLE shifted to 623.89 cm^{-1} in the AgNPs and was assigned to the stretching vibrations of C-Br groups and bending vibrations of C-H groups due to the presence of aliphatic bromo compounds and alkynes, respectively (Nandiyanto *et al.*, 2019; Coates, 2000).

The absence of peaks from the CLE-AgNPs which were initially present in the CLE suggests that these bioactive compounds were involved in reducing Ag^{+} to Ag^{0} and therefore are not found in the FTIR spectra of CLE-AgNPs (Jalani *et al.*, 2018). Based on the FTIR data, it was evident that some of the biomolecules present in the CLE were involved in the synthesis of CLE-AgNPs not only as reducing agents but as capping agents as well. The hydroxyl and carboxyl functional groups are responsible for the encapsulation of AgNPs which increases the stability of AgNPs (Dawadi *et al.*, 2021). A previous study showed that FT-IR analysis confirmed the presence of alkanes, carboxylic acid, esters, alkyl halide, and amines in the petroleum benzene leaf extract of *M. esculenta* (Manjula *et al.,* 2020*)*. The presence of amine, phenolic, primary alcohol, nitro, and aliphatic ether compounds was found in an aqueous extract of *M. esculenta* leaves (Kusuma *et al.*, 2022). These findings are in accordance with previous studies who identified the major functional groups of O-H, C-O, N-H, and N-O in cassava leaves (Kumar *et al.*, 2021b; Palupi *et al.*, 2020). The identified functional groups were attributed to the cellulose and chlorophyll present in the leaves (Kusuma *et al.*, 2022). In a previous study, a strong peak at 3400 cm^{-1} was also attributed to the intermolecular and intramolecular H bonds of free OH in cellulose as it is known that green leaves are primarily composed of lignocellulosic components (Sharif *et al.*, 2015; Razak *et al.*, 2013). Interestingly, no peaks occurred in the region of 2280-2220 cm^{-1} which would have indicated the presence of a nitrile CN, representative of cyanide, which is commonly found in cassava leaves (Nandiyanto *et al.*, 2019; Nkafamiya *et al.*, 2015).

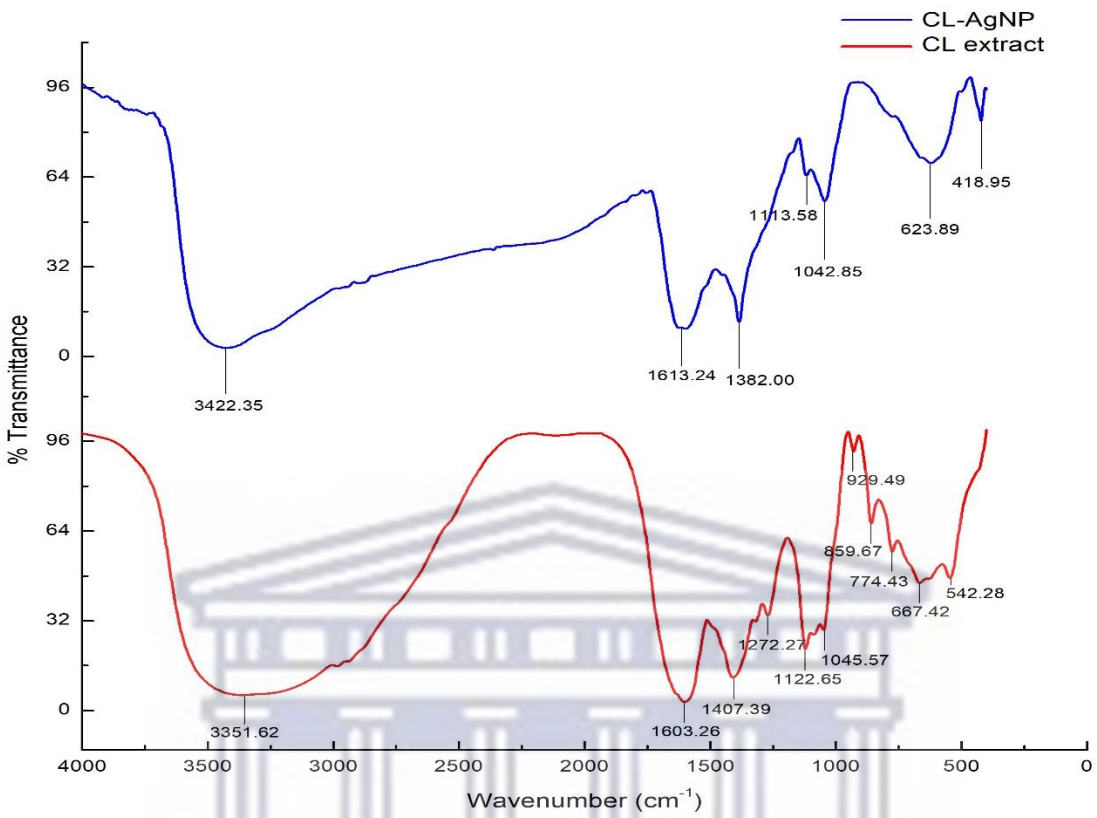

Figure 3.10: FTIR spectra of CLE and CLE-AgNPs.

Table 3.1: FTIR spectra peak values and peak shifts of CLE and CLE-AgNPs and their corresponding functional groups.

Peak values of CL extract (cm^{-1})	Peak values of CL-AgNP (cm^{-1})	Shift in peak values	Bond	Identified functional groups/ assignment
3351.62	3422.35	- 70.73	O-H stretch O-H (H-bonded) N-H stretch	Alcohols, Phenols 1°, 2° amines, amides Aliphatic primary amine
1603.26	1613.24	- 9.98	N-H bend	1° amines
1407.39	1382.00	+ 25.39	O-H bend	Phenol or tertiary alcohol
1272.27	-	-	C-H C-N stretch C-O stretch	Alkyl halides Aromatic primary amines Alcohols, Carboxylic acids, Esters, Ethers

1122.65	1113.58	+ 9.07	C-O stretch	Secondary alcohol, carboxylic acids, esters, ethers
1045.57	1042.85	+ 2.72	C-N stretch C-F stretch S=O stretch CO-O-CO stretch	Aliphatic amines Aliphatic fluoro compounds Sulfoxide Anhydride Phosphate ion
929.49	-	-	O-H bend =C-H bend	Carboxylic acids Alkenes Silicate ion
859.67	-	-	C-H N-H =C-H bend	Aromatics 1°, 2° amines Alkenes
774.48	-	-	C-Cl stretch C-H N-H =C-H bend	Alkyl halides Aromatics 1°, 2° amines Alkenes
667.42	623.89	+ 43.53	C-Br stretch C-H bend	Alkyl halides - Aliphatic bromo compounds Alkynes
542.28	-	-	C-I stretch	Alkyl halides - Aliphatic iodo compounds
-	418.95	-	C-Br stretch	Alkyl halides

3.2.6. Inductively coupled plasma optical emission spectrometry

Inductively coupled plasma optical emission spectrometry (ICP-OES) is a spectroscopic technique used to obtain qualitative and quantitative information about a given element within a liquid sample based on the emission intensity at specific wavelengths of the element of interest. Generally, a direct measure of ions dissolved at low concentrations can be provided by ICP-OES (Gasbarri *et al.*, 2019). Based on this knowledge, ICP-OES analysis was used to determine the concentration of silver in the CLE-AgNPs. The silver concentration in the CLE-AgNPs was found to be 43.489 ± 0.341 ug/ml. In a previous study, silver nanoparticles were synthesized using Gum Arabic and the silver concentration was found to be 10^4 µg/ml using ICP-OES (El-Adawy *et al.*, 2021).

3.3. Total phenolic content of CLE and CLE-AgNPs

The total phenolic content (TPC) of CLE and CLE-AgNPs was determined quantitatively by the Folin-Ciocalteu (FC) assay using the FC reagent and Gallic acid as the standard. The total phenolic content was expressed in terms of Gallic acid equivalents (GAE) in µg/ml and was calculated with the help of the Gallic acid calibration standard curve shown in **Figure 3.11**. The standard curve equation was y = 0.003x - 0.0203, where R^2 = 0.9979. Both the CLE and CLE-AgNPs showed the presence of phenolic compounds which corresponds to the FTIR data in this study. The TPC of the CLE and CLE-AgNPs was determined as 1131.21 ± 69.24 µg/ml and 86.36 ± 2.18 µg/ml (expressed as GAE), respectively (**Table 3.2**). The CLE had a higher content of phenolics as compared to the CLE-AgNPs. Nonetheless, the presence of phenols in the CLE-AgNPs suggests that the phytochemicals found in the CLE were involved in the synthesis of AgNPs as capping agents. In another study, it was discovered that *M. esculenta*, both tubers and leaves, contains phenolic compounds (Wattimena *et al.*, 2022). The presence of phenols in *M. esculenta* leaf extracts were also reported in other previous studies (Hasim *et al.*, 2016; Quartey *et al.*, 2016). Phytochemical screening analysis of the same plant may differ in the results obtained due to the location where the plants were harvested as soil nutrients in different regions has an effect on their phytochemical composition (Mustarichie *et al.*, 2020).

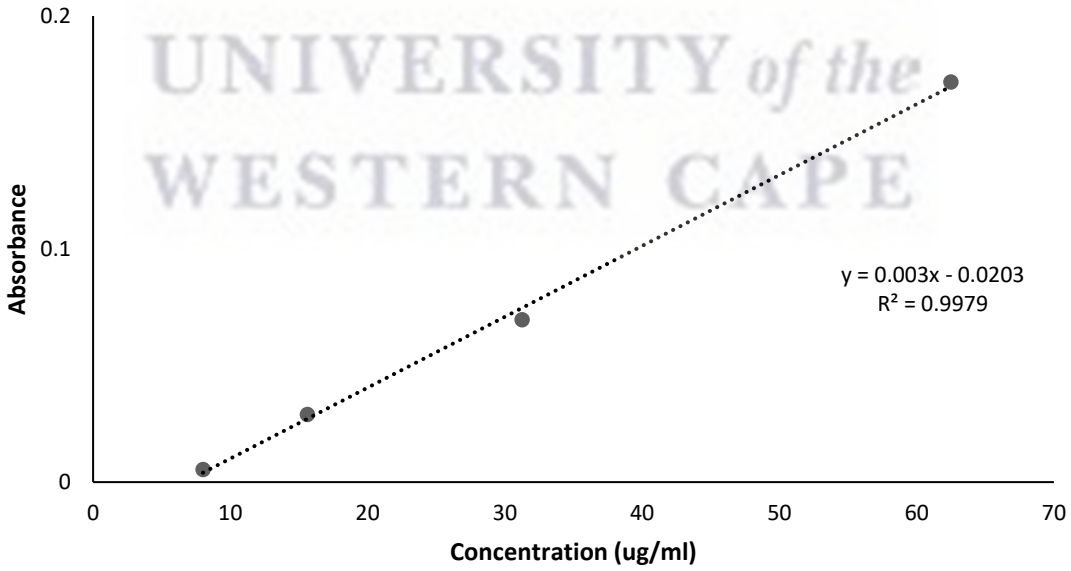

Figure 3.11: Gallic acid calibration standard curve for the determination of total phenolic content of CLE and CLE-AgNPs.

Table 3.2: Total phenolic content of CLE and CLE-AgNPs.

	Gallic acid equivalent (ug/ml)
CLE	1131.21 ± 69.24
CLE-AgNPs	86.36 ± 2.18

3.4. Stability analysis of CLE-AgNPs

For any potential biomedical application, nanoparticles need to remain stable under different biological conditions. Thus, the stability of the biogenic CLE-AgNPs was evaluated in MHB, dH_2O, and ddH_2O over a period of 24 hrs. UV-vis analysis was used to determine any changes in the stability of the nanoparticles as shown in **Figure 3.12**. The evaluation of the stability of the CLE-AgNPs was performed at 37 °C because most *in vitro* and *in vivo* applications are performed at this temperature. MHB, dH_2O, and ddH_2O were chosen due to their use in the biological assays conducted in this study. The CL-AgNPs appeared to be stable over the 24 hrs period for MHB, dH_2O, and ddH_2O as there were no significant changes in the UV-vis absorption spectra. Agglomeration of the CLE-AgNPs may have been prevented in the media used due to the biomass present on the surface of the AgNPs, which provide a stearic or electrostatic barrier (Khan *et al.*, 2020).

The findings of this study are in agreement with a study that reported on the absorbance peaks of biogenic AgNPs placed in MHB which had slight changes that were negligible in their UV-vis spectra over 24 hrs and implied that the AgNPs were stable in the respective media (Dube *et al.*, 2020). However, the findings of this study differed from the those from a study which showed that *Cotyledon orbiculata* AgNPs were not stable in MHB at 37 °C over a period of 24 hrs. The addition of *C. orbiculata*-AgNPs to MHB led to the flattening of the UV-vis absorption spectra indicating the possible aggregation of the NPs. MHB has a high protein content and low concentration of inorganic salts which may have affected the NPs (Tyavambiza *et al.*, 2021). Previous literature has shown that high protein content present in bacterial growth media may negatively affect the colloidal stability of the synthesized NPs resulting in agglomeration (Tyavambiza *et al.*, 2021; Moore *et al.*, 2015).

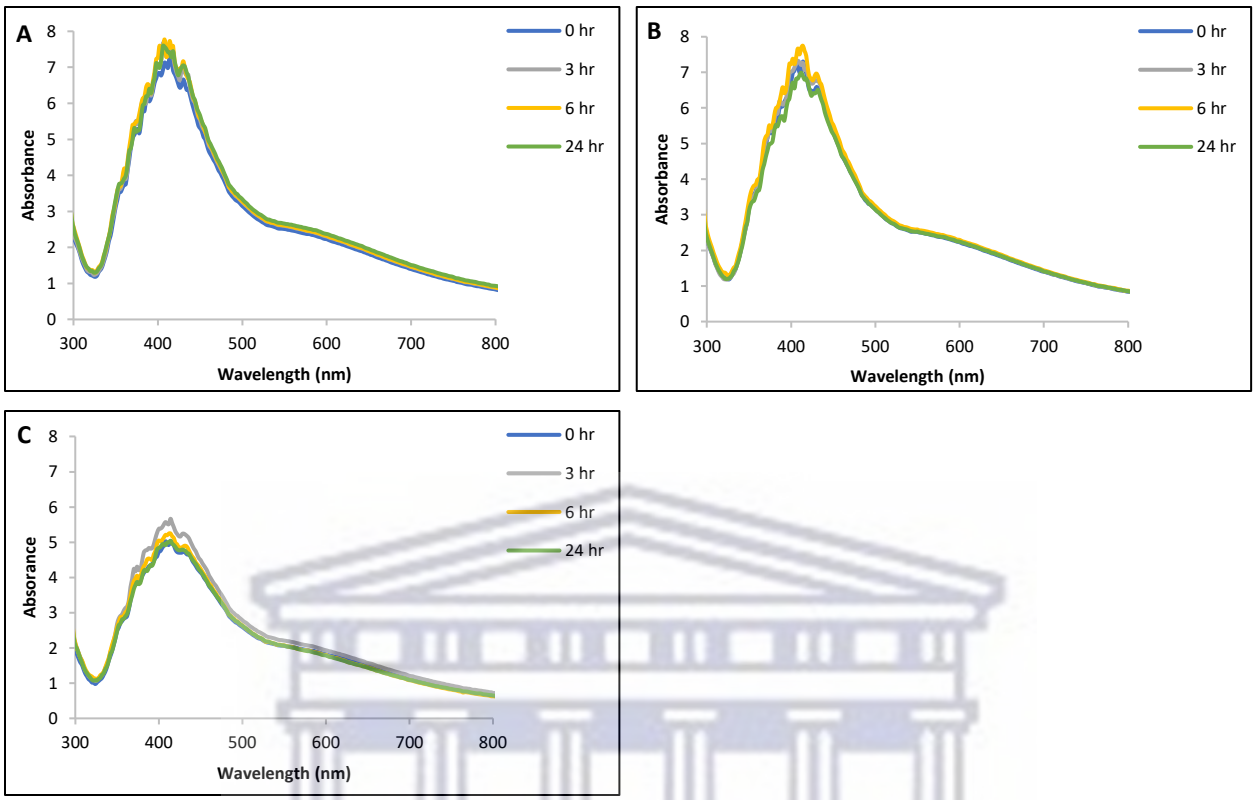

Figure 3.12: UV-vis absorption spectra showing the stability of the biogenic CLE-AgNPs in various media during incubation at 37 °C for 24 hrs (A: dH_2O, B: ddH_2O, C: MHB).

3.5. Antibacterial activity of CLE-AgNPs

3.5.1. Antibacterial activity of CLE-AgNPs using agar well diffusion assay

The antibacterial activity of CLE-AgNPs and CLE was studied against six human pathogenic bacteria, namely *S. aureus*, MRSA, *E. coli*, *K. pneumoniae*, *P. aeruginosa*, and *A. baumannii* using the agar well diffusion method. Ciprofloxacin and MHB were chosen as the positive control and negative control, respectively. The zone of inhibition (ZOI) surrounding each well for the various concentrations of CLE-AgNPs and CLE was measured to determine the antibacterial effect of the CLE-AgNPs and CLE on the microorganisms of interest.

The ZOI is the circular area around the antibacterial treatment in which bacteria colonies do not grow that can be used to measure the susceptibility of the bacteria towards the antibacterial treatment. The ZOI measurements for CLE-AgNP, CLE (unpH), and CLE (pH 10) are presented in **Table 3.2**, **Table 3.3**, and **Table 3.4**, respectively. The results shown in **Table 3.1** and **Figure 3.13** demonstrated that the CLE-AgNPs displayed broad spectrum antibacterial activity against all

the bacterial strains for all the concentrations (2.9-46.8 µg/ml) tested. The CLE-AgNPs were able to efficiently inhibit the growth of both gram-positive and gram-negative bacteria in a dose-dependent manner. The notable differences in the ZOIs can be observed in **Figure 3.13**.

For the gram-positive bacteria, MRSA was more susceptible to the CLE-AgNPs than *S. aureus*. The lowest concentration of CLE-AgNPs that was able to inhibit MRSA was 2.9 µg/ml with a ZOI of 7.17 ± 0.29 mm whilst the lowest concentration of CLE-AgNPs that inhibited *S. aureus* was 5.8 µg/ml with a ZOI of 7 ± 0 mm. *S. aureus* forms part of our skin flora, however, it is a common causative agent of various community-acquired and nosocomial infections. Interestingly, MRSA evolved from *S. aureus* due to long-term selection of methicillin and is genetically and structurally different compared to *S. aureus* (Hu *et al.*, 2020). Patients with MRSA infections are 64% more likely to die than those with drug-sensitive infections (World Health Organization, 2021). It is of great importance that effective strategies to treat bacterial infections with serious antibiotic resistance (Hu *et al.*, 2020). For the gram-negative bacteria, *E. coli* was more susceptible than *K. pneumoniae*, *P. aeruginosa*, and *A. baumannii*. The lowest concentration of CLE-AgNPs that was able to inhibit *E. coli* was 2.9 µg/ml with a ZOI of 8 ± 0.5 mm. *A. baumannii* was inhibited by 11.7 µg/ml CLE-AgNPs with a ZOI of 7.33 ± 0.29 mm. The least susceptible bacterial strains were *P. aeruginosa* and *K. pneumoniae* as they were inhibited by 23.4 µg/ml CLE-AgNPs with ZOI measurements of 7.67 ± 1.26 mm and 7.33 ± 0.29 mm, respectively. Nonetheless, CLE-AgNPs were able to inhibit the growth of all the pathogens tested in this study to some degree.

The positive control, Ciprofloxacin, was able to inhibit the growth of all the bacterial strains tested. On the contrary, the negative control, MHB, had no antibacterial activity as there were no ZOI for all the bacterial strains tested which ruled out the possibility of the growth medium influencing the antibacterial activity. Notably, the CLE (unpH and pH 10) did not display any significant antibacterial activity against the microorganisms tested in this study as shown in **Table 3.3** and **Table 3.4**. Based on the results, the CLE-AgNPs were solely responsible for the antibacterial activity, and not because of the phytochemicals involved in the synthesis of the CLE-AgNPs. In a study by Bold and colleagues (2022), the antibacterial activity of *R. rosea*-AgNPs was assessed using agar well diffusion. It was reported that *P. aeruginosa* was more susceptible to *R. rosea*-AgNPs compared to *S. aureus* (Bold *et al.*, 2022). This result may have been due to the difference

in bacterial cell wall structures (Vijayan *et al.*, 2018). Nonetheless, the *R. rosea*-AgNPs exhibited an effective antibacterial activity against both pathogens (Bold *et al.*, 2022).

Surprisingly, the highest concentration of aqueous CLE (2.5 mg/ml) did not show any antibacterial activity against the microorganisms used in this study. Other studies have shown that methanolic extracts of *M. esculenta* at lower concentrations has antibacterial activity against *P. aeruginosa, E. coli, E. cloacae, K. pneumoniae, Providencia stuartii* and *Enterobacter aerogenes* while another study showed that the chloroform extract of *M. esculenta* exhibited antibacterial activity against *L. monocytogenes, V. cholera, S. flexneri*, and *S. typhi*, and the ethanolic extract had antibacterial activity against *P. aeruginosa, C. diphtheriae*, and *V. cholera* (Noumedem *et al.*, 2013; Zakaria *et al.*, 2006). Another study also demonstrated the antibacterial activity of ethanolic extract of *M. esculenta* leaves against *S. epidermidis and Propionibacterium acnes* (Mustarichie *et al.*, 2020). It has been reported that ethanol is used as a solvent in the extraction process as it has the ability to extract almost all secondary metabolites present in the sample. Ethanol is classified as semipolar, due to the presence of the -OH group which is polar and the ethyl group (CH_3CH_2-) which is nonpolar, making it possible to dissolve both nonpolar and polar secondary metabolites (Mustarichie *et al.*, 2020).

Efficiency of the extraction of phytochemicals from plant material is greatly affected by extraction method, temperature, extraction time, the phytochemical composition and the solvent used. Solvents is one of the most important parameters as it has an influence on the yield and composition of biomolecules isolated (Kapadia *et al.*, 2022; Truong *et al.*, 2019). Results from a study showed that different solvents used to extract bioactive compounds from *S. buxifolia* branches resulted in various extraction yields due to the differences in the polarity of the extraction solvents which could cause an extensive variation in the level (and content) of isolated bioactive compounds (Truong *et al.*, 2019). Solvents with a polarity similar to a given solute leads to better extractions, thus, if the plant of interest contains a high level of polar biomolecules, then a polar solvent should be employed in order to extract the highest yield of phytochemicals, and the same would apply to nonpolar biomolecules (Kapadia *et al.*, 2022). Methanol was the best solvent to use in the extract preparation of *S. buxifolia* (Truong *et al.*, 2019). The biological activity of the extract is significantly influenced by the extraction yield and the content of bioactive compounds (Truong *et al.*, 2019). From the observations in this study, ddH_2O may not have isolated the

appropriate biomolecules from cassava leaves in order for the aqueous CLE to have significant antibacterial activity yet the biomolecules isolated were suitable for the synthesis of CLE-AgNPs which has been proven to possess antibacterial properties. Literature shows that other organic solvents, such as methanol and ethanol, are best for extracting high yields and composition of phytochemicals required from *M. esculenta* to obtain antibacterial activity in the extract itself (Mustarichie *et al.*, 2020; Noumedem *et al.*, 2013; Zakaria *et al.*, 2006).

The findings of this study were in agreement with the findings of a study that reported on a banana peel extract (BPE) preparation using distilled water and acetone. The BPE did not have any antibacterial activity, however, BPE-AgNPs showed antibacterial activity against *B. subtilis, S. aureus, P. aeruginosa,* and *E. coli* (Ibrahim, 2015). Another study tested the antibacterial activity of aqueous extracts of *Salvia Africana-lutea* (SAL) and *Sutherlandia frutescens* (SF) as well as the AgNPs synthesized from these extracts. Aqueous extracts of SAL and SF did not show any antibacterial activity against *S. epidermidis* and *P. aeruginosa* but the synthesized AgNPs showed antibacterial activity (Dube *et al.*, 2020). Other studies which report on plant mediated AgNPs synthesis have also described the enhanced antibacterial activity of biogenic AgNPs when compared to the antibacterial activity of the plant's extract (Dube *et al.*, 2020; Ahmed *et al.*, 2016b; Kathiravan *et al.*, 2015). Moreover, the antibacterial activity of *M. esculenta*-AgNPs synthesized from tuber and leaf extracts, respectively, were investigated by Wattimena and colleagues (2022). The results showed that both cassava leaf- and cassava tuber-AgNPs inhibited the growth of both *E. coli* and *S. aureus* (Wattimena *et al.*, 2022). The antibacterial action of the synthesized AgNPs were connected to the release of Ag^{+} ions where the positive ions favourably interact with the negatively charged membrane of the bacteria enabling the permeability of the membrane and leakage of the intracellular cytoplasmic contents, resulting in cell death (Dakal *et al.*, 2016; Feng *et al.*, 2000).The positive ions that penetrate the cell membrane are involved in the deactivation of respiratory enzymes which causes ROS formation that can cause cell membrane destruction and changes in the microbial DNA structure (Wattimena *et al.*, 2022; Ramkumar *et al.*, 2017).

S. aureus

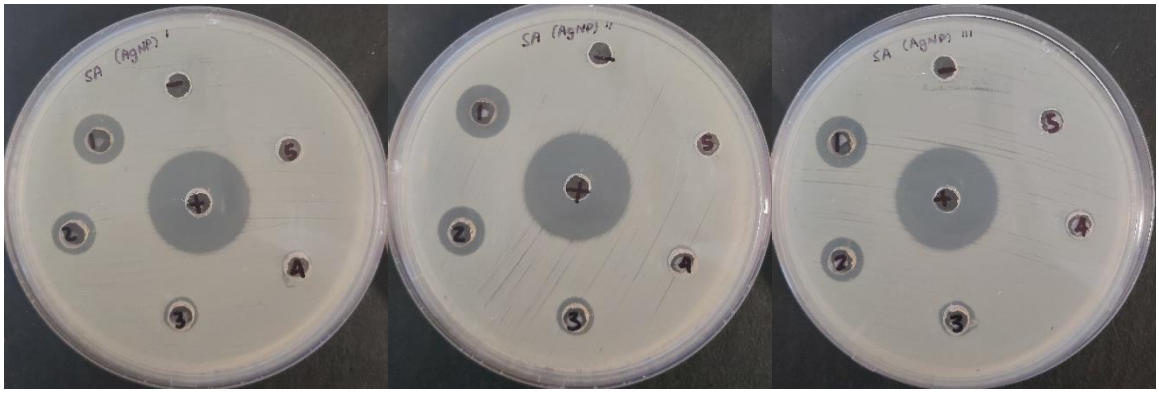

MRSA

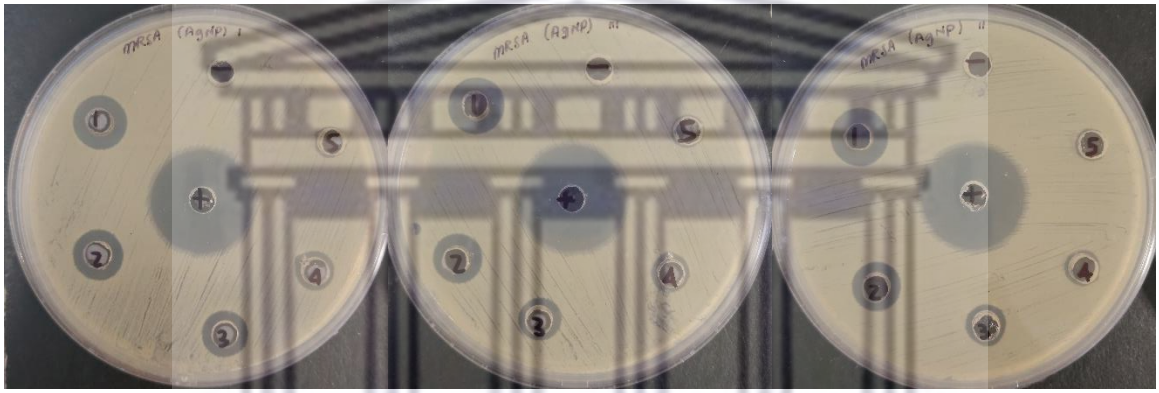

E. coli

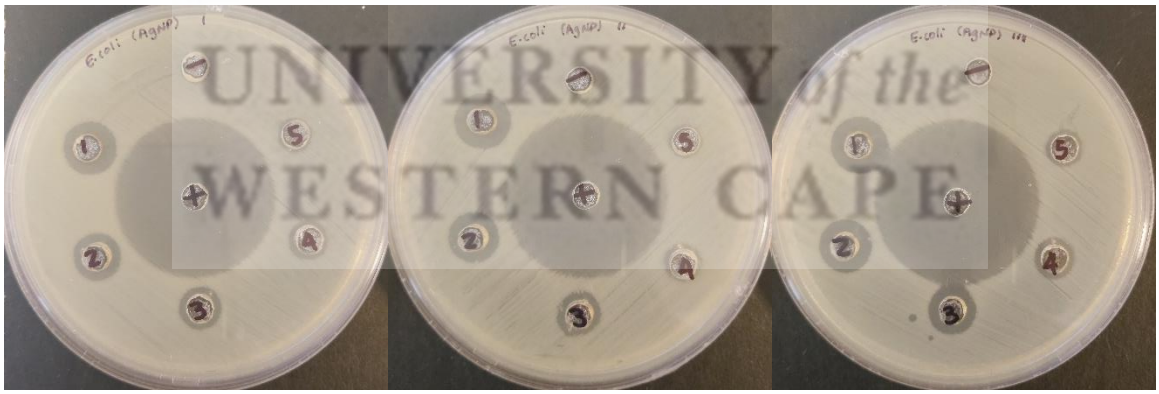

P. aeruginosa

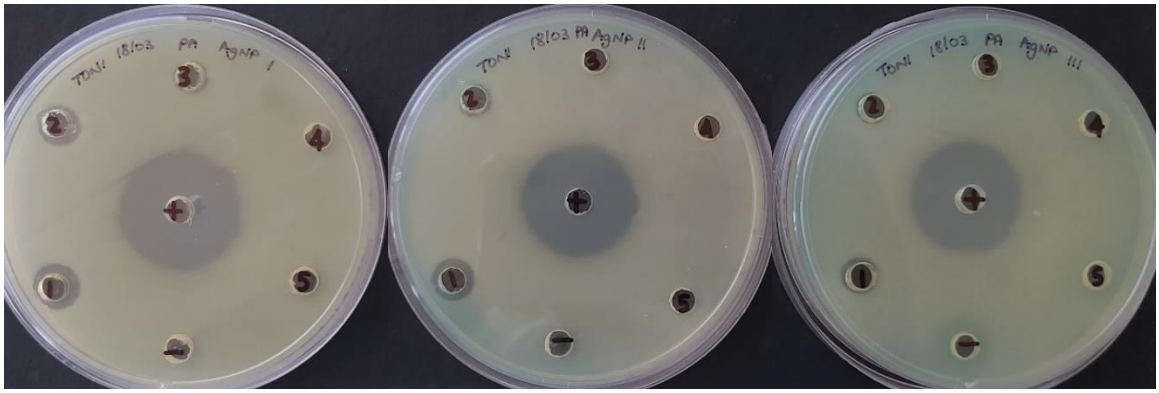

K. pneumoniae

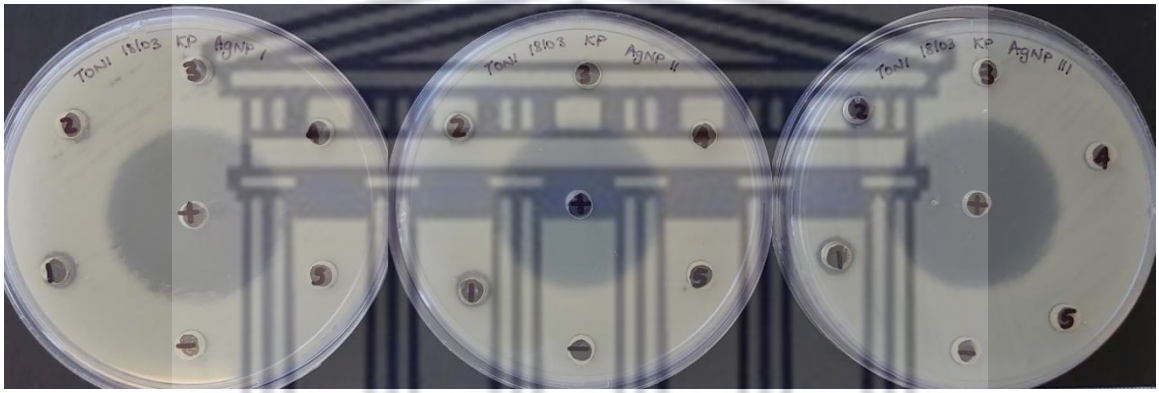

A. baumannii

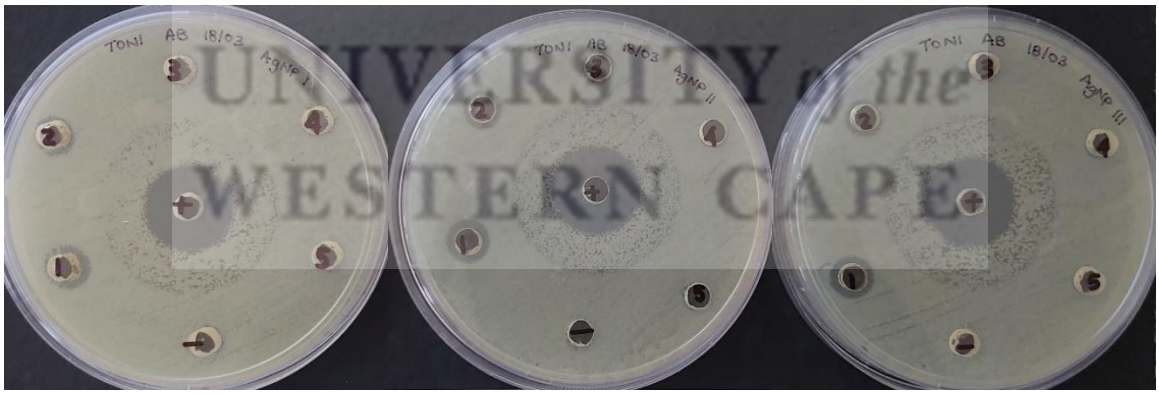

Figure 3.13: Antibacterial activity of CLE-AgNPs. The zone of inhibition of synthesized CLE-AgNPs (mm) on *S. aureus*, MRSA, *E. coli*, *P. aeruginosa*, *K. pneumoniae* and *A. baumannii*. (Concentrations of CLE-AgNPs - 1: 2.9 µg/ml, 2: 5.8 µg/ml, 3: 11.7 µg/ml, 4: 23.4 µg/ml and 5: 46.8 µg/ml CLE-AgNPs; +: Ciprofloxacin; –: MHB).

Table 3.3: The antibacterial effects of biogenic CLE-AgNPs against six human pathogenic bacteria tested at different doses ranging from 2.9-46.8 µg/ml (n=3).

	S. aureus	MRSA	*E. coli*	*P. aeruginosa*	*K. pneumoniae*	*A. baumannii*
	Zone of inhibition ± SD (mm)					
2.9 µg/ml (1)	0 ± 0	7.17 ± 0.29	8 ± 0.5	0 ± 0	0 ± 0	0 ± 0
5.8 µg/ml (2)	7 ± 0	8.67 ± 0.58	9 ± 0.5	0 ± 0	0 ± 0	0 ± 0
11.7 µg/ml (3)	8.17 ± 0.29	10 ± 1	10.33 ± 0.58	0 ± 0	0 ± 0	7.33 ± 0.29
23.4 µg/ml (4)	10.33 ± 0.58	11.33 ± 0.29	11.33 ± 0.76	7.67 ± 1.26	7.33 ± 0.29	8.67 ± 0.58
46.8 µg/ml (5)	12.17 ± 0.29	12.83 ± 0.29	12.67 ± 0.58	9.67 ± 1.53	8.83 ± 0.29	10.17 ± 0.29
Ciprofloxacin (+)	24.67 ± 0.29	24.17 ± 0.29	38 ± 0.5	26.33 ± 1.53	32.33 ± 0.58	19.83 ± 0.29
MHB (-)	0 ± 0	0 ± 0	0 ± 0	0 ± 0	0 ± 0	0 ± 0

Table 3.4: The antibacterial effects of CLE (unpH) against six human pathogenic bacteria tested at different doses ranging from 0.156-2.5 mg/ml (n=3).

	S. aureus	MRSA	*E. coli*	*P. aeruginosa*	*K. pneumoniae*	*A. baumannii*
	Zone of inhibition ± SD (mm)					
0.1563 mg/ml (1)	0 ± 0	0 ± 0	0 ± 0	0 ± 0	0 ± 0	0 ± 0
0.3125 mg/ml (2)	0 ± 0	0 ± 0	0 ± 0	0 ± 0	0 ± 0	0 ± 0
0.625 mg/ml (3)	0 ± 0	0 ± 0	0 ± 0	0 ± 0	0 ± 0	0 ± 0
1.25 mg/ml (4)	0 ± 0	0 ± 0	0 ± 0	0 ± 0	0 ± 0	0 ± 0
2.5 mg/ml (5)	0 ± 0	0 ± 0	0 ± 0	0 ± 0	0 ± 0	0 ± 0
Ciprofloxacin (+)	24.67 ± 0.58	24.83 ± 0.29	37.33 ± 0.58	26.33 ± 0.58	33 ± 2.65	19.67 ± 1.15
MHB (-)	0 ± 0	0 ± 0	0 ± 0	0 ± 0	0 ± 0	0 ± 0

Table 3.5: The antibacterial effects of CLE (pH 10) against six human pathogenic bacteria tested at different doses ranging from 0.156-2.5 mg/ml (n=3).

	S. aureus	MRSA	*E. coli*	*P. aeruginosa*	*K. pneumoniae*	*A. baumannii*
	Zone of inhibition ± SD (mm)					
0.1563 mg/ml (1)	0 ± 0	0 ± 0	0 ± 0	0 ± 0	0 ± 0	0 ± 0
0.3125 mg/ml (2)	0 ± 0	0 ± 0	0 ± 0	0 ± 0	0 ± 0	0 ± 0
0.625 mg/ml (3)	0 ± 0	0 ± 0	0 ± 0	0 ± 0	0 ± 0	0 ± 0
1.25 mg/ml (4)	0 ± 0	0 ± 0	0 ± 0	0 ± 0	0 ± 0	0 ± 0
2.5 mg/ml (5)	0 ± 0	0 ± 0	0 ± 0	0 ± 0	0 ± 0	0 ± 0
Ciprofloxacin (+)	24.83 ± 0.58	23.83 ± 0.29	37.17 ± 0.29	26.83 ± 0.29	34 ± 1	18 ± 1
MHB (-)	0 ± 0	0 ± 0	0 ± 0	0 ± 0	0 ± 0	0 ± 0

3.5.2. Antibacterial activity of CLE-AgNPs using microdilution assay

The microdilution assay was employed to further investigate the antibacterial activity of CLE-AgNPs against *S. aureus*, MRSA, *E. coli*, *K. pneumoniae*, *P. aeruginosa*, and *A. baumannii*. The minimum inhibitory concentration (MIC) and minimum bactericidal concentration (MBC) was determined against the microorganisms. MIC is defined as the lowest concentration of the treatments required to inhibit visible growth of the bacteria and MBC is defined as the minimum concentration of the treatments required to kill 99.9% of the bacteria in the original inoculum (Balouiri *et al.*, 2016). AlamarBlue™ dye was used as a bacterial viability indicator in combination with the microdilution assay (Henshaw, 2018).

CLE-AgNPs exhibited broad spectrum antibacterial activity against all the microorganisms tested in this study as indicated in **Table 3.6**. **Figure 3.14**, **Figure 3.15**, and **Figure 3.16** display the inhibitory and bactericidal effects of the CLE-AgNPs against the microorganisms tested in this study. The non-fluorescent AlamarBlue™ dye (resazurin) is reduced to resorufin, a highly fluorescent pink compound, in the presence of viable bacteria, and, thus, was used as a colourimetric indicator of viable bacteria (Henshaw, 2018). Moreover, the intensity of the pink colour and fluorescence was proportional to the number of viable cells present (**Figure 3.15**). The MIC was determined as the lowest concentration where no microbial growth was observed in the wells as well as by the spectrophotometer (Henshaw, 2018). It is advantageous to make use of AlamarBlue™ dye because it is non-toxic, sensitive, and cost-effective. AlamarBlue™ works on suspension cells and attached cells, making it incredibly useful for biofilms (Henshaw, 2018; Zachari *et al.*, 2014).

The CLE-AgNPs were able to efficiently inhibit the growth of both gram-positive and gram-negative bacteria in a dose-dependent manner. CLE-AgNPs were mostly active against the gram-negative bacteria as compared to the gram-positive bacteria. This may be due to the difference in their cell wall composition (Ibrahim, 2015). The cell wall of gram-positive bacteria is composed of a thick peptidoglycan layer which consists of linear polysaccharide cross linked by short peptides, therefore, a rigid structure is formed which makes the penetration of AgNPs more difficult to achieve. The cell wall of gram-negative bacteria is composed of a thinner peptidoglycan layer which gives AgNPs the advantage as it is easier for them to penetrate the cell (Ibrahim, 2015).

The highest antibacterial activity was observed against *K. pneumoniae* with the values for both MIC and MBC being 0.4 µg/ml. This is a remarkably low concentration of CLE-AgNPs that is required to inhibit the growth (and kill 99.9%) of *K. pneumoniae*. *K. pneumoniae* is a common bacterial pathogen found in the intestines. It is a major causative agent of nosocomial infections, such as pneumonia, BSIs, neonatal infections, and infections of intensive-care unit patients. Resistance in *K. pneumoniae* to last resort carbapenem antibiotic therapy has spread globally with some countries recording that carbapenem antibiotics do not work in more than half of the patients treated for *K. pneumoniae* infections (World Health Organization, 2021). The alternative antibiotic treatment, colistin, is the only last resort treatment for life-threatening infections caused by carbapenem-resistant Enterobacteriaceae, such as *E. coli* and *Klebsiella* sp.. However, colistin-resistant bacteria have been detected in various parts of the world and has already caused infections for which there is no effective antibiotic treatment at present (World Health Organization, 2021). Treatment options to treat bacterial infections of this nature is evidently limited. Moreover, colistin is not registered in the RSA and in order to access the antibiotic treatment, a Section 21 approval through the South African Health Products Regulatory Authority (SAHPRA) to procure is required. If treatment is not administered within a particular window of time, the patient is likely to die (NDoH-RSA, 2022).

The lowest antibacterial activity recorded for CLE-AgNPs was against *S. aureus*, MRSA and *E. coli* with the same MIC value of 5.8 µg/ml and same MBC value of 5.8 µg/ml, except for MRSA that had an MBC value of 11.7 µg/ml. Although, the inhibitory activity was the same for all three bacterial strains, the bactericidal effect of CLE-AgNPs was greater against *S. aureus* and *E. coli* as compared to MRSA. *P. aeruginosa* had the same MIC and MBC value of 1.5 µg/ml. *A. baumannii* required a higher concentration of CLE-AgNPs with the same MIC and MBC value of 2.9 µg/ml. A natural agent is considered significant to be used as an antibacterial agent if it has a MIC value of 1 mg/ml and below (Dube *et al.*, 2020; Van Vuuren, 2008). CLE-AgNPs had MIC values far below 1 mg/ml which proves that they have exceptional antibacterial properties and can be used in the treatment of bacterial infections that require urgent alternative treatment options. The results obtained in this study are in agreement with a previous study in which Coseri and

colleagues also showed that AgNPs exhibit potent antibacterial activity against gram-positive and gram-negative bacteria (Pal *et al.*, 2017; Coseri *et al.*, 2015).

The CLE-AgNPs performed well in comparison to the positive control, Ciprofloxacin, as the antibacterial activity for the CLE-AgNPs was similar to that of Ciprofloxacin. Even though the MIC and MBC values for Ciprofloxacin was not determined in this study, it is notable that the concentration of Ciprofloxacin used was 15 µg/ml for all the microorganisms tested, except for *E. coli* where 10 µg/ml Ciprofloxacin was used. At these concentrations, Ciprofloxacin was able to inhibit the growth of all the microorganisms as well as exert a bactericidal effect against all of the microorganisms. The MIC and MBC values of CLE-AgNPs for all the microorganisms was well below the concentration(s) of Ciprofloxacin used in their respective tests, thus it can be concluded that lower concentrations of CLE-AgNPs was required in order to exert similar antibacterial effects as Ciprofloxacin on all of the microorganisms. This is a significant finding of this study as it proves that CLE-AgNPs are more or equally as effective as conventional antibiotic therapy.

The antimicrobial mechanism of action of silver is still under scientific debate. Some authors have maintained that the bactericidal activity may be related to the release of silver ions and their interaction with bacterial components intra- and extracellularly whilst other authors claim that the effect of silver may be due to a physical effect exerted on the cell membrane through penetration and subsequent interference with cellular components (Montano *et al.*, 2019). Other important effects of silver that have been described include bacterial biofilm inhibition, anti-inflammatory effects, and wound healing potential (Montano *et al.*, 2019). The antimicrobial mechanism of action of AgNPs is not fully understood, however, it is thought that the mechanism is similar to that of Ag^+ ions which involves adhesion and destruction of the bacterial cell wall or membrane, interaction and disruption of biomolecules, and generation of ROS and free radicals (Dawadi *et al.*, 2021). AgNPs have been shown to have wide applications in the prevention of further injury and bacterial invasion of wounds, hence, the efficient recovery of damaged tissues is enhanced by the use of AgNPs (Montano *et al.*, 2019).

Tocco and colleagues reported that the antimicrobial activity of AgNPs appears high because of its multilevel (including MDR) antibacterial effects and low systemic toxicity that allows the provision of an antibacterial effect that greatly reduces the chances of developing resistance (Tocco *et al.*, 2012). Hambardzumyan and colleagues have suggested that the antibacterial mechanism of

action of AgNPs is the result of many antibacterial events taking place simultaneously: (i) penetration of AgNPs in the bacterial cell wall resulting in leakage of cellular contents, (ii) release of Ag^+ ions, and (iii) reaction with sulfhydryl groups within the cytosolic environment (Bold *et al.*, 2022; Hambardzumyan *et al.*, 2020; Rajesh *et al.*, 2020; Vorobyova *et al.*, 2020; Mickymaray, 2019). The extraordinary bactericidal activity of AgNPs is due to their large surface area which enables the AgNPs to have better contact with microorganisms (Ibrahim, 2015). Moreover, AgNPs function as reservoirs of the positively charged silver ions which is indisputably a magnificent bactericidal agent on its own. Cationic compounds are able to easily bind to negatively charged bacterial cell membrane to elicit antibacterial action while the amphiphilic structure of some NPs can induce bacterial cell membrane damage (Yeh *et al.*, 2020; Chen *et al.*, 2016; Ibrahim, 2015).

The synthesized CLE-AgNPs displayed significant antibacterial activity. The ability of CLE-AgNPs to inhibit and kill human pathogenic organisms of such medical importance showcases their capability of being used in various applications in the medical and pharmaceutical industries (Kowsalya *et al.*, 2020). Fifty-one nanomedicines, including antibacterial nanoformulations, have already been approved by the U.S. FDA (Yeh *et al.*, 2020; Bobo *et al.*, 2016). NPs allows for the opportunity of free drug "anti-virulence" therapy to be explored. In contrast to traditional antibiotics, NPs are unlikely to develop drug resistance as there is no bactericidal effect. The physical and non-specific structural disruption of bacterial cell membranes results in an increase in membrane permeation and bacterial cell death. This process is less likely to elicit the development of resistance (Franco *et al.*, 2022; Cano *et al.*, 2020; Wang *et al.*, 2017).

Table 3.6: The MIC and MBC values of CLE-AgNPs against six human pathogenic bacteria (n=3).

Microorganisms	MIC	MBC
S. aureus	5.8 µg/ml	5.8 µg/ml
MRSA	5.8 µg/ml	11.7 µg/ml
E. coli	5.8 µg/ml	5.8 µg/ml
P. aeruginosa	1.5 µg/ml	1.5 µg/ml
K. pneumoniae	0.4 µg/ml	0.4 µg/ml
A. baumannii	2.9 µg/ml	2.9 µg/ml

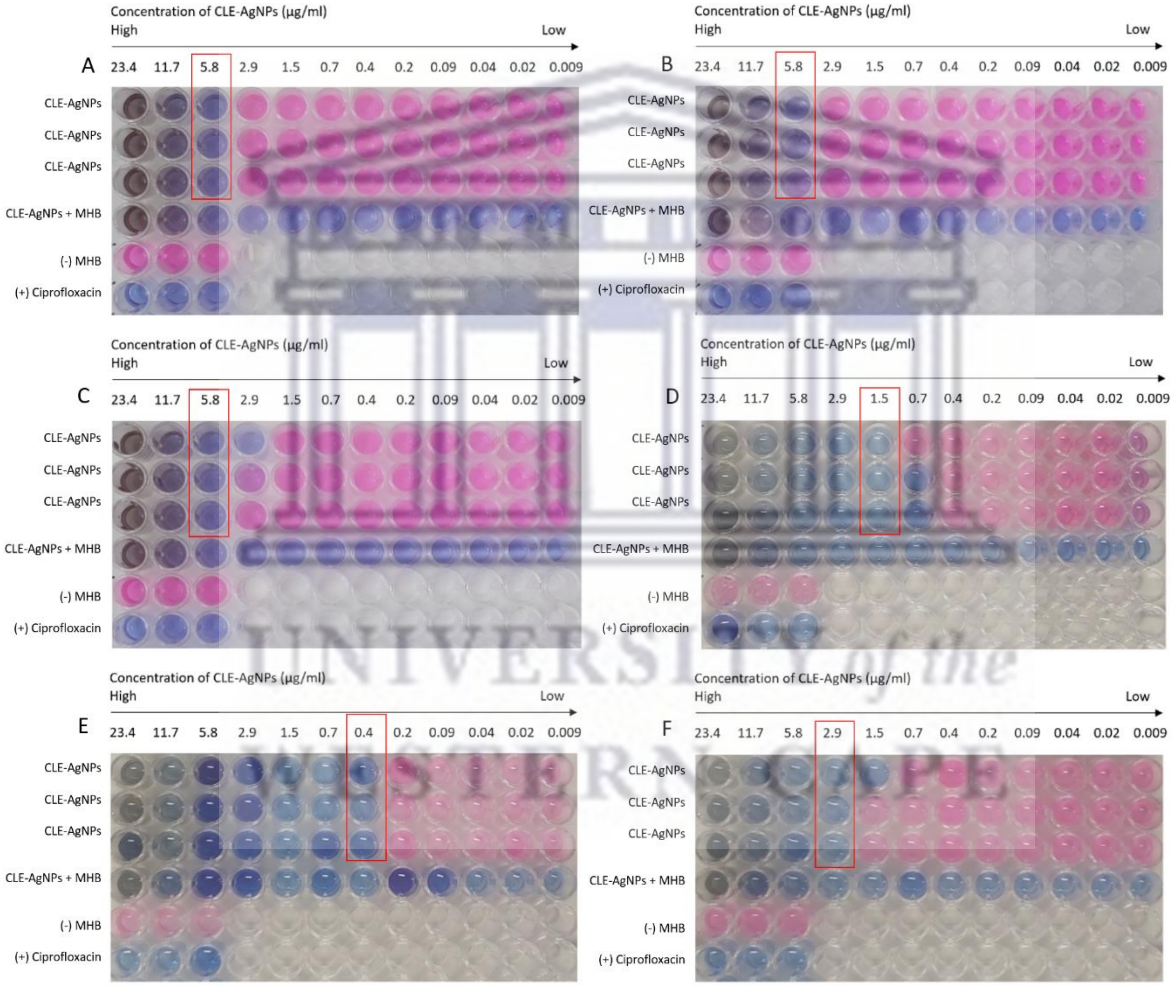

Figure 3.14: The inhibitory effects of CLE-AgNPs on bacterial growth using the microdilution assay in combination with AlamarBlue™ dye as a colourimetric indicator of viable bacteria. A colour change from blue to pink is observed in the presence of viable bacteria (A: *S. aureus*, B: MRSA, C: *E. coli*, D: *P. aeruginosa*, E: *K. pneumoniae*, and F: *A. baumannii*).

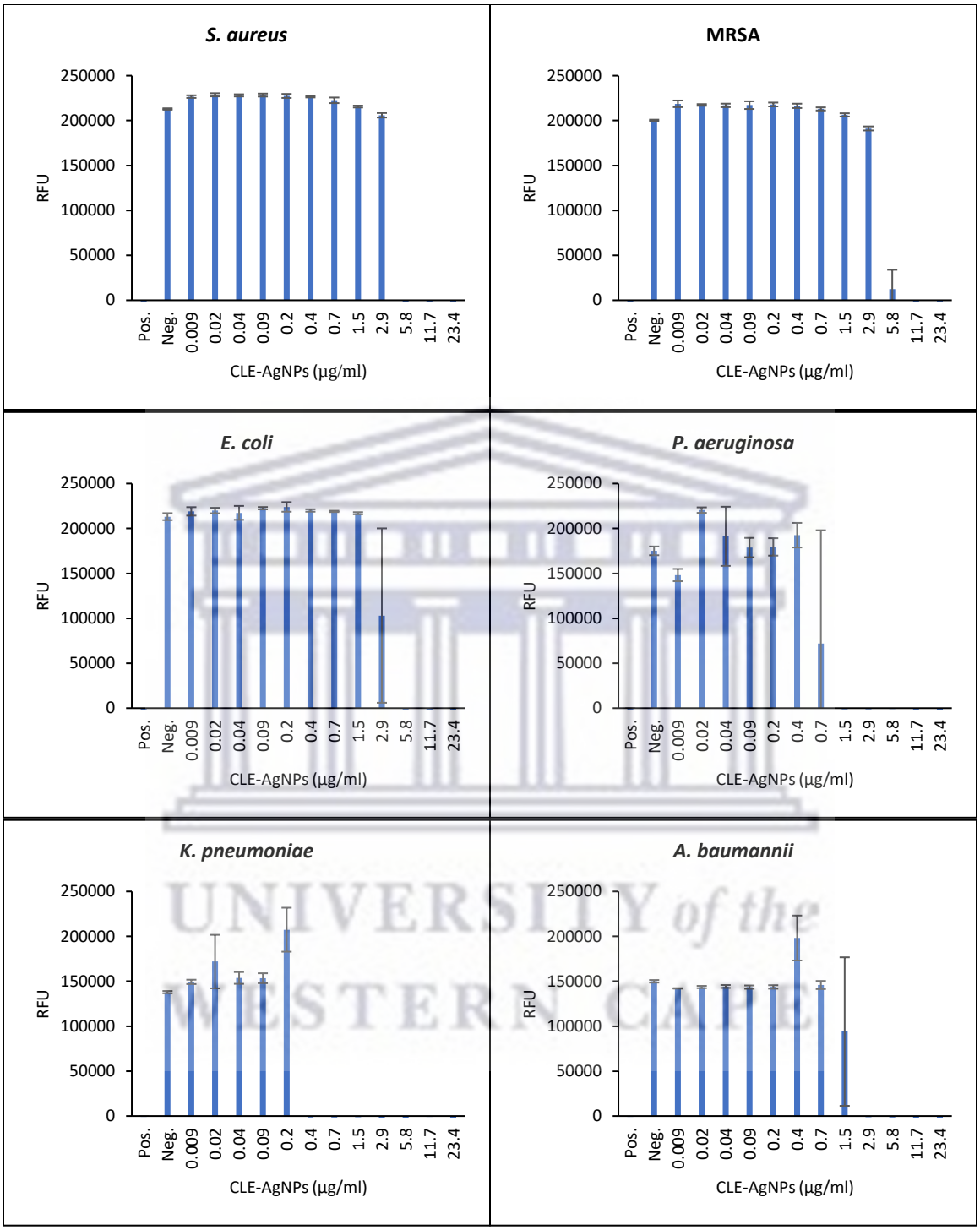

Figure 3.15: Graphs displaying the inhibitory effect of CLE-AgNPs on six different bacterial strains. The fluorescence of AlamarBlue™ was measured as a bacterial viability indicator and is directly proportional to the number of viable cells present (RFU: Relative Fluorescence Units).

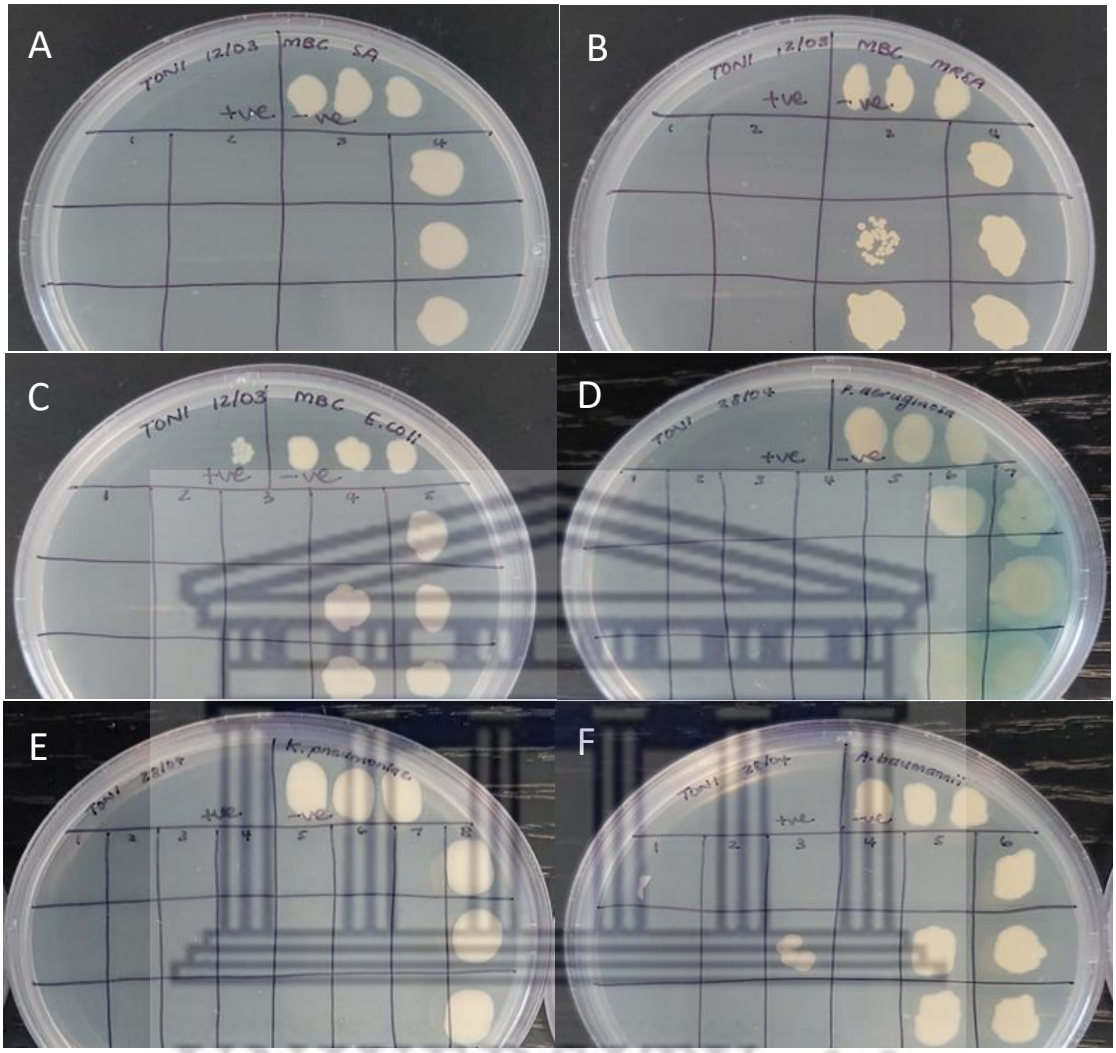

Figure 3.16: The bactericidal effects of CLE-AgNPs on six different bacterial strains (A: *S. aureus*, B: MRSA, C: *E. coli*, D: *P. aeruginosa*, E: *K. pneumoniae*, and F: *A. baumannii*).

CHAPTER 4: CONCLUSION AND RECOMMENDATIONS

"*Nanotechnology is an idea that most people simply didn't believe*." - Ralph Merkle

4.1 Conclusion

Antimicrobial resistance (AMR) is a major 'One Health' problem that needs to be addressed in order to achieve the Sustainable Development Goals. Infections caused by antibiotic-resistant bacteria are one of the leading causes of death for people of all ages. By 2050, more deaths will be attributed to AMR than all types of cancers which will cost the global economy an estimated US$100 trillion. Conventional treatments available for AMR infections are often inefficacious, require high or frequent dosages, are associated with side effects, and may further exacerbate AMR. Therefore, novel or alternative therapeutic strategies for the treatment of infections caused by antibiotic-resistant bacteria are urgently needed.

The main aim of the present study was to investigate the antibacterial effects of biogenic silver nanoparticles (AgNPs) synthesized using an aqueous *Manihot esculenta* (cassava) leaf extract, and their potential as anti-AMR agents. Thus, the study focused on the green synthesis of AgNPs using an aqueous cassava leaf extract (CLE) followed by the characterization of the synthesised CLE-AgNPs and the assessment of its *in vitro* antibacterial activity. The CLE-AgNPs were successfully synthesized and characterized.

The CLE-AgNPs demonstrated significant dose-dependent antibacterial activity against all six human pathogenic bacterial strains tested in this study. The CLE-AgNPs exhibited both growth inhibitory and bactericidal activity, with gram-negative bacteria being more susceptible to the antibacterial action of the CLE-AgNPs compared to gram-positive bacteria. These findings suggest that CLE-AgNPs may serve as a potential therapeutic agent for the treatment of bacterial infections associated with AMR for both gram-negative and gram-positive pathogenic bacteria.

In conclusion, the green synthesis, characterization, and assessment of the antibacterial activity of biogenic CLE-AgNPs were successfully performed, therefore, the aim and objectives of this study were achieved. This study has proven the hypothesis that phytochemicals present in the aqueous leaf extract from *M. esculenta* (cassava) may act as reducing, stabilizing, and capping agents in the formation of AgNPs with antibacterial properties. The biogenic CLE-AgNPs with significant antibacterial efficacy may be employed as a promising alternative strategy for the treatment of

antibiotic-resistant infections associated with AMR. The CLE-AgNPs have the potential to be applied in the biomedical field as a novel antimicrobial agent to eradicate the burden of AMR by combating bacterial infections. Nanotechnology can reshape the world through major revolutionary breakthroughs; some have already been made and others will continue to be made for the betterment of all humankind. In the words of Bernard Marcus, "*Nanotechnology in medicine is going to have a major impact on the survival of the human race.*"

4.2 Recommendations and future work

After the findings of this study were reviewed, it was evident that the CLE-AgNPs had vast potential and that the other biological activities of the CLE-AgNPs should be explored. Further investigations into the antibacterial activity of CLE-AgNPs tested against other medically important bacteria with antibiotic resistance can be conducted along with the determination of the antibacterial mechanism of action of CLE-AgNPs in each of these microorganisms that they are able to exert an antibacterial effect on. Additionally, the *in vitro* and *in vivo* antibacterial, antioxidant and anti-inflammatory activities of CLE-AgNPs should be evaluated. The cytotoxicity of the CLE-AgNPs in mammalian cells should be investigated in order to determine whether they can be used in further studies. Moreover, the wound healing potential of the biogenic CLE-AgNPs should be assessed as there is great potential for AgNPs being used as aids in wound healing. The long-term cytotoxicity and metabolism of the CLE-AgNPs should be considered as it is important to understand how NPs function at a cellular level in order to avoid the possible adverse side effects. It is imperative that more research is focused on the evaluation of the safety of nanotechnology-based approaches. Long-term *in vitro* and *in vivo* biosafety and experimental observations are essential as they play a key role in ensuring that innovative therapeutic strategies are transferred into clinical practice and other stages of the drug development process (Okkeh et al., 2021).

4.3 Limitations of the study

The present study had some limitations that need to be kept in mind when interpreting the findings of this study. Some of the limitations include limited accuracy and time required. Limited accuracy may refer to the equipment or machinery that may not have allowed the accurate collection of data, for example, the use of a ruler in the measurement of zone of inhibitions in the agar well diffusion

assays. The measurements may not be as accurate as it would have been had a different measuring tool (e.g., caliper) been used. Lastly, more time would have allowed me to perform further studies to understand the antibacterial mechanism of action of CLE-AgNPs and provide better insight into how the CLE-AgNPs are able to exert an inhibitory and bactericidal effect on the microorganisms.

REFERENCES

AGARWAL, H., KUMAR, S. V. & RAJESHKUMAR, S. 2021. Antidiabetic effect of silver nanoparticles synthesized using lemongrass (*Cymbopogon Citratus*) through conventional heating and microwave irradiation approach. *Journal of Microbiology, Biotechnology and Food Sciences,* 2021**,** 371-376.

AHMAD, N., SHARMA, S., ALAM, M. K., SINGH, V., SHAMSI, S., MEHTA, B. & FATMA, A. 2010. Rapid synthesis of silver nanoparticles using dried medicinal plant of basil. *Colloids and Surfaces B: Biointerfaces,* 81**,** 81-86.

AHMADI, M. & ADIBHESAMI, M. 2017. The effect of silver nanoparticles on wounds contaminated with *Pseudomonas aeruginosa* in mice: an experimental study. *Iranian Journal of Pharmaceutical Research: IJPR,* 16**,** 661.

AHMED, S., AHMAD, M., SWAMI, B. L. & IKRAM, S. 2016a. A review on plants extract mediated synthesis of silver nanoparticles for antimicrobial applications: a green expertise. *Journal of Advanced Research,* 7**,** 17-28.

AHMED, S. & IKRAM, S. 2016. Biosynthesis of gold nanoparticles: a green approach. *Journal of Photochemistry and Photobiology B: Biology,* 161**,** 141-153.

AHMED, S., SAIFULLAH, AHMAD, M., SWAMI, B. L. & IKRAM, S. 2016b. Green synthesis of silver nanoparticles using *Azadirachta indica* aqueous leaf extract. *Journal of Radiation Research and Applied Sciences,* 9**,** 1-7.

AL-ROFAAI, A., RAHMAN, W., SULAIMAN, S. & YAHAYA, Z. 2012. *In vitro* activity of neem (*Azadirachta indica*) and cassava (*Manihot esculenta*) on three pre-parasitic stages of susceptible and resistant strains of *Teladorsagia (Ostertagia) circumcincta*. *Veterinary Parasitology,* 188**,** 85-92.

AL AZAD, S., MORSHED, M. N., DEB, H., ALAM, M. A. M., HASAN, K. F. & SHEN, X. 2017. Localized Surface Plasmon Resonance Property of Ag-Nanoparticles and Prospects as Imminent Multi-Functional Colorant. *American Journal of Nanoscience and Nanotechnology Research,* 5**,** 1-20.

ALHARBI, N. S., KHALED, J. M., KADAIKUNNAN, S., ALOBAIDI, A. S., SHARAFADDIN, A. H., ALYAHYA, S. A., ALMANAA, T. N., ALSUGHAYIER, M. A. & SHEHU, M. R. 2019. Prevalence of *Escherichia coli* strains resistance to antibiotics in wound infections and raw milk. *Saudi Journal of Biological Sciences,* 26**,** 1557-1562.

ALJABALI, A. A., AKKAM, Y., AL ZOUBI, M. S., AL-BATAYNEH, K. M., AL-TRAD, B., ABO ALROB, O., ALKILANY, A. M., BENAMARA, M. & EVANS, D. J. 2018. Synthesis of gold nanoparticles using leaf extract of *Ziziphus zizyphus* and their antimicrobial activity. *Nanomaterials,* 8**,** 174.

AMADO-CORNEJO, N. D., ALDINE ATUSPARIA-FLORES, G., HUAMÁN-CABRERA, M. V., MÉNDEZ-PAJARES, Á., PRADO-ASENCIOS, E., JURUPE-CHICO, H. & HERENCIA-REYES, V. 2020. Anti-inflammatory activity of the ethanolic extract of the

leaves of *Manihot esculenta* crantz (yuca) in an experimental model of acute inflammation. *Revista de la Facultad de Medicina Humana,* 20**,** 94-98.

AMELEWORK, A. B., BAIRU, M. W., MAEMA, O., VENTER, S. L. & LAING, M. 2021. Adoption and promotion of resilient crops for climate risk mitigation and import substitution: A case analysis of cassava for South African agriculture. *Frontiers in Sustainable Food Systems,* 5**,** 617783.

ANAND, K., TILOKE, C., NAIDOO, P. & CHUTURGOON, A. 2017. Phytonanotherapy for management of diabetes using green synthesis nanoparticles. *Journal of Photochemistry and Photobiology B: Biology,* 173**,** 626-639.

ANASTAS, P. & WARNER, J. 1998. *Green chemistry: theory and practice*. New York: Oxford University Press, 30.

ANWAR, U. & BOHARI, S. P. M. 2019. Effect of *Manihot Esculenta* Aqueous Extract and Therapeutic Ultrasound In Accelerating the Wound Healing Process *In Vitro*. *Jurnal Teknologi,* 81.

ARYA, G., KUMARI, R. M., SHARMA, N., GUPTA, N., KUMAR, A., CHATTERJEE, S. & NIMESH, S. 2019. Catalytic, antibacterial and antibiofilm efficacy of biosynthesised silver nanoparticles using *Prosopis juliflora* leaf extract along with their wound healing potential. *Journal of Photochemistry and Photobiology B: Biology,* 190**,** 50-58.

AZELTINE, M., CLARK, A., ZGHEIB, C. & GHATAK, S. 2020. Nanotechnology in diabetic wound healing. *Wound Healing, Tissue Repair, and Regeneration in Diabetes.* Elsevier.

AZIMI, L., MOTEVALLIAN, A., EBRAHIMZADEH NAMVAR, A., ASGHARI, B. & LARI, A. R. 2011. Nosocomial infections in burned patients in Motahari hospital, Tehran, Iran. *Dermatology Research and Practice,* 2011.

BAHEKAR, S. & KALE, R. 2013. Phytopharmacological aspects of *Manihot esculenta* Crantz (cassava)—A Review. *Mintage Journal of Pharmaceutical and Medical Sciences,* 2**,** 4-5.

BAHRULOLUM, H., NOORAEI, S., JAVANSHIR, N., TARRAHIMOFRAD, H., MIRBAGHERI, V. S., EASTON, A. J. & AHMADIAN, G. 2021. Green synthesis of metal nanoparticles using microorganisms and their application in the agrifood sector. *Journal of Nanobiotechnology,* 19**,** 1-26.

BALAN, K., QING, W., WANG, Y., LIU, X., PALVANNAN, T., WANG, Y., MA, F. & ZHANG, Y. 2016. Antidiabetic activity of silver nanoparticles from green synthesis using *Lonicera japonica* leaf extract. *RSC Advances,* 6**,** 40162-40168.

BALOUIRI, M., SADIKI, M. & IBNSOUDA, S. K. 2016. Methods for *in vitro* evaluating antimicrobial activity: A review. *Journal of Pharmaceutical Analysis,* 6**,** 71-79.

BARISIK, M., ATALAY, S., BESKOK, A. & QIAN, S. 2014. Size dependent surface charge properties of silica nanoparticles. *The Journal of Physical Chemistry C,* 118**,** 1836-1842.

BENAKASHANI, F., ALLAFCHIAN, A. & JALALI, S. 2016. Biosynthesis of silver nanoparticles using *Capparis spinosa* L. leaf extract and their antibacterial activity. *Karbala International Journal of Modern Science,* 2**,** 251-258.

BEYENE, H. D., WERKNEH, A. A., BEZABH, H. K. & AMBAYE, T. G. 2017. Synthesis paradigm and applications of silver nanoparticles (AgNPs), a review. *Sustainable Materials and Technologies,* 13**,** 18-23.

BHARDWAJ, M., YADAV, P., DALAL, S. & KATARIA, S. K. 2020. A review on ameliorative green nanotechnological approaches in diabetes management. *Biomedicine and Pharmacotherapy,* 127**,** 110198.

BHATIA, P., SHARMA, A., GEORGE, A. J., ANVITHA, D., KUMAR, P., DWIVEDI, V. P. & CHANDRA, N. S. 2021. Antibacterial activity of medicinal plants against ESKAPE: An update. *Heliyon,* 7**,** e06310.

BOATENG, J. & CATANZANO, O. 2020. Silver and silver nanoparticle-based antimicrobial dressings. *Therapeutic Dressings and Wound Healing Applications***,** 157-184.

BOBO, D., ROBINSON, K. J., ISLAM, J., THURECHT, K. J. & CORRIE, S. R. 2016. Nanoparticle-based medicines: a review of FDA-approved materials and clinical trials to date. *Pharmaceutical Research,* 33**,** 2373-2387.

BOKANISEREME, U. F. Y. & OKECHUKWU, P. N. 2013. Anti-inflammatory, analgesic and anti-pyretic activity of cassava leaves extract. *Asian Journal of Pharmaceutical and Clinical Research,* 6**,** 89-92.

BOLD, B.-E., URNUKHSAIKHAN, E. & MISHIG-OCHIR, T. 2022. Biosynthesis of silver nanoparticles with antibacterial, antioxidant, anti-inflammatory properties and their burn wound healing efficacy. *Frontiers in Chemistry,* 10.

BOROUMAND, Z., GOLMAKANI, N. & BOROUMAND, S. 2018. Clinical trials on silver nanoparticles for wound healing. *Nanomedicine Journal,* 5**,** 186-191.

BRUNA, T., MALDONADO-BRAVO, F., JARA, P. & CARO, N. 2021. Silver nanoparticles and their antibacterial applications. *International Journal of Molecular Sciences,* 22**,** 7202.

BURDUȘEL, A.-C., GHERASIM, O., GRUMEZESCU, A. M., MOGOANTĂ, L., FICAI, A. & ANDRONESCU, E. 2018. Biomedical applications of silver nanoparticles: an up-to-date overview. *Nanomaterials,* 8**,** 681.

BURNS, A. E., GLEADOW, R. M., ZACARIAS, A. M., CUAMBE, C. E. O., MILLER, R. E. & CAVAGNARO, T. R. 2012. Variations in the chemical composition of cassava (*Manihot esculenta* Crantz) leaves and roots as affected by genotypic and environmental variation. *Journal of Agricultural and Food Chemistry,* 60**,** 4946-4956.

CANO, A., ETTCHETO, M., ESPINA, M., LÓPEZ-MACHADO, A., CAJAL, Y., RABANAL, F., SÁNCHEZ-LÓPEZ, E., CAMINS, A., GARCÍA, M. L. & SOUTO, E. B. 2020. State-of-the-art polymeric nanoparticles as promising therapeutic tools against human bacterial infections. *Journal of Nanobiotechnology,* 18**,** 1-24.

CENTERS FOR DISEASE CONTROL AND PREVENTION 2019. Antibiotic resistant threats in the United States 2019. Atlanta, GA.

CENTERS FOR DISEASE CONTROL AND PREVENTION. 2022a. *About Antimicrobial Resistance* [Online]. Atlanta, GA: U.S. Department of Health and Human Services, CDC. Available: https://www.cdc.gov/drugresistance/about.html [Accessed 12 December 2022].

CENTERS FOR DISEASE CONTROL AND PREVENTION. 2022b. *Antimicrobial Resistance Questions and Answers* [Online]. Atlanta, GA: U.S. Department of Health and Human Services, CDC. Available: https://www.cdc.gov/antibiotic-use/antibiotic-resistance.html#:~:text=CDC%20estimates%20about%2047%20million,play%20in%20improving%20antibiotic%20use. [Accessed 14 December 2022].

CENTERS FOR DISEASE CONTROL AND PREVENTION 2022c. COVID-19: U.S. Impact on Antimicrobial Resistance, Special Report 2022. Atlanta, GA.

CENTERS FOR DISEASE CONTROL AND PREVENTION. 2022d. *How Antimicrobial Resistance Happens* [Online]. Atlanta, GA: U.S. Department of Health and Human Services, CDC. Available: https://www.cdc.gov/drugresistance/about/how-resistance-happens.html [Accessed 12 December 2022].

CHAHARDOLI, A., KARIMI, N., SADEGHI, F. & FATTAHI, A. 2018. Green approach for synthesis of gold nanoparticles from *Nigella arvensis* leaf extract and evaluation of their antibacterial, antioxidant, cytotoxicity and catalytic activities. *Artificial Cells, Nanomedicine, and Biotechnology,* 46**,** 579-588.

CHEN, S.-L., YU, H., LUO, H.-M., WU, Q., LI, C.-F. & STEINMETZ, A. 2016. Conservation and sustainable use of medicinal plants: problems, progress, and prospects. *Chinese Medicine,* 11**,** 1-10.

CHETTY, S. 2021. South Africa's capacity to conduct antimicrobial stewardship. *Southern African Journal of Infectious Diseases,* 36.

CHINNASAMY, G., CHANDRASEKHARAN, S., KOH, T. W. & BHATNAGAR, S. 2021. Synthesis, characterization, antibacterial and wound healing efficacy of silver nanoparticles from *Azadirachta indica*. *Frontiers in Microbiology,* 12**,** 611560.

CHOUHAN, S., SHARMA, K. & GULERIA, S. 2017. Antimicrobial activity of some essential oils—present status and future perspectives. *Medicines,* 4**,** 58.

CHUNG, I.-M., PARK, I., SEUNG-HYUN, K., THIRUVENGADAM, M. & RAJAKUMAR, G. 2016. Plant-mediated synthesis of silver nanoparticles: their characteristic properties and therapeutic applications. *Nanoscale Research Letters,* 11**,** 1-14.

CLOGSTON, J. D. & PATRI, A. K. 2011. Zeta potential measurement. *In:* McNEIL, S. (ed.) *Characterization of Nanoparticles Intended for Drug Delivery.* Humana Press.

COATES, J. 2000. Interpretation of infrared spectra, a practical approach. *In:* MEYERS, R. (ed.) *Encyclopedia of Analytical Chemistry.* Chichester: John Wiley & Sons Ltd.

COSERI, S., SPATAREANU, A., SACARESCU, L., RIMBU, C., SUTEU, D., SPIRK, S. & HARABAGIU, V. 2015. Green synthesis of the silver nanoparticles mediated by pullulan and 6-carboxypullulan. *Carbohydrate Polymers,* 116**,** 9-17.

CRUZ, G., RODRIGUES, A. D. L. P., DA SILVA, D. F. & GOMES, W. C. 2021. Physical–chemical characterization and thermal behavior of cassava harvest waste for application in thermochemical processes. *Journal of Thermal Analysis and Calorimetry,* 143**,** 3611-3622.

DA COSTA MOUSINHO, N. M. H. 2013. *In vitro anti-diabetic activity of Sclerocarya birrea and Ziziphus mucronata.* M.Sc. Thesis, University of Pretoria.

DA'NA, E., TAHA, A. & AFKAR, E. 2018. Green synthesis of iron nanoparticles by *Acacia nilotica* pods extract and its catalytic, adsorption, and antibacterial activities. *Applied Sciences,* 8**,** 1922.

DADA, A. O., ADEKOLA, F. A., DADA, F. E., ADELANI-AKANDE, A. T., BELLO, M. O., OKONKWO, C. R., INYINBOR, A. A., OLUYORI, A. P., OLAYANJU, A., AJANAKU, K. O. & ADETUNJI, C. O. 2019. Silver nanoparticle synthesis by *Acalypha wilkesiana* extract: phytochemical screening, characterization, influence of operational parameters, and preliminary antibacterial testing. *Heliyon,* 5**,** e02517.

DAHL, J. A., MADDUX, B. L. & HUTCHISON, J. E. 2007. Toward greener nanosynthesis. *Chemical Reviews,* 107**,** 2228-2269.

DAKAL, T. C., KUMAR, A., MAJUMDAR, R. S. & YADAV, V. 2016. Mechanistic basis of antimicrobial actions of silver nanoparticles. *Frontiers in Microbiology,* 7**,** 1831.

DAWADI, S., KATUWAL, S., GUPTA, A., LAMICHHANE, U., THAPA, R., JAISI, S., LAMICHHANE, G., BHATTARAI, D. P. & PARAJULI, N. 2021. Current research on silver nanoparticles: Synthesis, characterization, and applications. *Journal of Nanomaterials,* 2021.

DE OLIVEIRA, D. M., FORDE, B. M., KIDD, T. J., HARRIS, P. N., SCHEMBRI, M. A., BEATSON, S. A., PATERSON, D. L. & WALKER, M. J. 2020. Antimicrobial resistance in ESKAPE pathogens. *Clinical Microbiology Reviews,* 33**,** e00181-19.

DREXLER, K. E. 1981. Molecular engineering: An approach to the development of general capabilities for molecular manipulation. *Proceedings of the National Academy of Sciences,* 78**,** 5275-5278.

DUBE, P., MEYER, S., MADIEHE, A. & MEYER, M. 2020. Antibacterial activity of biogenic silver and gold nanoparticles synthesized from *Salvia africana-lutea* and *Sutherlandia frutescens*. *Nanotechnology,* 31**,** 505607.

EKOP, I., SIMONYAN, K. & EVWIERHOMA, E. 2019. Utilization of cassava wastes for value added products: An overview. *International Journal of Scientific Engineering and Science,* 3**,** 31-39.

EL-SHARKAWY, M. A. 2004. Cassava biology and physiology. *Plant Molecular Biology,* 56**,** 481-501.

EL-ADAWY, M. M., EISSA, A. E., SHAALAN, M., AHMED, A. A., YOUNIS, N. A., ISMAIL, M. M. & ABDELSALAM, M. 2021. Green synthesis and physical properties of Gum Arabic-silver nanoparticles and its antibacterial efficacy against fish bacterial pathogens. *Aquaculture Research,* 52**,** 1247-1254.

ELIA, P., ZEIRI, Y., ZACH, R., HAZAN, S., KOLUSHEVA, S. & PORAT, Z. E. 2014. Green synthesis of gold nanoparticles using plant extracts as reducing agents. *International Journal of Nanomedicine***,** 4007.

ESSIEN, E. R., ATASIE, V. N., NWUDE, D. O., ADEKOLUREJO, E. & OWOEYE, F. T. 2022. Characterisation of ZnO nanoparticles prepared using aqueous leaf extracts of *Chromolaena odorata* (L.) and *Manihot esculenta* (Crantz). *South African Journal of Science,* 118**,** 1-8.

FENG, Q., WU, J., CHEN, C., CUI, F., KIM, T. & KIM, J. 2000. A mechanistic study of the antibacterial effect of silver ions on *Escherichia coli* and *Staphylococcus aureus*. *Journal of Biomedical Materials Research,* 52**,** 662-668.

FENG, Y., YU, Y., WANG, Y. & LIN, X. 2007. Biosorption and bioreduction of trivalent aurum by photosynthetic bacteria *Rhodobacter capsulatus*. *Current Microbiology,* 55**,** 402-408.

FERRARO, V., PICCIRILLO, C., TOMLINS, K. & PINTADO, M. E. 2016. Cassava (*Manihot esculenta* Crantz) and yam (*Dioscorea* spp.) crops and their derived foodstuffs: safety, security and nutritional value. *Critical Reviews in Food Science and Nutrition,* 56**,** 2714-2727.

FEYNMAN, R. P. Plenty of Room at the Bottom. APS annual meeting, 1959.

FONG, J., WOOD, F. & FOWLER, B. 2005. A silver coated dressing reduces the incidence of early burn wound cellulitis and associated costs of inpatient treatment: comparative patient care audits. *Burns,* 31**,** 562-567.

FOUNOU, R. C., FOUNOU, L. L. & ESSACK, S. Y. 2017. Clinical and economic impact of antibiotic resistance in developing countries: a systematic review and meta-analysis. *PloS ONE,* 12**,** e0189621.

FRANCO, D., CALABRESE, G., GUGLIELMINO, S. P. P. & CONOCI, S. 2022. Metal-based nanoparticles: Antibacterial mechanisms and biomedical application. *Microorganisms,* 10**,** 1778.

GAMBOA, S. M., ROJAS, E., MARTÍNEZ, V. & VEGA-BAUDRIT, J. 2019. Synthesis and characterization of silver nanoparticles and their application as an antibacterial agent. *International Journal of Biosensors and Bioelectronics,* 5**,** 166-173.

GASBARRI, C., RUGGIERI, F., FOSCHI, M., ACETO, A., SCOTTI, L. & ANGELINI, G. 2019. Simple determination of silver nanoparticles concentration as Ag+ by using ISE as potential alternative to ICP optical emission spectrometry. *Chemistry Select,* 4**,** 9501-9504.

GEBREYOHANNES, G., NYERERE, A., BII, C. & SBHATU, D. B. 2019. Challenges of intervention, treatment, and antibiotic resistance of biofilm-forming microorganisms. *Heliyon,* 5**,** e02192.

GEOPRINCY, G., SRRI, B. V., POONGUZHALI, U., GANDHI, N. N. & RENGANATHAN, S. 2013. A review on green synthesis of silver nanoparticles. *Asian Journal of Pharmaceutical and Clinical Research,* 6**,** 8-12.

GERAGHTY, T. & LAPORTA, G. 2019. Current health and economic burden of chronic diabetic osteomyelitis. *Expert Review of Pharmacoeconomics and Outcomes Research,* 19**,** 279-286.

GHIMIRE, A., SEN, R. & ANNACHHATRE, A. P. 2015. Biosolid management options in cassava starch industries of Thailand: present practice and future possibilities. *Procedia Chemistry,* 14**,** 66-75.

GHOSH, S., PATIL, S., AHIRE, M., KITTURE, R., KALE, S., PARDESI, K., CAMEOTRA, S. S., BELLARE, J., DHAVALE, D. D. & JABGUNDE, A. 2012. Synthesis of silver nanoparticles using *Dioscorea bulbifera* tuber extract and evaluation of its synergistic potential in combination with antimicrobial agents. *International Journal of Nanomedicine,* 7**,** 483.

GILBERTSON, L. M., ZIMMERMAN, J. B., PLATA, D. L., HUTCHISON, J. E. & ANASTAS, P. T. 2015. Designing nanomaterials to maximize performance and minimize undesirable implications guided by the Principles of Green Chemistry. *Chemical Society Reviews,* 44**,** 5758-5777.

GNANAJOBITHA, G., PAULKUMAR, K., VANAJA, M., RAJESHKUMAR, S., MALARKODI, C., ANNADURAI, G. & KANNAN, C. 2013. Fruit-mediated synthesis of silver nanoparticles using *Vitis vinifera* and evaluation of their antimicrobial efficacy. *Journal of Nanostructure in Chemistry,* 3**,** 1-6.

GOUR, A. & JAIN, N. K. 2019. Advances in green synthesis of nanoparticles. *Artificial Cells, Nanomedicine, and Biotechnology,* 47**,** 844-851.

GROSSMAN, L. D., ROSCOE, R., SHACK, A. R. & COMMITTEE, D. C. C. P. G. E. 2018. Complementary and alternative medicine for diabetes. *Canadian Journal of Diabetes,* 42**,** S154-S161.

GUISBIERS, G., MEJÍA-ROSALES, S. & DEEPAK, F. L. 2012. Nanomaterial properties: size and shape dependencies. *Journal of Nanomaterials,* 2012**,** 20-20.

GUNTI, L., DASS, R. S. & KALAGATUR, N. K. 2019. Phytofabrication of selenium nanoparticles from *Emblica officinalis* fruit extract and exploring its biopotential applications: antioxidant, antimicrobial, and biocompatibility. *Frontiers in Microbiology,* 10**,** 931.

HADZI-NIKOLOVA, M., DIMOV, G., MIRAKOVSKI, D., ZENDELSKA, A., DONEVA, N., ZLATKOVSKI, V., MARAGKAKI, A., PAPADAKI, A., SABATHIANAKIS, G. & THRASSYVOULOS, M. 2021. Biowaste Management and Circular Economy: Usage of Pay as you Throw System and Autonomous Composting Units in Municipality of Probishtip. *Circular Economy and Sustainability***,** 1-18.

HAMBARDZUMYAN, S., SAHAKYAN, N., PETROSYAN, M., NASIM, M. J., JACOB, C. & TRCHOUNIAN, A. 2020. *Origanum vulgare* L. extract-mediated synthesis of silver nanoparticles, their characterization and antibacterial activities. *AMB Express,* 10**,** 1-11.

HAMDAN, S., PASTAR, I., DRAKULICH, S., DIKICI, E., TOMIC-CANIC, M., DEO, S. & DAUNERT, S. 2017. Nanotechnology-driven therapeutic interventions in wound healing: potential uses and applications. *ACS Central Science,* 3**,** 163-175.

HASIM, H., FALAH, S. & DEWI, L. K. 2016. Effect of boiled cassava leaves (*Manihot esculenta* Crantz) on total phenolic, flavonoid and its antioxidant activity. *Current Biochemistry,* 3**,** 116-127.

HENSHAW, P. 2018. *Use of alamarBlue as an Indicator of Microbial Growth in Turbid Solutions for Antimicrobial Evaluation.* Masters Theses, University of Massachusetts Amherst.

HTWE, Y., CHOW, W., SUDA, Y. & MARIATTI, M. 2019. Effect of silver nitrate concentration on the production of silver nanoparticles by green method. *Materials Today: Proceedings,* 17**,** 568-573.

HU, D., ZOU, L., GAO, Y., JIN, Q. & JI, J. 2020. Emerging nanobiomaterials against bacterial infections in postantibiotic era. *View,* 1**,** 20200014.

HUSAIN, S., SARDAR, M. & FATMA, T. 2015. Screening of cyanobacterial extracts for synthesis of silver nanoparticles. *World Journal of Microbiology and Biotechnology,* 31**,** 1279-1283.

IBRAHIM, H. M. 2015. Green synthesis and characterization of silver nanoparticles using banana peel extract and their antimicrobial activity against representative microorganisms. *Journal of Radiation Research and Applied Sciences,* 8**,** 265-275.

ITOBA-TOMBO, E. F., NTWAMPE, S. K. O., NCHU, F. & MUDUMBI, J. B. 2019. Potential Challenges of Cassava Cultivation in South Africa. *16th SOUTH AFRICA International Conference on Agricultural, Chemical, Biological & Environmental Sciences (ACBES-19).* Johannesburg, South Africa.

IVANOV, D. 2015. How big is a nanoparticle?

JALANI, N. S., MICHELL, W., LIN, W. E., HANANI, S. Z., HASHIM, U. & ABDULLAH, R. 2018. Biosynthesis of silver nanoparticles using *Citrus grandis* peel extract. *Malaysian Journal of Analytical Sciences,* 22**,** 676-683.

JAMPA, M., SUTTHANUT, K., WEERAPREEYAKUL, N., TUKUMMEE, W., WATTANATHORN, J. & MUCHIMAPURA, S. 2022. Multiple Bioactivities of *Manihot esculenta* Leaves: UV Filter, Anti-Oxidation, Anti-Melanogenesis, Collagen Synthesis Enhancement, and Anti-Adipogenesis. *Molecules,* 27**,** 1556.

JAN, H. A., JAN, S., BUSSMANN, R. W., WALI, S., SISTO, F. & AHMAD, L. 2020. Complementary and alternative medicine research, prospects and limitations in Pakistan: a literature review. *Acta Ecologica Sinica,* 40**,** 451-463.

JANG, E.-Y., SON, Y.-J., PARK, S.-Y., YOO, J.-Y., CHO, Y.-N., JEONG, S.-Y., LIU, S. & SON, H.-J. 2018. Improved biosynthesis of silver nanoparticles using keratinase from *Stenotrophomonas maltophilia* R13: reaction optimization, structural characterization, and biomedical activity. *Bioprocess and Biosystems Engineering,* 41**,** 381-393.

JINI, D. & SHARMILA, S. 2020. Green synthesis of silver nanoparticles from *Allium cepa* and its *in vitro* antidiabetic activity. *Materials Today: Proceedings,* 22**,** 432-438.

JOUDEH, N. & LINKE, D. 2022. Nanoparticle classification, physicochemical properties, characterization, and applications: a comprehensive review for biologists. *Journal of Nanobiotechnology,* 20**,** 1-29.

KALANTARI, K., MOSTAFAVI, E., AFIFI, A. M., IZADIYAN, Z., JAHANGIRIAN, H., RAFIEE-MOGHADDAM, R. & WEBSTER, T. J. 2020. Wound dressings functionalized with silver nanoparticles: promises and pitfalls. *Nanoscale,* 12**,** 2268-2291.

KAPADIA, P., NEWELL, A. S., CUNNINGHAM, J., ROBERTS, M. R. & HARDY, J. G. 2022. Extraction of High-Value Chemicals from Plants for Technical and Medical Applications. *International Journal of Molecular Sciences,* 23**,** 10334.

KASITHEVAR, M., PERIAKARUPPAN, P., MUTHUPANDIAN, S. & MOHAN, M. 2017. Antibacterial efficacy of silver nanoparticles against multi-drug resistant clinical isolates from post-surgical wound infections. *Microbial Pathogenesis,* 107**,** 327-334.

KATHIRAVAN, V., RAVI, S., ASHOKKUMAR, S., VELMURUGAN, S., ELUMALAI, K. & KHATIWADA, C. P. 2015. Green synthesis of silver nanoparticles using *Croton sparsiflorus morong* leaf extract and their antibacterial and antifungal activities. *Spectrochimica Acta Part A: Molecular and Biomolecular Spectroscopy,* 139**,** 200-205.

KESHARI, A. K., SRIVASTAVA, R., SINGH, P., YADAV, V. B. & NATH, G. 2020. Antioxidant and antibacterial activity of silver nanoparticles synthesized by *Cestrum nocturnum*. *Journal of Ayurveda and Integrative Medicine,* 11**,** 37-44.

KGANYAGO, P., MAHLAULE-GLORY, L., MATHIPA, M., NTSENDWANA, B., MKETO, N., MBITA, Z. & HINTSHO-MBITA, N. 2018. Synthesis of NiO nanoparticles via a green route using *Monsonia burkeana*: the physical and biological properties. *Journal of Photochemistry and Photobiology B: Biology,* 182**,** 18-26.

KHALID, K., TAN, X., MOHD ZAID, H. F., TAO, Y., LYE CHEW, C., CHU, D.-T., LAM, M. K., HO, Y.-C., LIM, J. W. & CHIN WEI, L. 2020. Advanced in developmental organic and inorganic nanomaterial: A review. *Bioengineered,* 11**,** 328-355.

KHALIL, M. M., ISMAIL, E. H., EL-BAGHDADY, K. Z. & MOHAMED, D. 2014. Green synthesis of silver nanoparticles using olive leaf extract and its antibacterial activity. *Arabian Journal of Chemistry,* 7**,** 1131-1139.

KHAN, I., SAEED, K. & KHAN, I. 2019. Nanoparticles: Properties, applications and toxicities. *Arabian Journal of Chemistry,* 12**,** 908-931.

KHAN, S., SINGH, S., GAIKWAD, S., NAWANI, N., JUNNARKAR, M. & PAWAR, S. V. 2020. Optimization of process parameters for the synthesis of silver nanoparticles from *Piper betle* leaf aqueous extract, and evaluation of their antiphytofungal activity. *Environmental Science and Pollution Research,* 27**,** 27221-27233.

KHÉMIRI, I., ESSGHAIER HÉDI, B., SADFI ZOUAOUI, N., BEN GDARA, N. & BITRI, L. 2019. The antimicrobial and wound healing potential of *Opuntia ficus indica L. inermis*

extracted oil from Tunisia. *Evidence-Based Complementary and Alternative Medicine,* 2019.

KHORRAMI, S., ZARRABI, A., KHALEGHI, M., DANAEI, M. & MOZAFARI, M. 2018. Selective cytotoxicity of green synthesized silver nanoparticles against the MCF-7 tumor cell line and their enhanced antioxidant and antimicrobial properties. *International Journal of Nanomedicine,* Volume 13**,** 8013-8024.

KONOP, M., DAMPS, T., MISICKA, A. & RUDNICKA, L. 2016. Certain aspects of silver and silver nanoparticles in wound care: a minireview. *Journal of Nanomaterials,* 2016.

KOULENTI, D., SONG, A., ELLINGBOE, A., ABDUL-AZIZ, M. H., HARRIS, P., GAVEY, E. & LIPMAN, J. 2019. Infections by multidrug-resistant Gram-negative Bacteria: What's new in our arsenal and what's in the pipeline? *International Journal of Antimicrobial Agents,* 53**,** 211-224.

KOWSALYA, E., MOSACHRISTAS, K., BALASHANMUGAM, P., MANIVASAGAN, V., DEVASENA, T. & JAQULINE, C. R. I. 2021. Sustainable use of biowaste for synthesis of silver nanoparticles and its incorporation into gelatin-based nanocomposite films for antimicrobial food packaging applications. *Journal of Food Process Engineering,* 44**,** e13641.

KRISHNA, M., SYBIL, D., SHRIVASTAVA, P. K., PREMCHANDANI, S., KUMAR, H. & KUMAR, P. 2021. An innovative app (ExoDont) for postoperative care of patients after tooth extraction: prototype development and testing study. *JMIR Perioperative Medicine,* 4**,** e31852.

KUMAR, B., SMITA, K., CUMBAL, L. & DEBUT, A. 2017. Green synthesis of silver nanoparticles using Andean blackberry fruit extract. *Saudi Journal of Biological Sciences,* 24**,** 45-50.

KUMAR, B., SMITA, K., GALEAS, S., SHARMA, V., GUERRERO, V. H., DEBUT, A. & CUMBAL, L. 2020. Characterization and application of biosynthesized iron oxide nanoparticles using *Citrus paradisi* peel: A sustainable approach. *Inorganic Chemistry Communications,* 119**,** 108116.

KUMAR, M., SARMA, D. K., SHUBHAM, S., KUMAWAT, M., VERMA, V., NINA, P. B., JP, D., KUMAR, S., SINGH, B. & TIWARI, R. R. 2021a. Futuristic non-antibiotic therapies to combat antibiotic resistance: A review. *Frontiers in Microbiology,* 12**,** 609459.

KUMAR, S. S. D., RAJENDRAN, N. K., HOURELD, N. N. & ABRAHAMSE, H. 2018. Recent advances on silver nanoparticle and biopolymer-based biomaterials for wound healing applications. *International Journal of Biological Macromolecules,* 115**,** 165-175.

KUMAR, V., AL-GHEETHI, A., ASHARUDDIN, S. M. & OTHMAN, N. 2021b. Potential of cassava peels as a sustainable coagulant aid for institutional wastewater treatment: Characterisation, optimisation and techno-economic analysis. *Chemical Engineering Journal,* 420**,** 127642.

KURHADE, P., KODAPE, S. & CHOUDHURY, R. 2021. Overview on green synthesis of metallic nanoparticles. *Chemical Papers,* 75**,** 5187-5222.

KUSUMA, H. S., AMENAGHAWON, A. N., DARMOKOESOEMO, H., NEOLAKA, Y. A., WIDYANINGRUM, B. A., ONOWISE, S. U. & ANYALEWECHI, C. L. 2022. A comparative evaluation of statistical empirical and neural intelligence modeling of *Manihot esculenta*-derived leaves extract for optimized bio-coagulation-flocculation of turbid water. *Industrial Crops and Products,* 186**,** 115194.

LADE, B., D. & SHANWARE, A., S. 2020. Phytonanofabrication: Methodology and Factors Affecting Biosynthesis of Nanoparticles. *In:* SHABATINA, T. & BOCHENKOV, V. (eds.) *Smart Nanosystems for Biomedicine, Optoelectronics and Catalysis.* Rijeka: IntechOpen.

LAKKIM, V., REDDY, M. C., PALLAVALI, R. R., REDDY, K. R., REDDY, C. V., BILGRAMI, A. L. & LOMADA, D. 2020. Green synthesis of silver nanoparticles and evaluation of their antibacterial activity against multidrug-resistant bacteria and wound healing efficacy using a murine model. *Antibiotics,* 9**,** 902.

LAYA, A. & KOUBALA, B. B. 2020. Polyphenols in cassava leaves (*Manihot esculenta* Crantz) and their stability in antioxidant potential after in vitro gastrointestinal digestion. *Heliyon,* 6**,** e03567.

LEE, S. & JUN, B.-H. 2019. Silver Nanoparticles: Synthesis and Application for Nanomedicine. *International Journal of Molecular Sciences,* 20**,** 865.

LIM, J., YEAP, S. P., CHE, H. X. & LOW, S. C. 2013. Characterization of magnetic nanoparticle by dynamic light scattering. *Nanoscale Research Letters,* 8**,** 1-14.

LIMA, Z. M., DA TRINDADE, L. S., SANTANA, G. C., PADILHA, F. F., DA COSTA MENDONÇA, M., DA COSTA, L. P., LÓPEZ, J. A. & MACEDO, M. L. H. 2017. Effect of *Tamarindus indica* L. and *Manihot esculenta* extracts on antibiotic-resistant bacteria. *Pharmacognosy Research,* 9**,** 195.

LIU, W., ZHOU, Q., LIU, J., FU, J., LIU, S. & JIANG, G. 2011. Environmental and biological influences on the stability of silver nanoparticles. *Chinese Science Bulletin,* 56**,** 2009-2015.

LOZANO, C. 2022. *Nanotechnology* [Online]. Available: https://education.nationalgeographic.org/resource/nanotechnology [Accessed 10 November 2022 2022].

LU, M.-M., BAI, J., SHAO, D., QIU, J., LI, M., ZHENG, X., XIAO, Y., WANG, Z., CHANG, Z.-M. & CHEN, L. 2018. Antibacterial and biodegradable tissue nano-adhesives for rapid wound closure. *International Journal of Nanomedicine,* 13**,** 5849.

LUBIS, F. A., MALEK, N. A. N. N., SANI, N. S. & JEMON, K. 2022. Biogenic synthesis of silver nanoparticles using *Persicaria odorata* leaf extract: Antibacterial, cytocompatibility, and in vitro wound healing evaluation. *Particuology,* 70**,** 10-19.

MAGUIRE, C. M., RÖSSLEIN, M., WICK, P. & PRINA-MELLO, A. 2018. Characterisation of particles in solution – a perspective on light scattering and comparative technologies. *Science and Technology of Advanced Materials,* 19**,** 732-745.

MAKAROV, V., LOVE, A., SINITSYNA, O., MAKAROVA, S., YAMINSKY, I., TALIANSKY, M. & KALININA, N. 2014. "Green" nanotechnologies: synthesis of metal nanoparticles using plants. *Acta Naturae (англоязычная версия),* 6**,** 35-44.

MANJULA, P., LALITHA, K., VENGATESWARI, G., PATIL, J., NATHAN, S. S. & SHIVAKUMAR, M. S. 2020. Effect of *Manihot esculenta* (Crantz) leaf extracts on antioxidant and immune system of *Spodoptera litura* (Lepidoptera: Noctuidae). *Biocatalysis and Agricultural Biotechnology,* 23**,** 101476.

MARIE-MAGDELEINE, C., UDINO, L., PHILIBERT, L., BOCAGE, B. & ARCHIMÈDE, H. 2010. *In vitro* effects of Cassava (*Manihot esculenta*) leaf extracts on four development stages of *Haemonchus contortus*. *Veterinary Parasitology,* 173**,** 85-92.

MARTINELLI, C., PUCCI, C. & CIOFANI, G. 2019. Nanostructured carriers as innovative tools for cancer diagnosis and therapy. *APL Bioengineering,* 3**,** 011502.

MARTINS, C. S., SOUSA, H. & PRIOR, J. A. 2021. From Impure to Purified Silver Nanoparticles: Advances and Timeline in Separation Methods. *Nanomaterials,* 11**,** 3407.

MASSON-MEYERS, D. S., ANDRADE, T. A., CAETANO, G. F., GUIMARAES, F. R., LEITE, M. N., LEITE, S. N. & FRADE, M. A. C. 2020. Experimental models and methods for cutaneous wound healing assessment. *International Journal of Experimental Pathology,* 101**,** 21-37.

MATTEUCCI, F., GIANNANTONIO, R., CALABI, F., AGOSTIANO, A., GIGLI, G. & ROSSI, M. Deployment and exploitation of nanotechnology nanomaterials and nanomedicine. AIP conference proceedings, 2018. AIP Publishing LLC, 020001.

MEILAWATY, Z. 2013. Potensi ekstrak daun singkong (manihot utilissima) Dalam memodulasi ekspresi cox-2 pada monosit yang dipapar lps.

MERCHANT, S., PROUDFOOT, E. M., QUADRI, H. N., MCELROY, H. J., WRIGHT, W. R., GUPTA, A. & SARPONG, E. M. 2018. Risk factors for *Pseudomonas aeruginosa* infections in Asia-Pacific and consequences of inappropriate initial antimicrobial therapy: A systematic literature review and meta-analysis. *Journal of Global Antimicrobial Resistance,* 14**,** 33-44.

MICKYMARAY, S. 2019. One-step synthesis of silver nanoparticles using Saudi Arabian desert seasonal plant *Sisymbrium irio* and antibacterial activity against multidrug-resistant bacterial strains. *Biomolecules,* 9**,** 662.

MIHAI, M. M., DIMA, M. B., DIMA, B. & HOLBAN, A. M. 2019. Nanomaterials for wound healing and infection control. *Materials,* 12**,** 2176.

MIHAI, M. M., PREDA, M., LUNGU, I., GESTAL, M. C., POPA, M. I. & HOLBAN, A. M. 2018. Nanocoatings for chronic wound repair—modulation of microbial colonization and biofilm formation. *International Journal of Molecular Sciences,* 19**,** 1179.

MIRANDA, A., AKPOBOLOKEMI, T., CHUNG, E., REN, G. & RAIMI-ABRAHAM, B. T. 2022. pH Alteration in Plant-Mediated Green Synthesis and Its Resultant Impact on Antimicrobial Properties of Silver Nanoparticles (AgNPs). *Antibiotics,* 11**,** 1592.

MOHANTA, Y. K., BISWAS, K., JENA, S. K., HASHEM, A., ABD_ALLAH, E. F. & MOHANTA, T. K. 2020. Anti-biofilm and antibacterial activities of silver nanoparticles synthesized by the reducing activity of phytoconstituents present in the Indian medicinal plants. *Frontiers in Microbiology***,** 1143.

MOHANTA, Y. K., PANDA, S. K., JAYABALAN, R., SHARMA, N., BASTIA, A. K. & MOHANTA, T. K. 2017. Antimicrobial, antioxidant and cytotoxic activity of silver nanoparticles synthesized by leaf extract of *Erythrina suberosa* (Roxb.). *Frontiers in Molecular Biosciences,* 4**,** 14.

MOINS-TEISSERENC, H., CORDEIRO, D. J., AUDIGIER, V., RESSAIRE, Q., BENYAMINA, M., LAMBERT, J., MAKI, G., HOMYRDA, L., TOUBERT, A. & LEGRAND, M. 2021. Severe altered immune status after burn injury is associated with bacterial infection and septic shock. *Frontiers in Immunology,* 12**,** 586195.

MONIKA, P., CHANDRAPRABHA, M. N., RANGARAJAN, A., WAIKER, P. V. & CHIDAMBARA MURTHY, K. N. 2022. Challenges in healing wound: role of complementary and alternative medicine. *Frontiers in Nutrition,* 8**,** 1198.

MONTANO, E., VIVO, M., GUARINO, A. M., DI MARTINO, O., DI LUCCIA, B., CALABRÒ, V., CASERTA, S. & POLLICE, A. 2019. Colloidal silver induces cytoskeleton reorganization and E-cadherin recruitment at cell-cell contacts in HaCaT cells. *Pharmaceuticals,* 12**,** 72.

MOOLLA, M., REDDY, K., FWEMBA, I., NYASULU, P., TALJAARD, J., PARKER, A., LOUW, E., NORTJE, A., PARKER, M. & LALLA, U. 2021. Bacterial infection, antibiotic use and COVID-19: Lessons from the intensive care unit. *South African Medical Journal,* 111**,** 575-581.

MOORE, T. L., RODRIGUEZ-LORENZO, L., HIRSCH, V., BALOG, S., URBAN, D., JUD, C., ROTHEN-RUTISHAUSER, B., LATTUADA, M. & PETRI-FINK, A. 2015. Nanoparticle colloidal stability in cell culture media and impact on cellular interactions. *Chemical Society Reviews,* 44**,** 6287-6305.

MOULTON, M. C., BRAYDICH-STOLLE, L. K., NADAGOUDA, M. N., KUNZELMAN, S., HUSSAIN, S. M. & VARMA, R. S. 2010. Synthesis, characterization and biocompatibility of "green" synthesized silver nanoparticles using tea polyphenols. *Nanoscale,* 2**,** 763-770.

MOUNTAIN HERB ESTATE. 2022. *Plant Information* [Online]. Mountain Herb Estate. Available: https://www.herbgarden.co.za/mountainherb/herbinfo.php?id=654 [Accessed 14 October 2022].

MOUNTRICHAS, G., PISPAS, S. & KAMITSOS, E. I. 2014. Effect of temperature on the direct synthesis of gold nanoparticles mediated by poly (dimethylaminoethyl methacrylate) homopolymer. *The Journal of Physical Chemistry C,* 118**,** 22754-22759.

MUBEEN, B., ANSAR, A. N., RASOOL, R., ULLAH, I., IMAM, S. S., ALSHEHRI, S., GHONEIM, M. M., ALZAREA, S. I., NADEEM, M. S. & KAZMI, I. 2021. Nanotechnology as a Novel Approach in Combating Microbes Providing an Alternative to Antibiotics. *Antibiotics,* 10**,** 1473.

MULANI, M. S., KAMBLE, E. E., KUMKAR, S. N., TAWRE, M. S. & PARDESI, K. R. 2019. Emerging strategies to combat ESKAPE pathogens in the era of antimicrobial resistance: a review. *Frontiers in Microbiology,* 10**,** 539.

MULDER, P. P., KOENEN, H. J., VLIG, M., JOOSTEN, I., DE VRIES, R. B. & BOEKEMA, B. K. 2022. Burn-Induced Local and Systemic Immune Response: Systematic Review and Meta-Analysis of Animal Studies. *Journal of Investigative Dermatology*.

MURRAY, C. J., IKUTA, K. S., SHARARA, F., SWETSCHINSKI, L., AGUILAR, G. R., GRAY, A., HAN, C., BISIGNANO, C., RAO, P. & WOOL, E. 2022. Global burden of bacterial antimicrobial resistance in 2019: a systematic analysis. *The Lancet,* 399**,** 629-655.

MUSTARICHIE, R., SULISTYANINGSIH, S. & RUNADI, D. 2020. Antibacterial activity test of extracts and fractions of cassava leaves (*Manihot esculenta* Crantz) against clinical isolates of *Staphylococcus epidermidis* and *Propionibacterium acnes* causing acne. *International Journal of Microbiology,* 2020.

MYERS, R. 2003. *The basics of chemistry,* Wesport**,** London, Greenwood Publishing Group.

NANDIYANTO, A. B. D., OKTIANI, R. & RAGADHITA, R. 2019. How to Read and Interpret FTIR Spectroscope of Organic Material. *Indonesian Journal of Science and Technology,* 4**,** 97.

NARINA, S. & ODENY, D. 2011. Cassava. *In:* KOLE, C., JOSHI, C. P. & SHINNARD, D. R. (eds.) *Handbook of Bioenergy Crop Plants.* Boca Raton, Florida, USA: Taylor and Francis Group.

NDOH-RSA, N. D. O. H. R. O. S. A. 2022. Surveillance for Antimicrobial Resistance and Consumption of Antimicrobials in South Africa 2021. South Africa.

NIKNEJAD, F., NABILI, M., DAIE GHAZVINI, R. & MOAZENI, M. 2015. Green synthesis of silver nanoparticles: Another honor for the yeast model *Saccharomyces cerevisiae*. *Current Medical Mycology,* 1**,** 17-24.

NILASHI, M., SAMAD, S., YUSUF, S. Y. M. & AKBARI, E. 2020. Can complementary and alternative medicines be beneficial in the treatment of COVID-19 through improving immune system function? *Journal of Infection and Public Health,* 13**,** 893.

NISKA, K., ZIELINSKA, E., RADOMSKI, M. W. & INKIELEWICZ-STEPNIAK, I. 2018. Metal nanoparticles in dermatology and cosmetology: Interactions with human skin cells. *Chemico-biological Interactions,* 295**,** 38-51.

NKAFAMIYA, I., OSEMEAHON, S., ANDEMA, A. & AKINTERINWA, A. 2015. Evaluation of Cyanogenic Glucoside Contents in Some Edible Nuts and Seeds in Girei, Adamawa State, Nigeria. *IOSR Journal of Environmental Science, Toxicology and Food Technology,* 9**,** 27-33.

NOAH, N. 2019. Green synthesis: Characterization and application of silver and gold nanoparticles. *In:* SHUKLA, A. I., S (ed.) *Green Synthesis, Characterization and Applications of Nanoparticles.* Amsterdam: Elsevier.

NORUZI, M. 2015. Biosynthesis of gold nanoparticles using plant extracts. *Bioprocess and Biosystems Engineering,* 38**,** 1-14.

OGHENEJOBOH, K. M., ORUGBA, H. O., OGHENEJOBOH, U. M. & AGARRY, S. E. 2021. Value added cassava waste management and environmental sustainability in Nigeria: A review. *Environmental Challenges,* 4**,** 100127.

OGOLA, J. B. O. & MATHEWS, C. 2011. Adaptation of cassava (*Manihot esculenta*) to the dry environments of Limpopo, South Africa: growth, yield and yield components. *African Journal of Agricultural Research,* 6**,** 6082-6088.

OKKEH, M., BLOISE, N., RESTIVO, E., DE VITA, L., PALLAVICINI, P. & VISAI, L. 2021. Gold nanoparticles: can they be the next magic bullet for multidrug-resistant bacteria? *Nanomaterials,* 11**,** 312.

OLUKANNI, D. O. & OLATUNJI, T. O. 2018. Cassava waste management and biogas generation potential in selected local government areas in Ogun State, Nigeria. *Recycling,* 3**,** 58.

OMRAN, B. A., NASSAR, H. N., FATTHALLAH, N. A., HAMDY, A., EL-SHATOURY, E. H. & EL-GENDY, N. S. 2018. Waste upcycling of *Citrus sinensis* peels as a green route for the synthesis of silver nanoparticles. *Energy Sources, Part A: Recovery, Utilization, and Environmental Effects,* 40**,** 227-236.

ORCHARD, A. & VAN VUUREN, S. 2017. Commercial essential oils as potential antimicrobials to treat skin diseases. *Evidence-Based Complementary and Alternative Medicine,* 2017.

ORLOWSKI, P., ZMIGRODZKA, M., TOMASZEWSKA, E., RANOSZEK-SOLIWODA, K., CZUPRYN, M., ANTOS-BIELSKA, M., SZEMRAJ, J., CELICHOWSKI, G., GROBELNY, J. & KRZYZOWSKA, M. 2018. Tannic acid-modified silver nanoparticles for wound healing: the importance of size. *International Journal of Nanomedicine,* 13**,** 991.

ORTEGA, F., VERSINO, F., LÓPEZ, O. V. & GARCÍA, M. A. 2022. Biobased composites from agro-industrial wastes and by-products. *Emergent Materials,* 5**,** 873-921.

OWAID, M. N., RAMAN, J., LAKSHMANAN, H., AL-SAEEDI, S. S. S., SABARATNAM, V. & ABED, I. A. 2015. Mycosynthesis of silver nanoparticles by *Pleurotus cornucopiae* var. *citrinopileatus* and its inhibitory effects against *Candida* sp. *Materials Letters,* 153**,** 186-190.

PAL, S., NISI, R., STOPPA, M. & LICCIULLI, A. 2017. Silver-functionalized bacterial cellulose as antibacterial membrane for wound-healing applications. *ACS Omega,* 2**,** 3632-3639.

PALADINI, F. & POLLINI, M. 2019. Antimicrobial silver nanoparticles for wound healing application: progress and future trends. *Materials,* 12**,** 2540.

PALLEJA, A., MIKKELSEN, K. H., FORSLUND, S. K., KASHANI, A., ALLIN, K. H., NIELSEN, T., HANSEN, T. H., LIANG, S., FENG, Q. & ZHANG, C. 2018. Recovery of gut microbiota of healthy adults following antibiotic exposure. *Nature Microbiology,* 3**,** 1255-1265.

PALUPI, E. K., NAZOPATUL, P., UMAM, R., ANDRIANA, B. B., SATO, H. & ALATAS, H. Molecular functional group and optical analysis on chlorophyll of green choy sum and

cassava leaves extracts. IOP Conference Series: Earth and Environmental Science, 2020. IOP Publishing, 012030.

PARK, Y. 2014. A new paradigm shift for the green synthesis of antibacterial silver nanoparticles utilizing plant extracts. *Toxicological Research,* 30**,** 169-178.

PARVEEN, K., BANSE, V. & LEDWANI, L. Green synthesis of nanoparticles: their advantages and disadvantages. AIP conference proceedings, 2016. AIP Publishing LLC, 020048.

PATIL, S. & CHANDRASEKARAN, R. 2020. Biogenic nanoparticles: A comprehensive perspective in synthesis, characterization, application and its challenges. *Journal of Genetic Engineering and Biotechnology,* 18**,** 1-23.

PATRA, J. K. & BAEK, K.-H. 2015. Green nanobiotechnology: factors affecting synthesis and characterization techniques. *Journal of Nanomaterials,* 2014**,** 219.

PHILIP, D., UNNI, C., AROMAL, S. A. & VIDHU, V. 2011. *Murraya koenigii* leaf-assisted rapid green synthesis of silver and gold nanoparticles. *Spectrochimica Acta Part A: Molecular and Biomolecular Spectroscopy,* 78**,** 899-904.

PICRAUX, T. 2022. *Nanotechnology* [Online]. Encyclopedia Britannica. Available: https://www.britannica.com/technology/nanotechnology [Accessed 16 November 2022].

PINTO, A. M., CERQUEIRA, M. A., BAÑOBRE-LÓPES, M., PASTRANA, L. M. & SILLANKORVA, S. 2020. Bacteriophages for chronic wound treatment: From traditional to novel delivery systems. *Viruses,* 12**,** 235.

PIZZOLATO-CEZAR, L. R., OKUDA-SHINAGAWA, N. M. & MACHINI, M. T. 2019. Combinatory therapy antimicrobial peptide-antibiotic to minimize the ongoing rise of resistance. *Frontiers in Microbiology,* 10**,** 1703.

PRATHNA, T., CHANDRASEKARAN, N., RAICHUR, A. M. & MUKHERJEE, A. 2011. Biomimetic synthesis of silver nanoparticles by *Citrus limon* (lemon) aqueous extract and theoretical prediction of particle size. *Colloids and Surfaces B: Biointerfaces,* 82**,** 152-159.

PUGAZHENTHIRAN, N., ANANDAN, S., KATHIRAVAN, G., UDAYA PRAKASH, N. K., CRAWFORD, S. & ASHOKKUMAR, M. 2009. Microbial synthesis of silver nanoparticles by *Bacillus* sp. *Journal of Nanoparticle Research,* 11**,** 1811-1815.

QUARTEY, E., AMOATEY, H., ACHORIBO, E., OWUSU-ANSAH, M., NUNEKPEKU, W., DONKOR, S., APPIAH, A. & OFORI, E. 2016. Phytochemical constituents and antioxidant activities in leaves of 14 breeding lines of cassava (*Manihot esculenta* Crantz). *American Journal of Experimental Agriculture,* 12**,** 1-10.

RADULESCU, M., ANDRONESCU, E., DOLETE, G., POPESCU, R. C., FUFĂ, O., CHIFIRIUC, M. C., MOGOANTĂ, L., BĂLŞEANU, T.-A., MOGOŞANU, G. D. & GRUMEZESCU, A. M. 2016. Silver nanocoatings for reducing the exogenous microbial colonization of wound dressings. *Materials,* 9**,** 345.

RAFIQUE, M., SADAF, I., RAFIQUE, M. S. & TAHIR, M. B. 2017. A review on green synthesis of silver nanoparticles and their applications. *Artificial Cells, Nanomedicine, and Biotechnology,* 45**,** 1272-1291.

RAJ, S., MALI, S. C. & TRIVEDI, R. 2018. Green synthesis and characterization of silver nanoparticles using *Enicostemma axillare* (Lam.) leaf extract. *Biochemical and Biophysical Research Communications,* 503**,** 2814-2819.

RAJESH, M., MURALIKRISHNA, K., NAIR, S. S., KRISHNA, K. B., SUBRAHMANYA, T., SONU, K., SUBAHARAN, K., SWETA, H., KESHAVA, P. T. & NEELI, C. 2020. Facile coconut inflorescence sap mediated synthesis of silver nanoparticles and its diverse antimicrobial and cytotoxic properties. *Materials Science and Engineering: C,* 111**,** 110834.

RAJESHKUMAR, S., KUMAR, S. V., MALARKODI, C., VANAJA, M., PAULKUMAR, K. & ANNADURAI, G. 2017. Optimized Synthesis of Gold Nanoparticles Using Green Chemical Process and Its *In vitro* Anticancer Activity Against HepG2 and A549 Cell Lines. *Mechanics, Materials Science and Engineering Journal,* 9.

RAMESH, C., PRASAD, M. H. & RAGUNATHAN, V. 2013. Biosynthesis of Silver Nanoparticles Using *Manihot esculenta* Leaf Extract**.** *Advanced Science, Engineering and Medicine,* 5**,** 864-868.

RAMKUMAR, V. S., PUGAZHENDHI, A., GOPALAKRISHNAN, K., SIVAGURUNATHAN, P., SARATALE, G. D., DUNG, T. N. B. & KANNAPIRAN, E. 2017. Biofabrication and characterization of silver nanoparticles using aqueous extract of seaweed *Enteromorpha compressa* and its biomedical properties. *Biotechnology Reports,* 14**,** 1-7.

RAZAK, S. I. A., RAHMAN, W. A. W. A., HASHIM, S. & YAHYA, M. Y. 2013. Enhanced interfacial interaction and electronic properties of novel conducting kenaf/polyaniline biofibers. *Polymer-Plastics Technology and Engineering,* 52**,** 51-57.

REYES, D. F., CABRERA, G. F. S., MATA, S. M. V., SAN PEDRO, J. P. D., PALIOC, J. C. C. & TANDINGAN, G. S. 2020. Effect of pH on Size and Concentration of Silver Nanoparticles Synthesized using Ixora coccinea Linn. Leaf Extracts. *Oriental Journal of Chemistry,* 36.

RIGO, C., FERRONI, L., TOCCO, I., ROMAN, M., MUNIVRANA, I., GARDIN, C., CAIRNS, W. R., VINDIGNI, V., AZZENA, B. & BARBANTE, C. 2013. Active silver nanoparticles for wound healing. *International Journal of Molecular Sciences,* 14**,** 4817-4840.

ROBERTSON, J. D., RIZZELLO, L., AVILA-OLIAS, M., GAITZSCH, J., CONTINI, C., MAGOŃ, M. S., RENSHAW, S. A. & BATTAGLIA, G. 2016. Purification of nanoparticles by size and shape. *Scientific Reports,* 6**,** 1-9.

RODRÍGUEZ-RODRÍGUEZ, N., MARTÍNEZ-JIMÉNEZ, I., GARCÍA-OJALVO, A., MENDOZA-MARI, Y., GUILLÉN-NIETO, G., ARMSTRONG, D. G. & BERLANGA-ACOSTA, J. 2022. Wound chronicity, impaired immunity and infection in diabetic patients. *MEDICC Review,* 24**,** 44-58.

ROSIQUE, R. G., ROSIQUE, M. J. & FARINA JUNIOR, J. A. 2015. Curbing inflammation in skin wound healing: a review. *International Journal of Inflammation,* 2015.

ROSLI, N. A., TEOW, Y. H. & MAHMOUDI, E. 2021. Current approaches for the exploration of antimicrobial activities of nanoparticles. *Science and Technology of Advanced Materials,* 22**,** 885-907.

SAKA, R. & CHELLA, N. 2021. Nanotechnology for delivery of natural therapeutic substances: a review. *Environmental Chemistry Letters,* 19**,** 1097-1106.

SÁNCHEZ-LÓPEZ, E., GOMES, D., ESTERUELAS, G., BONILLA, L., LOPEZ-MACHADO, A. L., GALINDO, R., CANO, A., ESPINA, M., ETTCHETO, M. & CAMINS, A. 2020. Metal-based nanoparticles as antimicrobial agents: an overview. *Nanomaterials,* 10**,** 292.

SANKAR, R., KARTHIK, A., PRABU, A., KARTHIK, S., SHIVASHANGARI, K. S. & RAVIKUMAR, V. 2013. *Origanum vulgare* mediated biosynthesis of silver nanoparticles for its antibacterial and anticancer activity. *Colloids and Surfaces B: Biointerfaces,* 108**,** 80-84.

SANTAJIT, S. & INDRAWATTANA, N. 2016. Mechanisms of antimicrobial resistance in ESKAPE pathogens. *BioMed Research International*, 2016.

SELVARAJAN, V., OBUOBI, S. & EE, P. L. R. 2020. Silica nanoparticles—a versatile tool for the treatment of bacterial infections. *Frontiers in Chemistry,* 8**,** 602.

SHAH, M., FAWCETT, D., SHARMA, S., TRIPATHY, S. K. & POINERN, G. E. J. 2015. Green synthesis of metallic nanoparticles via biological entities. *Materials,* 8**,** 7278-7308.

SHAIKH, W. A., CHAKRABORTY, S., OWENS, G. & ISLAM, R. U. 2021. A review of the phytochemical mediated synthesis of AgNP (silver nanoparticle): the wonder particle of the past decade. *Applied Nanoscience,* 11**,** 2625-2660.

SHALABY, M. A., ANWAR, M. M. & SAEED, H. 2022. Nanomaterials for application in wound Healing: Current state-of-the-art and future perspectives. *Journal of Polymer Research,* 29**,** 1-37.

SHARIF, N. F. A., ABD RAZAK, S. I., RAHMAN, W. A. W. A., NAYAN, N. H. M., RAHMAT, A. R. & YAHYA, M. Y. 2015. Preparation and characterization of cassava leaves/cassava starch acetate biocomposite sheets. *BioResources,* 10**,** 4339-4349.

SHARMA, A., KHANNA, S., KAUR, G. & SINGH, I. 2021. Medicinal plants and their components for wound healing applications. *Future Journal of Pharmaceutical Sciences,* 7**,** 1-13.

SHARMA, D., KANCHI, S. & BISETTY, K. 2019. Biogenic synthesis of nanoparticles: a review. *Arabian Journal of Chemistry,* 12**,** 3576-3600.

SHARMA, P., GULERIA, P. & KUMAR, V. 2020. Green nanotechnology for bioactive compounds delivery. *Biotechnological Production of Bioactive Compounds.* Elsevier.

SHEDOEVA, A., LEAVESLEY, D., UPTON, Z. & FAN, C. 2019. Wound healing and the use of medicinal plants. *Evidence-Based Complementary and Alternative Medicine,* 2019.

SHOLIKHAH, U. N., PRANOWO, D., ARVIANTO, R. I., SARMINI, E. & WIDYANINGRUM, T. 2020. Purification Method of Silver Nanoparticles (AgNPs) and its Identification Using UV-Vis Spectrophotometer. *Key Engineering Materials,* 840**,** 484-491.

SIBBALD, R. G., CONTRERAS-RUIZ, J., COUTTS, P., FIERHELLER, M., ROTHMAN, A. & WOO, K. 2007. Bacteriology, inflammation, and healing: a study of nanocrystalline silver dressings in chronic venous leg ulcers. *Advances in Skin and Wound Care,* 20**,** 549-558.

SIDDIQI, K. S., HUSEN, A. & RAO, R. A. 2018. A review on biosynthesis of silver nanoparticles and their biocidal properties. *Journal of Nanobiotechnology,* 16**,** 1-28.

SIDHU, A. K., VERMA, N. & KAUSHAL, P. 2022. Role of Biogenic Capping Agents in the Synthesis of Metallic Nanoparticles and Evaluation of Their Therapeutic Potential. *Frontiers in Nanotechnology*.3, 801620.

SIMÕES, M. F., OTTONI, C. A. & ANTUNES, A. 2020. Biogenic metal nanoparticles: A new approach to detect life on Mars? *Life,* 10**,** 28.

SINCLAIR, A. 2016. *There is No Escape from the ESKAPE Pathogens* [Online]. Available: https://emerypharma.com/blog/eskape-pathogens-explained/ [Accessed 30 September 2022].

SINGH, A., GAUD, B. & JAYBHAYE, S. 2020. Optimization of synthesis parameters of silver nanoparticles and its antimicrobial activity. *Materials Science for Energy Technologies,* 3**,** 232-236.

SINTUBIN, L., DE WINDT, W., DICK, J., MAST, J., VAN DER HA, D., VERSTRAETE, W. & BOON, N. 2009. Lactic acid bacteria as reducing and capping agent for the fast and efficient production of silver nanoparticles. *Applied Microbiology and Biotechnology,* 84**,** 741-749.

SKÓRA, B., KRAJEWSKA, U., NOWAK, A., DZIEDZIC, A., BARYLYAK, A. & KUS-LIŚKIEWICZ, M. 2021. Noncytotoxic silver nanoparticles as a new antimicrobial strategy. *Scientific Reports,* 11**,** 1-13.

SOLTYS, L., OLKHOVYY, O., TATARCHUK, T. & NAUSHAD, M. 2021. Green synthesis of metal and metal oxide nanoparticles: Principles of green chemistry and raw materials. *Magnetochemistry,* 7**,** 145.

SONI, R. A., RIZWAN, M. A. & SINGH, S. 2022. Opportunities and potential of green chemistry in nanotechnology. *Nanotechnology for Environmental Engineering,* 7**,** 661-673.

SOOD, R. & CHOPRA, D. S. 2018. Optimization of reaction conditions to fabricate *Ocimum sanctum* synthesized silver nanoparticles and its application to nano-gel systems for burn wounds. *Materials Science and Engineering: C,* 92**,** 575-589.

SPAMPINATO, S. F., CARUSO, G. I., DE PASQUALE, R., SORTINO, M. A. & MERLO, S. 2020. The treatment of impaired wound healing in diabetes: looking among old drugs. *Pharmaceuticals,* 13**,** 60.

SRIKAR, S. K., GIRI, D. D., PAL, D. B., MISHRA, P. K. & UPADHYAY, S. N. 2016. Green synthesis of silver nanoparticles: a review. *Green and Sustainable Chemistry,* 6**,** 34-56.

SYAFIUDDIN, A., SALMIATI, HADIBARATA, T., SALIM, M. R., KUEH, A. B. H. & SARI, A. A. 2017. A purely green synthesis of silver nanoparticles using *Carica papaya*, *Manihot esculenta*, and *Morinda citrifolia*: synthesis and antibacterial evaluations. *Bioprocess and Biosystems Engineering,* 40**,** 1349-1361.

TACCONELLI, E. 2017. Global Priority List of Antibiotic-Resistant Bacteria to Guide Research, Discovery, and Development.

TACHE, A. M., DINU, L. D. & VAMANU, E. 2022. Novel Insights on Plant Extracts to Prevent and Treat Recurrent Urinary Tract Infections. *Applied Sciences,* 12**,** 2635.

TARANNUM, N., DIVYA, D. & GAUTAM, Y. K. 2019. Facile green synthesis and applications of silver nanoparticles: a state-of-the-art review. *RSC Advances,* 9**,** 34926-34948.

TENDERWEALTH, C. J., BERNARD, O. P. & NTIIDO, N. U. 2018. Surface plasmon resonance and antimicrobial properties of novel silver nanoparticles prepared from some indigenous plants in Uyo, Nigeria. *African Journal of Biotechnology,* 17**,** 748-752.

TEOH, S. L. & DAS, S. 2018. Phytochemicals and their effective role in the treatment of diabetes mellitus: a short review. *Phytochemistry Reviews,* 17**,** 1111-1128.

TOCCO, I., ZAVAN, B., BASSETTO, F. & VINDIGNI, V. 2012. Nanotechnology-based therapies for skin wound regeneration. *Journal of Nanomaterials,* 2012.

TORRES-RIVERO, K., BASTOS-ARRIETA, J., FIOL, N. & FLORIDO, A. 2021. Metal and metal oxide nanoparticles: An integrated perspective of the green synthesis methods by natural products and waste valorization: applications and challenges. *Comprehensive Analytical Chemistry,* 94**,** 433-469.

TRAIWATCHARANON, P., TIMSORN, K. & WONGCHOOSUK, C. 2016. Effect of pH on the green synthesis of silver nanoparticles through reduction with *Pistiastratiotes* L. extract. *Advanced Materials Research,* , 223-226.

TRIPATHY, A., RAICHUR, A. M., CHANDRASEKARAN, N., PRATHNA, T. & MUKHERJEE, A. 2010. Process variables in biomimetic synthesis of silver nanoparticles by aqueous extract of *Azadirachta indica* (Neem) leaves. *Journal of Nanoparticle Research,* 12**,** 237-246.

TRUONG, D.-H., NGUYEN, D. H., TA, N. T. A., BUI, A. V., DO, T. H. & NGUYEN, H. C. 2019. Evaluation of the use of different solvents for phytochemical constituents, antioxidants, and in vitro anti-inflammatory activities of *Severinia buxifolia*. *Journal of Food Quality,* 2019.

TYAVAMBIZA, C., ELBAGORY, A. M., MADIEHE, A. M., MEYER, M. & MEYER, S. 2021. The antimicrobial and anti-inflammatory effects of silver nanoparticles synthesised from *Cotyledon orbiculata* aqueous extract. *Nanomaterials,* 11**,** 1343.

UMAR, H., KAVAZ, D. & RIZANER, N. 2019. Biosynthesis of zinc oxide nanoparticles using *Albizia lebbeck* stem bark, and evaluation of its antimicrobial, antioxidant, and cytotoxic activities on human breast cancer cell lines. *International Journal of Nanomedicine,* 14**,** 87.

UMMARTYOTIN, S., BUNNAK, N., JUNTARO, J., SAIN, M. & MANUSPIYA, H. 2012. Synthesis of colloidal silver nanoparticles for printed electronics. *Comptes Rendus Chimie,* 15**,** 539-544.

URZEDO, A. L., GONCALVES, M. C., NASCIMENTO, M. H., LOMBELLO, C. B., NAKAZATO, G. & SEABRA, A. B. 2020. Multifunctional alginate nanoparticles containing nitric oxide donor and silver nanoparticles for biomedical applications. *Materials Science and Engineering: C,* 112**,** 110933.

VAN VUUREN, S. 2008. Antimicrobial activity of South African medicinal plants. *Journal of Ethnopharmacology,* 119**,** 462-472.

VAN WYK, A. & PRINSLOO, G. 2018. Medicinal plant harvesting, sustainability and cultivation in South Africa. *Biological Conservation,* 227**,** 335-342.

VELAYUTHAM, K., RAMANIBAI, R. & UMADEVI, M. 2016. Green synthesis of silver nanoparticles using *Manihot esculenta* leaves against *Aedes aegypti* and *Culex quinquefasciatus*. *The Journal of Basic and Applied Zoology,* 74**,** 37-40.

VELAZQUEZ-MEZA, M. E., GALARDE-LÓPEZ, M., CARRILLO-QUIRÓZ, B. & ALPUCHE-ARANDA, C. M. 2022. Antimicrobial resistance: One Health approach. *Veterinary World,* 15**,** 743.

VENUGOPAL, K., AHMAD, H., MANIKANDAN, E., ARUL, K. T., KAVITHA, K., MOODLEY, M., RAJAGOPAL, K., BALABHASKAR, R. & BHASKAR, M. 2017. The impact of anticancer activity upon *Beta vulgaris* extract mediated biosynthesized silver nanoparticles (ag-NPs) against human breast (MCF-7), lung (A549) and pharynx (Hep-2) cancer cell lines. *Journal of Photochemistry and Photobiology B: Biology,* 173**,** 99-107.

VIJAYAKUMAR, V., SAMAL, S. K., MOHANTY, S. & NAYAK, S. K. 2019. Recent advancements in biopolymer and metal nanoparticle-based materials in diabetic wound healing management. *International Journal of Biological Macromolecules,* 122**,** 137-148.

VIJAYAN, R., JOSEPH, S. & MATHEW, B. 2018. Eco-friendly synthesis of silver and gold nanoparticles with enhanced antimicrobial, antioxidant, and catalytic activities. *IET Nanobiotechnology,* 12**,** 850-856.

VOROBYOVA, V., VASYLIEV, G. & SKIBA, M. 2020. Eco-friendly "green" synthesis of silver nanoparticles with the black currant pomace extract and its antibacterial, electrochemical, and antioxidant activity. *Applied Nanoscience,* 10**,** 4523-4534.

WANG, L., HU, C. & SHAO, L. 2017. The antimicrobial activity of nanoparticles: present situation and prospects for the future. *International Journal of Nanomedicine,* 12**,** 1227.

WATTIMENA, S. C., AYUNINGRUM, D. A., LATUASAN, L. Y., SAMSON, E. & PATTY, P. J. 2022. Properties of Bio-Silver Nanoparticles Mediated by Tuber and Leaf Extracts of *Manihot esculenta* Crantz. *Biosaintifika: Journal of Biology and Biology Education,* 14.

WEN, L., ZENG, P., ZHANG, L., HUANG, W., WANG, H. & CHEN, G. 2016. Symbiosis theory-directed green synthesis of silver nanoparticles and their application in infected wound healing. *International Journal of Nanomedicine,* 11**,** 2757.

WILHELM, K. P., WILHELM, D. & BIELFELDT, S. 2017. Models of wound healing: an emphasis on clinical studies. *Skin Research and Technology,* 23**,** 3-12.

WILKINSON, H. N. & HARDMAN, M. J. 2020. Wound healing: Cellular mechanisms and pathological outcomes. *Open Biology,* 10**,** 200223.

WORLD HEALTH ORGANIZATION. 2020. *WHO calls for global action on sepsis - cause of 1 in 5 deaths worldwide* [Online]. Geneva: World Health Organization. Available: https://www.who.int/news/item/08-09-2020-who-calls-for-global-action-on-sepsis---cause-of-1-in-5-deaths-worldwide [Accessed 11 December 2022].

WORLD HEALTH ORGANIZATION. 2021. *Antimicrobial resistance* [Online]. Geneva: World Health Organization. Available: https://www.who.int/news-room/fact-sheets/detail/antimicrobial-resistance [Accessed 20 December 2022].

YANG, J. & YANG, H. 2019. Non-antibiotic therapy for *Clostridioides difficile* infection: a review. *Critical Reviews in Clinical Laboratory Sciences,* 56**,** 493-509.

YE, J. & CHEN, X. 2023. Current Promising Strategies against Antibiotic-Resistant Bacterial Infections. *Antibiotics,* 12**,** 67.

YEH, Y.-C., HUANG, T.-H., YANG, S.-C., CHEN, C.-C. & FANG, J.-Y. 2020. Nano-based drug delivery or targeting to eradicate bacteria for infection mitigation: a review of recent advances. *Frontiers in Chemistry,* 8**,** 286.

ZACHARI, M. A., CHONDROU, P. S., POULILIOU, S. E., MITRAKAS, A. G., ABATZOGLOU, I., ZOIS, C. E. & KOUKOURAKIS, M. I. 2014. Evaluation of the alamarblue assay for adherent cell irradiation experiments. *Dose-Response,* 12**,** dose-response. 13-024. Koukourakis.

ZAKARIA, Z., KHAIRI, H., SOMCHIT, M., SULAIMAN, M., MAT JAIS, A., REEZAL, I., MAT ZAID, N., ABDUL WAHAB, S., FADZIL, N. & ABDULLAH, M. 2006. The *in vitro antibacterial* activity and brine shrimp toxicity of Manihot esculenta var. Sri Pontian extracts. *International Journal of Pharmacology,* 2**,** 216-220.

ZHANG, D., MA, X.-L., GU, Y., HUANG, H. & ZHANG, G.-W. 2020a. Green synthesis of metallic nanoparticles and their potential applications to treat cancer. *Frontiers in Chemistry,* 8**,** 799.

ZHANG, L., BAO, M., LIU, B., ZHAO, H., ZHANG, Y., JI, X., ZHAO, N., ZHANG, C., HE, X. & YI, J. 2020b. Effect of andrographolide and its analogs on bacterial infection: a review. *Pharmacology,* 105**,** 123-134.

ZHANG, X., QU, Y., SHEN, W., WANG, J., LI, H., ZHANG, Z., LI, S. & ZHOU, J. 2016. Biogenic synthesis of gold nanoparticles by yeast *Magnusiomyces ingens* LH-F1 for catalytic reduction of nitrophenols. *Colloids and Surfaces A: Physicochemical and Engineering Aspects,* 497**,** 280-285.

ZHONG, L., SHI, C., HOU, Q., YANG, R., LI, M. & FU, X. 2022. Promotive effects of four herbal medicine ARCC on wound healing in mice and human. *Health Science Reports,* 5**,** e494.